TÉCNICO LISBOA

Techno-economical potential of photovoltaic solutions in the urban environment

A web-based decision support model at high spatio-temporal resolution for residential buildings in Portugal

Miguel Eduardo Correia Duarte

Thesis to obtain the Master of Science Degree in

Civil Engineering

Supervisors: Prof.ª Ana Paula Martins Falcão Flor

Prof. António Morais Aguiar da Costa

Examination Committee

Chairperson: Prof. João Torres de Quinhones Levy

Supervisor: Prof.ª Ana Paula Martins Falcão Flor

Member of the Committee: Prof.ª Maria da Glória De Almeida Gomes

June 2018

Declaração

Declaro que o presente documento é um trabalho original da minha autoria e que cumpre todos os requisitos do Código de Conduta e Boas Práticas da Universidade de Lisboa

Declaration

I declare this document is an original work of my own authorship and that it fulfills all the requirements of the Code of Conduct and Good Practices of the Universidade de Lisboa

Acknowledgements

I would like to extend my deep gratitude to the following people:

To my thesis advisors, Profª. Ana Paula Falcão and Prof. António Aguiar Costa, whose insights, guidance, feedback and support were instrumental in the execution of this work;

To Rita Machete, for the help and support in procuring and understanding the information, data and research on which this dissertation was built;

To Paul Gilman from NREL for the timeliness, thoroughness and patience in responding to all my queries regarding the SAM software;

To my friends who supported me throughout this period and gave me the will to proceed. A special thank you to Gaspar Costa, whose programming skills help put me on the right track;

To my girlfriend Inês Silva, who was patient and kind enough to bear with me the weight of the long hours I had to dedicate;

And finally to my parents, Paula Correia and José Duarte, without whose guidance this dissertation wouldn´t have been achieved, and to my grandfather, José Nunes Correia, whose wisdom and integrity were instrumental in pulling me towards my final objective.

Resumo

Atualmente existe uma multiplicidade de ferramentas para o cálculo do potencial técnico e económico de instalações fotovoltaicas em ambientes urbanos. Esta dissertação visa colmatar lacunas identificadas nessas ferramentas que comprometem a aplicabilidade das informações geradas por estas, em particular no que diz respeito à escala, ao potencial de utilização de BIPV em fachadas, integração de informação morfológica e meteorológica de elevada granularidade e modelação detalhada do funcionamento dos sistemas fotovoltaicos.

Para tal foi desenvolvida e implementada uma metodologia de cálculo de desempenho técnico e económico de soluções fotovoltaicas à escala local para edificios residenciais urbanos, adaptada à realidade Portuguesa. Foi feito um levantamento exaustivo de informação sobre o estado atual da tecnologia, métodos de análise e enquadramento legal destas tecnologias, daí resultando uma nova metodologia que permite integrar informação morfológica e meteorológica em formato SIG 3D e cruzá-la com modelos de desempenho técnico e económico de soluções fotovoltaicas e com o ambiente legal e fiscal em que se inserem, permitindo obter indicadores de desempenho financeiro para soluções fotovoltaicas desenhadas pelo utilizador.

Esta metodologia é subsequentemente aplicada a um caso de estudo na freguesia de Alvalade em Lisboa, e os resultados de sistemas fotovoltaicos no telhado e na fachada são analisados e discutidos, sendo que revelam boa concordância com a realidade atual de mercado e reforçam a noção da viabilidade económica de ambos os sistemas fotovoltaicos, contribuindo para a sua potencial disseminação. A inclusão de sistemas fotovoltaicos em fachada, como complemento de instalações de telhado, revela-se desejável e economicamente vantajosa, suportando a utilização do SIG 3D para este tipo de aplicações.

Palavras Chave: PV BIPV Modelação Técnica Económica Local SIG 3D

Abstract

There are currently multiple tools available for the assessment of the technical and economic potential of photovoltaic installations in urban environments. This dissertation aims to close some gaps identified in these tools which compromise the applicability of the information obtained, namely in respect to the scale, potential use of BIPV on façades, integration of high granularity morphological and meteorological information and detailed modeling of the performance of photovoltaic systems.

To this end, a calculation methodology for the technical and economic performance of photovoltaic solutions at the local scale for urban residential buildings was developed and implemented, adapting it to the Portuguese reality. A comprehensive gathering of information about the current state of the art, analysis methods and legal framework was carried out, and from it a new methodology was derived to integrate 3D-GIS morphological and meteorological information with technical and economic performance models of photovoltaic systems and their legal and fiscal constraints, enabling the determination of financial performance indicators for user designed photovoltaic solutions.

This methodology is subsequently applied to a case study in the borough of Alvalade in Lisboa, and the results for rooftop and façade mounted photovoltaic systems are analyzed and discussed, revealing good agreement with current market reality and reinforcing the notion of the economic viability of both types of photovoltaic systems, contributing to their potential for dissemination. The inclusion of façade PV systems as a complement to rooftop systems is desirable and economically advantageous, lending support to further uses of 3D-GIS for these applications.

Key Words: *PV BIPV Modeling Technical Economic Local 3D-GIS*

Table of Contents

Table of Figures

Table of Tables

Acronyms and Abbreviations

AC – Alternate Current
AOI – Angle of Incidence
API – Application Programming Interface
BAPV – Building Attached Photovoltaics
BIPV – Building Integrated Photovoltaics
c-Si – Crystalline Silicon
CAPEX – Capital Expenditure
CEC – California Energy Commission
CGA – Computer Generated Architecture
CIEG – *Compensação de Interesse Económico Geral*
CIGS - Copper-Indium-Gallium-Selenide Solar Cells
CIM – City Information Model
CIS - Copper Indium Selenide
CUR – *Comercializador de Último Recurso*
DC – Direct Current
DL – Decreto-Lei
DHI – Diffuse Horizontal Irradiance
DNI – Direct Normal Irradiance
DR – *Diário da República*
DSM – Digital Surface Model
DTM – Digital Terrain Model
FiT – Feed-in-Tariff
GCR – Ground Coverage Ratio
GHG – Green House Gases
GHI – Global Horizontal Irradiance
GIS – Geographic Information System
HVAC – Heating, Ventilation & Air-conditioning
INOCT – Installed Nominal Operating Temperature
IMI – *Imposto Municipal sobre Imóveis*
IMT – *Imposto Municipal sobre as Transmissões Onerosas de Imóveis*
ILR – Inverter Load Ratio
IRC – *Imposto sobre Rendimentos de Pessoas Colectivas*
IRR – Internal Rate of Revenue
IRS – *Imposto sobre Rendimentos Singulares*
LCOE – Levelized Cost of Energy
LiDAR - Light Detection And Ranging
MPP – Maximum Power Point
NOCT – Nominal Operating Cell Temperature
NPV – Net Present Value
NREL – National Renewable Energy Laboratory
O&M – Operation & Maintenance
OMIE – *Operador do Mercado Ibérico de Energia – Pólo Espanhol*
OMIP – *Operador do Mercado Ibérico de Energia – Pólo Português*
OPEX – Operational Expenditure
PN – Positive/Negative junction
POA – Plane of Array
PPA – Power Purchase Agreement
PV - Photovoltaic
RC – Resistor/Capacitor thermal network model
RES – Renewable Energy Source
RESP – *Rede Eléctrica de Serviço Público*
SERUP - *Sistema Electrónico de Registo de Unidades de Produção*
SAM – System Advisor Model
SDK – Software Development Kit
SSC – SAM Simulation Core
ST – Solar Thermal
STC – Standard Test Conditions
TF – Thin film PV
TOU – Time of Use
TMY -Typical Meteorological Year
UAV – Unmanned Aerial Vehicle
UP – *Unidade de Produção*
UPAC – *Unidade de Produção de Auto-consumo*
UPP – *Unidade de Pequena Produção*
VAT – Value Added Tax
VBA – Visual Basic for Applications
WACC – Weighted Average Cost of Capital
W_{DC} – Direct Current Power in Watts

List of Symbols

A_{apt} – Area of each apartment
A_{total} – Total building area

B_t – Auxiliary power cost in year t

C – Yearly electricity cost without the system
C_{air} – Air capacitance
C_{area} – Average annual electricity consumption per household in kWh/year/m^2
C_{AT} – After-tax annual costs
$C_{building}$ – Total annual energy consumption of building
C_{cap} – Capacity Costs
C_{debt} – Total debt
C_{env} – Building envelope capacitance
C_{equity} – Total equity
C_{inst} – Total installed system costs
C_{loan} – Annual debt payments
C_{mass} – Thermal mass capacitance
C_{occ} – Average annual electricity consumption per household in kWh/year/person
C_{oper} – Operating Costs
$C_{O\&M}$ – OPEX costs
C_{reg} – Registration fee costs
C_{string} – String inverter cost
C_{sys} – Yearly electricity cost with system
C_{tax} – Taxable yearly income
C_{total} – Total installed system cost
C_{var} – Variable Costs
CF – Pre-tax cash flow
CF_{AT} – After-tax cash flow
CF_P – Project cash flow
CF_{cum} – Cumulative cash flow

D – Yearly panel degradation
D_{bal} – Debt balance

E_i – Hourly system expense
$E_{supplied,m}$ – Energy sold in month m
E_t – Energy produced in year t
E_{val} – Annual energy value

f_{debt} – Debt fraction

G_i – Energy bought/sold to grid in hour i

h_{surf} – Convection coefficient

I – Interest payments
I_b – Beam normal irradiance
$I_{d,ground}$ – Ground reflected irradiance
$I_{d,sky}$ – Sky diffuse irradiance
I_{poa} – Incident POA irradiance
I_t – CAPEX in year t
I_{tr} – Transmitted Irradiance

L – Hourly building energy load
$L_{total}(\%)$ - Total DC loss

M_t – OPEX in year t

n_{apt} – Number of apartments in building

O_{apt} – Apartment occupancy
O_{total} – Building occupancy
$OMIE_m$ – Sale rate for month m

P – Principal payments
P_{ac} – AC power output
P_{ac0} – Inverter AC nameplate rating
P'_{dc} – Derated DC Power Output
P_{dc0} – Panel DC nameplate rating
P_{dc} – DC Power Output
$P_{inv,dc0}$ – Inverter effective DC input rating
PB – Payback period

Q_{conv} – Convective thermal gains
Q_{inf} – Infiltration thermal gains
Q_{rad} – Radiative thermal gains
Q_{sol} – Solar thermal gains

R_{env} – Building envelope resistance
$R_{UPAC,m}$ – Monthly remuneration from grid sales
r_{buy} – Electricity buy rate
r_{loan} – Loan nominal interest rate
r_{inf} – Inflation rate
r_{IRS} – Income tax rate
r_{nom} – Nominal discount rate
r_{real} – Real discount rate
r_{sell} – Electricity sell rate
r_{VAT} – VAT rate

S_i – Hourly system income

T_{air} – Air temperature
T_{amb} – Ambient temperature
T_{cell} – Operating cell temperature
T_{mass} – Thermal mass temperature
T_{ref} – Reference cell temperature
T_{S-A} – Sol-air temperature
T_{surf} – Interior wall surface temperature
Tax – Yearly tax collection
t_{loan} – Loan term

ξ_{sys} – System derate factor
η_{inv} – Inverter efficiency loss
ξ_{dc} – DC derate factor
α – Angle of incidence
β – Panel tilt angle
γ – Panel azimuth angle
φ – Temperature coefficient
θ – Zenith angle
ω – Altitude angle
η_{op} – Inverter conversion efficiency at operating conditions

Introduction

In 2015, for the first time, a worldwide agreement encompassing 195 countries was reached, for the need to move from fossil fuels towards innovative technologies and low carbon economy, in a collective bid to avert a climatic catastrophe (COP 21, 2016).

The European commission set itself ambitious goals towards decarbonization of the economy, with targets to reduce GHG emissions to 40% below their 1990 level by 2030 (Psomopoulos et al., 2015), whilst making energy systems more competitive, secure and sustainable.

The current EU goal for renewable energy share of final consumption for 2020 stands at 20% (31% in Portugal). While currently well on track to meet and exceed those goals (in 2016 the renewable share of gross final energy consumption stood at 17% (Eurostat, 2018)), there is still a lot of uncertainty as to what RES mix will provide a lasting and sustainable solution.

Solar radiation is a clean and abundant source of energy. Every year it's estimated that between 1.575 and 49.837 exajoules[1] of primary [2] solar energy reaches the earth's surface (UNDP, 2000). Out of a total world energy consumption of 394.6 exajoules (IEA, 2016c), only 0.99 exajoules (IEA, 2015) is produced by solar power technology. This gap reveals the potential of solar power, if correctly harnessed, to supply well and beyond current and future consumption estimates.

Rapid technological development and deployment, coupled with decreasing costs and wider public acceptance have seen solar power technologies permeate the urban fabric, with the proliferation of solar photovoltaic (PV) and solar thermal (ST) collectors. Due to their high modularity and increasing cost competitiveness, these technologies are driving power and heat production away from utility scale generation towards an ever more decentralized system.

In this context PV technologies play a decisive role towards a future of less dependence on traditional electrical supply by way of a thorough integration of renewable energy sources at the urban level.

Nowadays 40% of PV installations occur on buildings, so the building sector has a significant role to play in PV development, reflected in the directive delivered by the EU on Energy Performance in Buildings (EU, 2010). This directive presents new ways to decrease local energy consumption from 2020 onwards, striving for Near Zero Energy Buildings (NZEBs), with reduced energy consumption but still consuming) and Positive Energy Buildings (PEBs), producing more than what is consumed (IEA, 2017).

[1] Wide estimation interval given rough estimation of high impact variables on primary solar energy availability (e.g. a region's geographic position, typical weather conditions and land availability)
[2] Before conversion to secondary or final energy

Objectives

The main goal of this dissertation is to create a web-based decision support tool for residential PV systems in urban buildings in Portugal.

To this end, it includes the study and development of a methodology to assess the technical and economic potential of urban PV solutions on rooftops and façades, adapting the existing approaches to the requirements of a web-based GIS user interface and its underlying datasets.

The methodology will employ commonly used tools in wide scale urban solar potential estimation for a local, bespoke application on tilted rooftops and façades within a 3DGIS/CIM model, with high spatio-temporal detail, explicitly modeling the PV and BIPV system technical and economic performance, its behavior throughout the lifecycle, and tailoring it to the constraints of Portuguese urban PV legal and fiscal framework.

This methodology will quantify the technical and economic potential of Urban PV and BIPV solutions on rooftops and façades, with a view to support decision making by the stakeholders of different urban photovoltaic systems.

Throughout the dissertation, current limitations to full deployment of BIPV are identified and the current state of affairs in BIPV is reviewed, including its technical and legal hurdles, and how that may affect the future of the technology deployment.

Research methodology and dissertation structure

A thorough review of publications pertaining to the dissertation´s objectives was undertaken, including a wide range of journals and conference proceedings, and diverse websites such as industry blogs, companies, governmental organizations and research institutes. The results of this research can be found in the State of the Art section, and include an overview of solar potential assessment methods in cities (page 3), technical and performance characteristics of PV technologies (page 6), PV system technical, production and economic assessment methods (page 10), cost breakdown of PV systems components (page 18) and the legal framework for this kind of technological deployment (page 21).

The possible contributions to the current state of the art were thus identified and formed the basis for the development of a conceptual model (page 23), starting with the choice of a software tool for the PV simulation (page 23) and its adaptation for the stated objectives (page 27). The review of the model is broken down into three components, Input Data (page 52), Interface (page 56) and Simulator (page 59), exhaustively detailing each step in the calculation methodology.

The conceptual model is then applied as a case study in Lisbon (page 64) with both rooftop (page 68) and façade (page 74) systems´ performances and sensitivities to external factors analyzed in depth. The dissertation concludes with the appraisal of the limitations of the approach (page 78) and its contributions to the current literature (page 79).

I State of the Art

One of the aims of this dissertation is finding a suitable way to estimate the technical and economic solar energy potential of an urban PV system, and as such one must be able to define what that potential is. According to Gagnon et al. (2016), technical potential is the generation available from a particular technology in a region and requires knowledge of the resource availability and quality, the technical system performance and the physical availability of area for deployment. As for economic potential it is the quantity of possible generation that would result in a positive return on investment of constructing the system, and requires accounting for projected technology costs, available vs. required revenue for energy project, project financing details and life cycle performance.

The literature pertaining to the acquisition, modeling and analysis methods of resource availability and area for deployment is reviewed in section I.1. A review of technical characteristics of the components of PV systems and respective modeling can be found in I.2 & I.3, the cost assessment of which are further analyzed in section I.4. An overview of the applicable legislation and support schemes for this technology is made in section I.5.

I.1. Assessing Solar Energy Potential in Cities

For the determination of solar radiation on any surface, the usual approach is taking meteorological data (satellite, local measurements or typical meteorological year (TMY) data) that accurately represent the weather at a system's location (Yates & Hibberd, 2010). In case no such data is available, indirect methods can be used such as the Kumar radiation model (Kumar et al., 1997). The amount of solar radiation incident on a surface on the earth can be divided into three categories: direct (DNI, direct normal radiation), diffuse (DHI, diffuse horizontal radiation) or reflected. Direct radiation describes solar radiation travelling from the sun to the surface of the earth without obstacles and it´s the strongest component among the three. Diffuse radiation describes solar radiation that has been scattered by molecules and particles in the atmosphere but that has still made it down to the surface of the earth. Reflected radiation is the component that has been reflected off of a non-atmospheric source such as the ground or urban elements, a function of the reflecting surface´s albedo (Machete, R., 2016, & Yates & Hibberd, 2010).

While occasionally installed flat, PV systems usually have a tilt and an azimuth or employ single or dual-axis trackers, and as such a mathematical model is needed to translate horizontal radiation values into plane-of-array (POA) irradiance, which is the portion of the total radiation that falls onto the PV array. Numerous models can be used to make this translation, including isotropic sky model (Liu & Jordan, 1960), Hay model (Hay, 1979), and the Perez model (Perez et al., 1987). In general these empirical radiation models treat the direct beam component the same way, and where they differ is in the treatment of diffuse radiation (Freitas et al., 2015). A general review of solar radiation models can be found in Teke et al., (2015) and Despotovica et al., (2015).

However, for complex 3D urban environments, physically based solar radiation formulations cannot reproduce the range of phenomena that impact available solar radiation. Computational modeling of the physical context is required to achieve reliable and granular spatio-temporal assessment of available

radiation, accounting for obstructions to sunlight, variable diffuse radiation due to anisotropy, amount of visible sky at any given point and complex 3D geometries and textures at a large scale.

Bearing this in mind, besides the geographic location and natural features of the surrounding area being determining factors in the solar irradiance, other topographical features such as the building´s footprints, volumetric distribution, shape, color and albedo can all have a significant impact on the amount and quality of available sunlight for electricity production (Compagnon, 2004). As such, a detailed model of the study area is recommended to account for all impacting variables.

GIS tools are particularly adequate for solar exposure and shadowing calculations (Biljecki et al., 2015), given the extensive availability of GIS databases with planimetry, altimetry and surface features of many urban areas, and many energy models and techniques have been developed for this purpose in recent years (Ratti et al., 2005). For solar radiation, 3D representation of the environment is necessary, leading to 2.5D and 3D approaches.

In 2.5D models for each planimetric position (x,y) there is a single elevation value (H), making the distinction of elements on different planes impossible, such as overhangs or caves. Consequently, it is not possible to distinguish radiation values for those planes, resulting in models with only one solar radiation value for each location (x,y), an approach that is most adequate for non-urban scenarios or rooftop analyses. This can be partially mitigated by the hyper point approach described in Catita et al. (2014) but that requires façades to be contiguous to the roof edges greatly limiting the urban form variability that can be modeled.

In 3D models the object is defined by a set of points with three-dimensional coordinates (x,y,H), where each (x,y) pair can have different corresponding altitude values (H). From this point cloud, the surfaces that define the entity are derived and each surface has a defined normal vector for orientation and inclination information. In these models solar radiation values are calculated for each surface allowing different values at different altitudes for the same (x,y) position (Machete, Falcão, & Gomes, 2015). Extensive reviews of the multiple solar potential analysis models and their evolution can be found in Freitas et al., (2015) and Martin et al., (2015).

Examples of implementation of a 2.5D approach include the *r.sun* tool implemented in *Grass GIS* used by Hofierka & Suri (2002), the *Area Solar Radiation* tool implemented in ESRI *ArcGIS* used by Santos et al., (2011) and Chow et al. (2014) with LIDAR and 3D area model respectively, and the hybrid approach described by Carneiro et al. (2010). Recent refinements to these methods applied to urban planning, solar energy and vegetation modelling can be found in Bizjak et al. (2015), Horvath et al. (2016) and Fogl & Moudry (2016) respectively.

3D-GIS approaches are currently implemented in commercial software products specific for climatic and energy analysis, often by integrating tools for quantifying the incident solar radiation such as *EnergyPlus* and *Ecotect* (Marsh, 2004). Other less generic approaches can be used for specific problems, such as in Hofierka e Zlocha (2012) or the methods described by Redweik et al. (2013) and Catita et al. (2014). Recent applications of 3D solar potential assessment methodologies include Eicker et al. (2015), Liang et al. (2015), Sarralde et al. (2015), Peronato & Rey (2016), Machete et al., (2015) and Rodriguez et al. (2017),

which address a wide range of issues in the fields of urban planning, solar exposure estimation, vegetation modeling and urban PV production.

All the GIS solar radiation models estimate the extent of radiation incident, at specific point at the earth's surface, direct or indirectly by taking into consideration geographic, meteorological and temporal factors. At an urban scale this implies that a digital surface model (DSM) is necessary, by combining the digital terrain model (DTM) with building and urban elements.

There are two methods to obtain a DSM in urban environment: i) through the acquisition of a 3D point cloud that allows geometric reconstruction of the surveyed elements; ii) by means of procedural and/or parametric modelling (Machete, Falcão, & Gomes, 2015). Usually in the first approach data is acquired by aerial photography of an unmanned aerial vehicle (UAV) or light detection and ranging (LiDAR) system (Carneiro et al., 2008). In the second approach the 3D models are built based on attributes, stored in a geodatabase, and are generally referred to as 3DGIS/CIM models (Gil et al., 2011). The accuracy of these models depends on the LiDAR data quality, allows for the creation of 3D models in a very expedite way and is best applied in an urban environment with clear repetition and symmetry of the architectural elements in order to best capture the local identity (Aliaga, 2012). The steps for the application of this method are further detailed in Falcão et al. (2016).

Solar radiation is time, location and condition dependent, particularly for cityscapes with their complex 3D environment. It requires obstruction analysis to account for shadows cast on surfaces by buildings, vegetation or other structural elements (Freitas et al., 2015). In PV production analysis, shading must be accounted for because large distant objects, close obstructions and the system itself may block some of the available sunlight. The complexity of the performance-modeling tool and quality of the urban model dictate whether these types of shading are treated separately or grouped together.

In the latter case, and the most common, 2.5D models are used and shading is accounted for by a single derate factor (see Levinson et al., 2009; Tooke et al., 2012; Horvath et al., 2016; Fogl & Moudry, 2016; and Rodriguez et al., 2017), which simplistically assumes that the system experiences the same losses due to shade for every hour of the year and that the effects of shade on PV production are linear (when in fact shading of a single cell in a module can disproportionately impact the whole module, the string or even the entire PV array, see section I.2).To accurately represent shading behavior throughout the day, a full 3D approach is required, implying more time consuming calculations and usage of detailed 3D models, as employed in Jakubiec & Reinhart (2013) and Peronato & Rey (2016).

PV production is dependent on the available irradiated area for PV deployment, with most studies focusing on large urban areas for the estimation of PV deployment. Melius et al. (2013) identify three methods to evaluate available deployment area: constant-value, manual selection, and GIS-based methods. Constant-value methods for estimating rooftop suitability simply assume a certain percentage of building rooftop area is suitable for hosting PV (see Paidipati et al., 2008). It is quick and easy but ignores the nuances such as HVACs, tree shadows, and lacks validation. Manual selection evaluates buildings individually to determine the total suitable area with sources such as aerial photography providing visual clues to rooftop PV

installation locations, being the most precise and time consuming of the methods. GIS methods use 3D models to account for area limitations to deployment given a range of constraints, including but not limited to construction constraints (e.g. HVACs, chimneys, antennas), legal constraints (e.g. protected buildings), shading effects, and service and separation requirements of PV panels (e.g. ground coverage ratio (GCR[3]) and service areas (see Gagnon et al., 2016 and Rodriguez et al., 2017). A complete review of existing methods for estimating the fraction of rooftop area suitable for PV deployment over large areas can be found in Melius et al., (2013), and a methodology for the estimation of façade suitability can be found in Esclapes et al., (2014).

Solar and photovoltaic energy potential analysis is progressively adapting to detailed 3D representations and spatial analysis, with no standardized procedures, or consensus on methodologies. Most of the research has focused on urban-scale assessment of solar radiation of PV yield, with simplistic assumptions regarding the technical performance of PV panels when installed in complex 3D environments. The current open-source state of the art for spatial attribute query and manipulation is CityGML, while another common option is the ESRI CityEngine (complemented with analysis tools from ArcGIS, see Freitas et al., 2015). Much effort is still needed to accomplish the creation of a 3D urban model that brings together all the features that existing 2D models can offer.

I.2. Photovoltaic systems

Typical photovoltaic Crystalline-Silicon (c-Si) solar panels are made up of multiple solar cells, which are combined in series into solar modules. These can also be combined in series, forming a solar string, with a higher voltage but same current. Multiple strings can be combined into an array, by arranging them in parallel, keeping the voltage of the strings constant but increasing the current level (Figure 1).

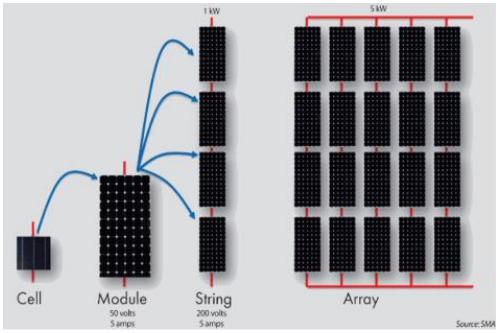

Figure 1 - PV system components (Pickerel, 2011)

This array outputs direct current (DC), which, to be fed into a local grid or to be used by ordinary AC-powered equipment, must be converted into alternate current (AC). An inverter (see section I.2.2), which is a critical balance of system (BoS) component, executes this conversion. PV installations vary greatly in size, and can be ground mounted, rooftop mounted, or wall mounted. The mounting systems may be fixed or, alternatively, use a solar tracker to keep the panels perpendicular to the sun´s rays throughout the day

Solar panels can be broken down into two major categories: crystalline solar cells and thin film solar cells. Crystalline solar cells, which account for the largest share of the market (Fraunhofer ISE, 2017), are based on silicon, and can be either monocrystalline or polycrystalline, with the former presenting higher efficiency (typically around 20%, can go up to 28%) and costs, and the latter representing most of the worldwide production, being cheaper and easier to produce, although its efficiency is quite lower (between 12% and 15%, see Tyiagi at al., (2013)). Thin film (TF) solar cells are much cheaper to produce, as they use very

[3] Measure of the total module area relative to the rooftop or ground space on which it is mounted

few materials, but have usually very low efficiencies (normally around 5%) and the materials used can be very detrimental to the environment. They include amorphous silicon (a-Si), CdTe (Cadmium Telluride, the most common), CdS (Cadmium Sulphide), CIGS (Cadmium Indium Gallium Selenide) and CIS (Copper Indium Selenide), which vary quite significantly in their properties (e.g. temperature coefficient). Since their first appearance in the 1950´s, solar cells´ efficiency have grown, thanks in part to newly developed technologies and systematic improvements in industrial manufacturing processes. For further details on this evolution, refer to Barbose & Dargouth (2016), Fraunhofer ISE (2017) and NREL (2017c).

Besides the technology choice, other factors impact the efficiency of a solar cell during operation, the most important being temperature (efficiency decreases with increase in temperature). Soiling and shading are highly impacting as well (e.g. from other buildings, chimneys, HVACs, dust or snow), as even one partly shaded module will lead to a significant loss of power in all the modules connected in series within the same circuit, all being reduced to the same power as the shaded module. These issues are partially addressed by either the use of micro inverters attached to each individual module, or the use of TF technology, which is less sensitive to thermal variations and to partial shading (Heinstein et al., 2013).

TF technologies have had very little market penetration, in part due to some misunderstandings regarding their efficiency. While under ideal lab conditions TF technology does indeed perform worse than crystalline modules, the differences might not be significant in annual energy production under real weather conditions, meaning the real life economic performance of TF can be superior to c-Si modules. This is due to the better thermal and shaded performance, and to the lower costs/m^2 outweighing the lower efficiency under certain real-life conditions (Heinstein et al., 2013).

2.1. Building Integrated Photovoltaics

PV systems used on buildings can be classified into two main groups: Building attached PVs (BAPVs) and Building integrated PVs (BIPVs). BAPVs are simply attached to the building structure, and thus do not affect any of the building´s functions. BIPVs refer to photovoltaic or solar cells that are integrated into the building envelope. They form a subsector of PV applications where PV cells replace conventional building materials with impact on the structure´s functionality and can be considered an integral part of the energy system of the building. As such they must fulfil multiple requirements in parameters such as buildability, design, durability, environmental impacts, maintenance, performance, safety standards and regulations (Biyik et al., 2017). Concerning durability, they must be able to withstand solar radiation, ambient infrared, high and low temperatures (as well as their rapid change) water, snow loads, wind, erosion, pollution, microorganisms, oxygen and time for all these factors to work (Jelle et al., 2012).

BIPV are usually implemented in new buildings (although they can also be retrofitted to existing buildings) and have an estimated life-span of 25 to 30 years. The most common application of PV integration in buildings are rack mounted PV modules on roofs (BAPVs), while other BIPV products haven't yet reached widespread distribution or application (Yang & Zou, 2016). The potential for BIPV must not be underestimated, with an average 18m^2 of roof area per capita potentially useable for photovoltaics in western Europe (IEA, 2016b).

BIPVs can be categorized according to solar cell type, application or market name, and can typically be installed as tiles, foils, modules and solar glazing products, and carry out the normal building material functions (e.g. heat insulation, noise protection, weather protection, shading modulation, electromagnetic shielding, privacy), beyond electricity generation (Heinstein et al., 2013).

Foil products are lightweight and flexible, with easy installation, few weight constraints on the underlying structure, and can be applied on roofs or façades. The solar cells are usually made from TF technology, whose disadvantages (lower efficiency than crystalline modules and not many producers with weather tight solutions (Jelle et al., 2012) can be compensated by lower temperature coefficients, better performance in shaded or partially shaded areas, and adaptability to complex geometries of existing building envelopes (Heinstein et al., 2013).

Tile products can cover part or the entirety of the roof, are normally arranged in modules with the appearance and properties of standard roof tiles and are considered a good option for retrofitting in existing buildings. Their shape varies, with products mimicking the curvature of curved ceramic tiles (usually less area effective due to the curved surface area) and others laying flat like a shale roof shingle. The highest efficiency solar tiles can reach 20% and are made of monocrystalline silicon (Jelle et al., 2012).

BIPV modules are very similar to standard PV modules, except they are made with weather resistance in mind, and can either replace part of the roof or be mounted on racks provided by the manufacturer.

Solar cell glazing products are glass with a PV substract (e.g. sprayed silicon nanoparticles), can function as a PV module, with varying degrees of opacity normally inversely related to the PV production (the more opaque the more energy produced). They provide wide-ranging options in color and transparencies (16 to 41% transparency) and can be used for windows, glass façades and glass roofs (Jelle et al., 2012).

Roof mounting accounts for 80% of BIPV installations (Shukla et al., 2017), as they are the most cost effective of all BIPV due to prime solar resource and may reduce maintenance costs of roof systems by providing protection and insulation to the underlying membranes (Eiffert & Kiss, 2000).

The remaining BIPV installations are usually on façades, due to the active and passive benefits they confer buildings, and are especially suited for higher latitudes where they achieve higher outputs (Jelle et al., 2012). For façades, one normally overlooked technology is TF, which offers high adaptability to complex geometries of the building envelope, improved low illumination performance, improved temperature coefficient (Shukla et al., 2017) and a very drastic reduction in cost relative to c-Si modules (see section I.4.1).

Less common uses for BIPV include atriums or skylights (Jesus et al., 2005), sun shades for windows, canopies, walkable floors, parking lot structures with EV charging ports, and urban furniture such as benches, tables and street lighting. A thorough review of current BIPV systems can be found in Biyik et al. (2017).

2.1.1. Barriers to BIPV

BIPV does not represent any standardized industrial product, but a whole range of applications of PV in construction, placing BIPV in a very demanding context and its full integration dependent on a complex and

tight interlocking of all stakeholders (Heinstein et al. 2013), with technology and application driven barriers to overcome.

In their extensive review of over 115 BIPV system studies Biyik et al., (2017) failed to find any comparable performance indicators, due to the lack of standardized approach to the assessments, including varied solar cell technologies, applications on the buildings, products and test conditions, leading, for example, to estimations of efficiency ranging from 5% to 18% and generation capacities from a few MWh/yr to more than 100 MWh/yr. As further discussed in section I4.2, the lack of systematic studies on this subject also lends itself to wide estimations regarding the economic benefit of building material cost offset in BIPV solutions. There is no large-scale implementation from which to draw conclusive data and the heterogeneity of technological and design choices make for poor analysis. This is a situation which may improve soon with the appearance of mass market solutions in BIPV application (e.g. Tesla´s recently announced entry into the BIPV market (Tesla, 2017)).

There is also a lack of validated prediction simulations that are required to make conscious economic decisions related to BIPV, with projects to compare BIPV performance to PV simulation estimations running over many years, with no consistency regarding input parameters to describe BIPV performance for existing PV simulation models. Simulation models specifically designed for BIPV assessment range from empirical studies (Lee et al., 2014), to detailed fluid and thermal analysis to determine performance evaluation, power generation and energy potential of the BIPV solution (Chen et al., 2012), with the most popular software suites being *TRNSYS* and *EnergyPlus* (Biyik et al., 2017).

The broadness of the BIPV concept and its still embryonic market also leads to lack of dissemination of knowledge among interested parties, namely academia, engineers, architects, builders, installers, planners politicians and the public (Jesus et al., 2005 & Heinstein et al., 2013), hampered further still by the difficulty in getting specific product properties (either because they are not available through manufacturers´ public channels or because of the very bespoke nature of their installations (Jelle et al., 2012) and the lack of databases of exemplary projects.

Beyond these technology dependent barriers, BIPV real life application is not without its drawbacks. One of the main limitations of BIPV proliferation in the urban environment is its suitability for solar power production. Limited area availability, geometric constraints leading to sub-optimal orientations of systems and complex shading and reflections in the urban 3D environment limit the attainment of full solar potential and deployment. Fully integrated roof mounted BIPV solutions still suffer from relatively low efficiency, high capital cost, low government support, inflated costs associated with customized design, poor public understanding and low competitiveness when compared with current electricity prices and traditional roof mounted PV. As for façade solutions, the existing heterogeneity of façade types and elements coupled with their early stage deployment lead to low penetration and to projects bespoke in nature, making it nearly impossible to attain standardization, and exacerbating the difficulty in generating cost estimates for these types of systems (Yang & Zou, 2016).

For both roof and façade applications, the most impacting factor in PV performance is the module temperature and as such all BIPV must account for adequate ventilation in order to guarantee a level of performance (Biyik et al., 2017), which may not always be easily achievable, in particular when retrofitting to existing infrastructure. Moreover, not all buildings can incorporate façade solutions, due to aesthetic requirements of the surrounding area (zoning laws or societal unacceptability), dimensional requirements (i.e. the space required between the façade and the existing solid wall isn´t enough for the integration), or functional requirements, namely shadow limitation, optimal orientation, compatibility with existing insulation materials or state of the local electricity grid (Biyik et al., 2017).

Beyond all the above stated, other barriers to BIPV acceleration include: immature business models, little insight on the part of producers and installers regarding the applicable regulations, certifications, requirements and specifications, environmental aspects of BIPV not being comparable to traditional building components, demonstration and testing projects are fragmented and their adaptability to various climates is still unclear (IEA, 2016b). Some of these issues are being catered to in current BIPV research, a comprehensive analysis of which can be found in Biyik et al. (2017) and Jelle et al. (2012).

2.2. Inverters

Inverters are an essential BoS component of PV systems, and convert the DC output of the PV modules into AC, to be injected into the electricity grid. For grid tied systems, the inverter also monitors the inputs and outputs to and from the utility grid, bringing power in from the utility grid when the solar cells are not producing enough, and pushing it out when production exceeds consumption.

A standard inverter (also known as a string-inverter) is a standalone box that is typically installed close to the fuse box and electricity meter, and functions in a series circuit coupled to a string of solar panels. Micro inverters perform the same basic function but are attached to each individual panel, creating a parallel circuit within the string of panels. A full characterization and list of advantages of one choice over the other can be found on Solar Reviews (2018) & Free Clean Solar (2018), the most relevant ones for this analysis being: i) cost (string inverters are cheaper, see section I.4.1); ii) yield, as micro inverters can potentially yield higher production (PV panels wired in series will cap the voltage of the system to the lowest voltage panel on the string, a particularly relevant problem for partially shaded systems or different oriented panels in the same string, circumvented for parallel system layouts made possible by the inclusion of micro inverters); and iii) warranty, as micro inverters typically have 25 year warranty while standard inverters have 10 year, meaning substitution is likely mid-way through the lifecycle of the system for string inverters. When designing a system with varying performance characteristics (for example, due to angles or shading), the underlying assumption is that micro inverters are used (Mapdwell, 2013).

I.3. PV Technical, Production and Economic Performance

Many studies and tools for estimation of PV technical potential have opted for an oversimplified calculation that incorporates available area, panel efficiency, losses and irradiance to derive PV electricity production (Defaix et al., 2012) without explicitly modeling the PV panel performance. To simulate PV system performance in detail, one must model the technical performance of the underlying components of the PV

panel (section I.3.1), the production performance throughout the year (section I.3.2), and how that affects the economics of energy production and consumption (section I.3.3). The most complete simulation methods that generate solar maps detailing the potential for PV production with varying levels of spatiotemporal resolution are reviewed in section I.3.4.

3.1. PV Technical Performance Simulation

To calculate how efficient a PV system is at converting sunlight into power, multiple technical performance models have been proposed to replicate the behavior of the system components. These are the mathematical underpinnings for some of the most popular software suites, including PVGIS, PVWatts and SAM (see European Commission, 2017, Dobos, A., 2013, Dobos, A., 2014 and Gilman, P., 2015)

When the power of a PV module is measured in the laboratory or at the factory, this is done under Standard Test Conditions (STC) which include: i) irradiance should be 1000W/m² on the whole surface of the module; ii) The module temperature should be 25°C. The power measured at STC is called the nominal power or peak power (European Comission, 2017). Any departure from these standard test conditions impacts the efficiency and thus the power output of the PV module.

3.1.1. Module Cover

When light hits the PV module surface some of it will be reflected away without entering the module, with higher losses the lower the angle of incidence (almost complete loss for parallel incidence). This can be calculated using empirical mathematical models (as described in Martin & Ruiz, 2001, Martin & Ruiz, 2013), empirical polynomial models such as the Sandia PV Array Performance Model polynomial correction (Dobos A. P., 2013), or physical transmittance models by application of Snell and Fresnel equations (Dobos, A.P., 2014 & DeSoto et al., 2006). Generally, this effect causes a loss of 2-4% of the sunlight, though this will be lower for sun-tracking PV systems (Huld & Amillo, 2015).

3.1.2. Thermal Model

Generally, the efficiency of a PV panel decreases with increasing temperature, and the strength of this effect depends on the PV technology. The module temperature calculation can be done by empirically derived formulae, as devised in Faiman (2008) or by heat transfer energy balance models (Dobos, A., 2013 & Fuentes, 1987), and accounts for POA irradiance, air temperature, wind speed, and in the case of the Fuentes model, wind speed at height of installation, dry bulb temperature and thermal capacitance of the module, enabling the conversion of Nominal Operating Cell Temperature (NOCT, the expected operating cell temperature of the cell in conditions closer to real life (PVEducation, 2018)) into INOCT (installed NOCT, see Fuentes, 1987).

3.1.3. PV Cell DC Output

For most module types, the efficiency is nearly constant for irradiances from about 400W/m^2 to at least 1000W/m^2 (for constant module temperature), but at lower irradiance the efficiency tends to decrease. Since the standard test conditions measure module power at high irradiance (1000W/m^2) and fairly low

temperature (NOCT of 25°C) the overall result is that for most places the average module efficiency is a bit lower than the efficiency measured at the factory.

To predict the power output of a solar cell, empirical models (Huld et al., 2011, Sandia PV (Gilman P. , 2015) and PVFORM (Dobos A. P., 2013)) or equivalent circuit models (Singh, G., 2013) and CEC PV Model (Gilman P. , 2015) can be used. All of them model the efficiency variations due to temperature and irradiance other than the STC conditions, as seen in Figure 2, which are the main, but not the only factors affecting DC output of a solar cell.

Sandia model is one of the most robust models available, developed by Sandia Laboratories. Based on extensive empirical analysis, for each solar panel a formula is derived to create a 5 point curve that approximates the real IV curve (current-voltage curve) of the specific PV panel model, requiring close to 30 coefficients related to, among other things, module construction and racking technique, solar spectral influences, angle of incidence effects and the irradiance dependence of electrical characteristics such as the temperature coefficients of power, voltage and current (Yates & Hibberd, 2010). This technical model is available on most PV modeling software (available in SAM, section II.1) and has been shown to predict power output to within 1% of measured power.

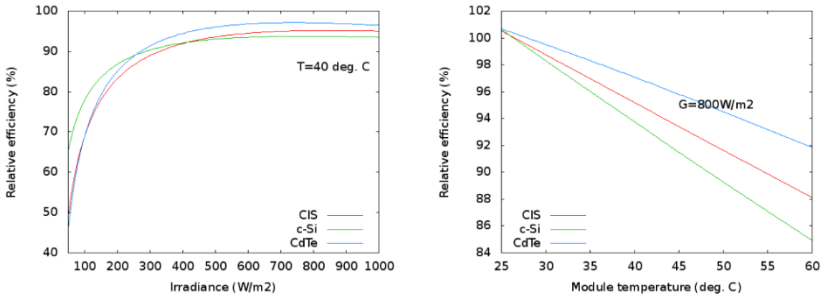

Figure 2 – Relative efficiency dependence on Irradiance and Module Temperature (European Comission, 2017)

The PVFORM model, developed by NREL, is a simplification of the Sandia model, implemented in PVWatts (NREL´s simplified PV simulator, section II.1) it calculates the power output of the system by adjusting the STC capacity rating of the array based on the POA irradiance and the cell temperature at every time-step (Yates & Hibberd, 2010).

The CEC PV model (also available in SAM, section II.1) is based on the single-diode performance model, which assumes that the behavior of a PV cell can be simulated by an equivalent circuit consisting of a current source, a diode and two or three resistors. The current source and diode represent the ideal behavior of a solar cell, and the series and shunt resistors are modeling real-world losses (e.g. current leaks). By using circuit theory, equations can be defined that describe the current and voltage characteristics of the equivalent circuit (Yates & Hibberd, 2010).

3.1.4. Inverter AC Output

An inverter´s efficiency depends on both the loading of the inverter and the input voltage of the array, meaning an accurate inverter modeling should account for power shaving due to overloading and inverter shutdowns due to input voltage being out of range.

The Sandia inverter model, as for the PV model of the same name, is based on empirically derived equations that take the DC input power and voltage and convert it to AC power output. Several coefficients

are used to derive the inverter´s equation, usually available on the manufacturer´s spec sheet. The Sandia model has been shown to be accurate to within 0.2% when compared to measured results (Yates & Hibberd, 2010). The single-point efficiency model (implemented in NREL´s PVWatts, running the PVFORM algorithm, see section II.1) specifies a conversion efficiency that is used for all operating conditions, which is an oversimplification. However, due to the flatness of the efficiency curve of inverters as a function of DC input load (Figure 3), it is an admissible one. These models are empirically derived, and are further detailed in Yates & Hibberd (2010), Dobos, A.P. (2013) and Gilman, P. (2015).

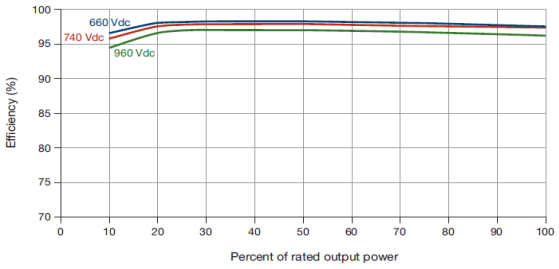

Figure 3 -Typical Inverter Efficiency as a function of DC input (Yates & Hibberd, 2010)

3.1.5. DC & AC Losses

The power output of PV panels is prone to losses that may come from multiple sources, including but not limited to (see Dobos, A.P. , 2013; Dobos A.P., 2014; Gilman, P., 2015; and Yates & Hibberd, 2010): i) inaccuracies in the model nameplate rating (usually a +/- 5% accuracy is assumed in the specified STC nameplate rating); ii) DC and AC wiring resistive losses; iii) module mismatch (no two modules are the same due to manufacturing imperfections, thus even though the inverter´s Maximum Power Point Tracker (MPPT) keeps the array at its MPP, the individual modules that constitute may not be at the MPP); iii) soiling (caused by the accumulation of particulates, such as dust, snow, pollutants and bird droppings); iv) system availability (e.g. reductions in the system's output or complete system outages for maintenance, forced outages due to grid constraints); v) diode losses (due to voltage drops across blocking diodes and electrical connections); vi) tracking errors (in the case of tracking systems when they are not able to accurately track the sun´s position); vii) shading losses (besides shades cast on the PV panels by nearby objects or the urban form, self-shading in PV panels can be significant when no backtracking[4] exists for tracking systems); viii) inverter losses (they are not 100% efficient at converting DC to AC); ix) light induced degradation of the photovoltaic cells in the first few months of operation; x) age induced degradation; and xi) transformer losses (not all power from the inverter makes it onto the grid).

There are two approaches to accounting for these losses: the most common is the use of derate factors (see Jakubiec & Reinhart, 2013; Chow et al.,2016; and Rodriguez et al., 2017), which separately or jointly account for the total loss of power caused by these multiple causes and effectively reduce the overall power output; otherwise, these losses are modeled explicitly, with equations for each loss being modeled (an example of such an approach can be found in SAM´s Photovoltaic Model (Gilman P. , 2015)).

[4] Real-time adjustment of the tilt of the modules to a suboptimal angle, whose lower incident irradiance is compensated by the diminished self-shading resulting from the new orientation (Smalley, 2015).

3.2. PV Production Simulation

PV hourly production simulation aggregates all the above models under a single roof (Figure 4). The inputs consist of: i) the solar resource (hourly irradiance and weather data); ii) the sun position (derived by knowing time of day, latitude and longitude); iii) tracking system (fixed or tracking PV array, impacting the angle of incidence of the sun´s rays at each time step); and iv) the system design (tilt, azimuth, module nameplate capacity, inverter nameplate capacity and PV type).

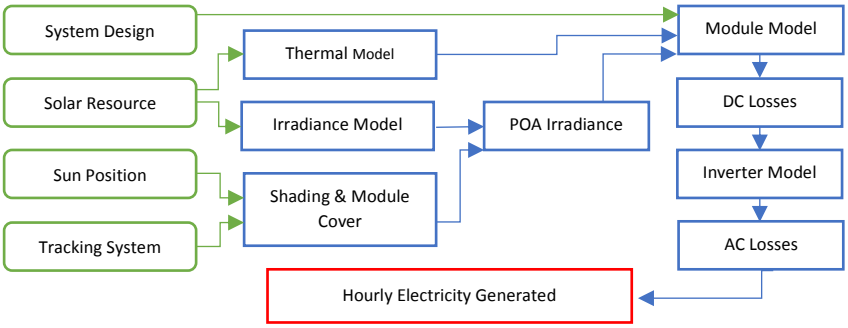

Figure 4 – Typical Steps in PV Production Simulation

These are then fed into the computation modules which will calculate the irradiance (which, for the purposes of this work, will be an input previously calculated and accounting for shading phenomena in urban settings) and the shading and module cover losses (accounting for self-shading of the PV modules, backtracking and reflected radiation losses due to angle of incidence) to derive the POA irradiance. This, together with the thermal model results is processed by the module model, simulating the performance of the PV panels to derive their DC output, which is then corrected by the appropriate DC losses. Finally, this electrical output is fed into the inverter module, which computes the final AC production in Wh/h, corrected for the appropriate AC losses, and giving us the final output of hourly electricity generated by the PV system.

Examples of PV system models include SAM, PVWatts, PVGIS, PVsyst, PV Design Pro, PVSol, PVSim, PV F-Chart, and Polysun, some of which are further detailed in section II.3.4. For a complete overview of these models see Yates & Hibberd (2010), and for an application of this methodology consult Jakubiec & Reinhart (2013) and Chow et al. (2016).

3.3. PV Economic Performance Simulation

PV Economic Performance Simulation aggregates the PV performance simulation results to project analysis inputs, enabling a life cycle economic assessment of the performance of the system and informing decision makers of the main metrics required for investment decisions (Figure 5). The inputs consist of: i) the Hourly electricity generated for the first year, derived from the previously reviewed PV production simulation (see section I.3.2); ii) the installation and operation system costs (CAPEX and OPEX, e.g. system hardware,

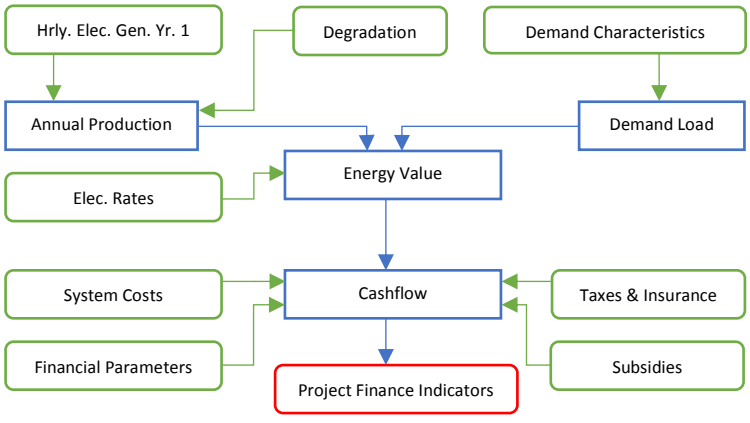

Figure 5 – Typical steps in PV economic performance simulation

labor costs, permitting, inspection, interconnection and overhead, a review of which can be found in Fu et al. (2017), and further detailed in section II2.2.1); iii) lifetime degradation (reflecting the decrease in output of the PV system throughout its lifetime due to physical degradation); iv) financial parameters (predicted lifetime of the system, loan parameters (e.g. debt percentage and interest), inflation, applicable discount rate); v) taxation and insurance rates (applicable to the project throughout its lifetime); vi) subsidies (a common feature of renewable energy projects, which can be the recipients of cash incentives, accelerated depreciation schedules, tax reductions and/or exemptions); vii) electricity demand characteristics (in case the PV system output is used to satisfy local demand); and viii) electricity rates (to calculate the monetary value of electricity bought from and sold to the grid).

Inputs i) and iii) are fed into the Annual Production module (that will calculate hourly annual PV production profiles for each year of the system´s lifetime) and input vii) is used by Demand Load module (to estimate an hourly annual load profile of consumption, in case one isn´t provided). The results of these two modules are joined with input viii) to calculate Annual Energy Value (reflecting the annual income from electricity sales and/or the savings accrued from the demand load shift from grid electricity to self-consumption over the life time of the project). Finally, these annual values, along with the remaining four inputs, are processed in a Project Cash Flow analysis from which one can then derive the outputs (e.g. project finance indicators such as Payback Period, Net Present Value (NPV), Internal Rate of Return (IRR) and LCOE).

Methodologies for PV and BIPV economic performance assessment are further discussed in Short et al. (1995), Eiffert & Thompson (2000), Eiffert (2003), and Brown et al. (2016), with application examples found in Bortolini et al. (2014); Fath et al. (2015); Lang et al. (2016); Pereira et al. (2016b); Lazard (2017); and Fu et al. (2017).

3.3.1. Project Finance Indicators

When analyzing a project for an energy producing system, the most commonly used tool of economic analysis is cash flow analysis, enabling cost assessment throughout the lifetime of the project, and estimation of the relevant indicators such as NPV (Net Present Value, the excess discounted cash flow (positive or negative) for the lifetime of the project, indicates value of the investment), IRR (Internal Rate of Return, the annualized effective compounded return rate, indicates the yield of the investment and can be used to compared to alternative investments) and Payback Period (period of time required for the yearly revenues to make up for the original investment). In the reviewed literature, most assessments are high level, without accounting for site-specific legal and fiscal framework for PV projects. For applications and definitions of these indicators and methodologies, see Jakubiec & Reinhart (2013), Bortolini et al., (2014), Fath et al., (2015), Pereira et al., (2016a), Fu et al., (2017) & Lazard (2017).

Specific to energy producing systems, another metric is usually calculated, the LCOE (Levelized Cost of Energy). It can be used to compare different electricity generation sources and is an economic assessment of total average expenditure to build and operate a power generating asset over its life time, divided by the expected total energy generation in that timeframe, yielding a €/MWh figure. It can also be regarded as the average minimum cost at which the energy generated must be sold in order to

break even over the project´s lifetime and is the main metric for assessing competitiveness of an energy producing project, by comparing alternative solutions´ LCOE. While not perfect, it incorporates many other PV metrics important to the energy costs beyond upfront installation costs (Fu et al.,2017), accounting for the electricity produced over the lifetime of the project, initial investment (CAPEX) and operational and maintenance costs (OPEX) throughout the life-cycle, according to Equation (1) (Pereira et al., 2016b):

$$LCOE = \frac{\sum_{t=1}^{n} \frac{I_t + M_t + B_t}{(1+r)^t}}{\sum_{t=1}^{n} \frac{E_t}{(1+r)^t}} \quad (1)$$

n - system lifetime [years]; r - discount rate [%]; It – Initial investment at t=1, or replacement cost in specific year (CAPEX); Mt – Operation and Maintenance costs (OPEX) in year t; Bt – Auxiliary power cost in year t; Et – Energy Produced in year t

One can´t compare LCOE directly to the market price[5], only between projects (see Lazard (2017)). A key variable to keep in mind when comparing LCOE is the impact of the availability and cost of capital. In Lazard (2017), their analysis shows that a +3.8% increase in WACC can result in a +37% in average LCOE for rooftop residential systems, demonstrating the high sensitivity of this indicator to financing conditions.

3.4. Review of PV Technical, Production and Financial Performance Models

The most complete simulation methods to estimate PV technical and economic performance start out by generating a solar map, detailing the potential for PV production with varying levels of spatiotemporal resolution, then combine this information with technical and economic variables specific to photovoltaic performance, enabling analysis of bespoke PV solutions for a certain area or building, while detailing the costs and savings associated with it. Making it web-based (web-based solar maps) and user-friendly allows for a wider audience (e.g. residents, business owners. urban & energy planners and decision makers) to analyze the potential for solar PV, facilitating the proliferation of distributed renewable energy generation (Dean et al., 2009).

The most common output data from web-based solar mapping tools include technical properties of the system (type, model, size, etc.), electricity production, installed cost, financial indicators, environmental indicators, links to local suppliers and installers of PV solutions, information on how to be eligible and capture local incentives and educational resources for further understanding of the technology (Dean et al., 2009).

Reviewing the literature it is clear that there are a series of common issues with current modeling tools of urban solar PV potential, including (see Chow et al., 2016, and Freitas et al., 2015) : i) a lack of generalizable, unified and comprehensive approach; ii) inefficient modeling approaches; iii) lack of information sources for high level of detail (LoD) leading to high computational times to accurately estimate solar energy potential at high spatiotemporal detail; iv) differing levels of accuracy among the several layers of input data; v) spatial detail and temporal resolution mismatch compromising the results; and vi)

[5] The resulting price from a merit-order supply stack curve in each time step, with the market price being the cost to call upon the last, most expensive generation source required to enter the supply curve at any given moment.

differences in accuracy of between interpolation of ground based measurements and satellite derived data (LiDAR data presents particular limitations, beyond possible obsolescence and outdating, in particular in façades due to the relative proximity and the multi-path effects of LiDAR surveys).

Also representations come with multiple caveats namely (see Freitas et al., 2015): i) some radiation models adopt an isotropic representation of diffuse and reflected radiation, as a compromise between acceptable results and reasonable computation time (even though it is established that an anisotropic representation is more accurate); ii) the representation of surfaces is heterogeneous as some models don't even consider slope or aspect, and others consider flat surfaces, ignoring chimneys, HVACs and other structures; iii) the representation of windows is lacking in most models, which would require either photogrammetric methods or local assessment for particular façades; and iv) representation of trees is often done as solid shadow casters instead of translucid.

Problems specific to the PV part of the model include (see Freitas et al., 2015): i) the conversion of solar radiation into PV output requires accounting for ambient and/or module temperature, and the latter is often assumed to be the same as the former; ii) PV installation requirements and regulatory limitations are usually unaccounted for leading to a mismatch between estimated usable areas for PV systems and real life useable areas; and iii) validation procedures for the models are lacking, as they present quite a challenge, particularly in an urban setting, requiring a great amount of case studies due to the complexity and technology dependent phenomena involved (there aren't many measurement systems (pyranometers) in cities, and not many PV or BIPV systems installed to serve as reference data).

General methodologies to evaluate specific PV solutions with the tools developed for large-scale assessments are lacking, presenting wide ranging possibilities for the refinement and adaptation of these tools for more detailed and site-specific assessments, of more relevance for individuals evaluating investment opportunities. An extensive review of commercially available web-based solar mapping tools was undertaken, which included: Mapdwell, PVGIS, PVWatts, SAM, CH2M Hill, RET Screen, Solargis and HOMER, the most relevant of which being the first four.

PVGIS is an online free solar photovoltaic energy calculator for stand-alone or connected to grid PV systems and provides a large and accurate solar radiation database for Europe, Africa, the Mediterranean basin and South-West Asia. It calculates solar radiation including terrain shadowing losses for each location and can simulate PV panel operation (see Freitas et al., 2015 and Psomopoulos et al., 2015). PVWatts and PVSAM (whose details are further explored in section II.1) add a financial model to the analysis, providing a more detailed PV production, more modularity and detail than any other free option in the market. They still ignore the impacts of the urban fabric on irradiation but provide multiple project and finance structures to choose from, making them versatile and accurate tools. Mapdwell Solarsystem brings it all together with the GIS database, detailing the rooftop morphology, structures, existing systems and tree foliage (based on LiDAR and GIS data) on a map along with the respective yearly irradiation. On this map the user can size and design his PV system and financing details for a specific rooftop, returning financial, technical and environmental information (Mapdwell, 2013). The full access to this tool is paid, with a limited trial version

available upon sign-up. While it is beyond the scope of this dissertation to analyze all of the available PV production and economic modeling tools, in depth comparisons can be found in Dean et al. (2009); Yates & Hibberd (2010); Kuiper et al. (2013); Psomopoulos et al., (2015); and Freitas et al., (2015).

I.4. Cost of PV and BIPV – Evolution and Assessment

Since the 1980's the price of PV modules in the world has dropped drastically (Yang & Zou, 2016). Throughout the last 20 years there has been a steep decrease in module costs, to less than a fifth of their cost in the mid 90´s (EPIA, 2011) with marked declines between 2009 and 2012, spurred by reductions in global PV module prices mainly due to over production and price dumping in the Far East (Heinstein et al., 2013), sustained since through reductions in non-module costs. These include BoS (balance of system) hardware costs (inverter and racking system price decreases) and soft costs such as increased module efficiency and system size, marketing and customer acquisition, system design, installation labor, permitting and inspection costs, installer margins and widespread policy and industry efforts aimed at reducing soft costs (Barbose & Darghouth, 2016).

Table 1 – Relative weight of cost categories for residential PV system in Q1 2017 in the U.S.A. (Fu et al.,2017)

Installation Cost	Module	Hard Costs	12.50%	64.30%
	Inverter		6.80%	
	Structural BoS		3.90%	
	Electrical BoS		8.60%	
	Supply Chain	Soft Costs	15%	
	Sales Tax		3.20%	
	Installation Labor		10.70%	
	Permitting, Inspection and Interconnection		3.60%	
Other Costs	Sales and Marketing (customer acquisition)		12.13%	35.70%
	Overhead(General and Admin)		11.07%	
	Net Profit		12.50%	

Fu et al. (2017) computed the US national benchmark breakdown in Q1 2017 for all cost categories in the residential PV sector, weighted to reflect the market share of various inverter options available and types of installers in the market. They arrived at an average estimated installed cost of residential PV systems of 2.8$/W (Figure 6), with the relative weight of each cost category presented in Table 1, with hard costs accounting for 31.8% of total installed system cost.

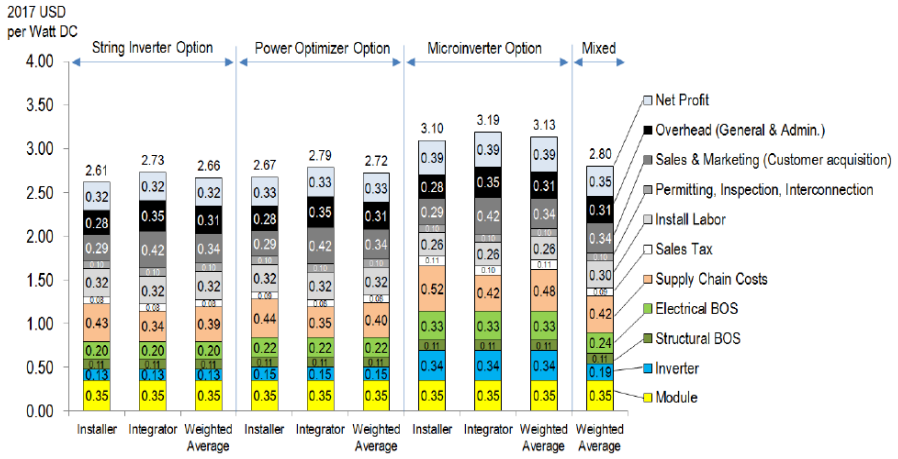

Figure 6 – Cost breakdown for residential PV system installed cost in Q1 2017 in the U.S.A. (Fu et al.,2017)

4.1. Variations in installed system cost

Installed costs vary quite significantly from country to country, as do the relative weights of each cost category. This can largely be attributed to soft costs (as hardware costs, with the exception of USA and Japan (IEA, 2017), are quite uniform across countries) but is also influenced by different deployment scales, solar industry business models, customer awareness, incentive levels and design, building architecture, system sizing and design, interconnection standards, labor wages and permitting and interconnection process (Barbose & Darghouth, 2016). In the case of Portugal, IEA (2017) reports a 2.43$/W ([6]2.2€/W) residential installed system price (excluding VAT) in 2016, with hard costs accounting for 77.39% of total installed system cost (Table 2), which is a significant difference when compared to the USA but is very much in line with reported figures throughout most of the European Union (IEA, 2017). A summary market research of Portuguese PV Kit suppliers in 2018 (Table 3) reveals this estimate to be a bit on the conservative side, with reported hard costs from these suppliers consistently below this estimate[7]. As it is beyond the scope of this dissertation to ascertain the current actual cost of PV kits in the Portuguese market, the more conservative IEA estimate will be used.

Table 2 – Relative weight of installed cost in 2016 for a grid-connected residential PV system in Portugal (adapted from IEA (2017))

Installation Cost*	Module	Hard Costs	45.37%
	Inverter		16.01%
	Structural BoS		16.01%
	Electrical BoS		
	Supply Chain	Soft Costs	22.61%
	Installation Labor		
	Permitting, Inspection and Interconnection		
Other Costs	Sales and Marketing (customer acquisition)		
	Overhead(General and Admin)		
	Net Profit		

*Not including VAT

Table 3 – Summary analysis of prices (€/W_{DC}) of PV Kit suppliers in Portugal in 2018

	Installed cost (no VAT)	Hard costs (77.39%)	Hard costs (+VAT)	Source
Portugal 2016	2.20	1.70	2.09	(IEA,2017)
	Min Hard Costs (+VAT)	Max Hard Costs (+VAT)	Avg. Hard Costs (+VAT)	
Futursolutions	1.97	2.26	2.06	(Futursolutions, 2018)
Sunenergy	1.73	2.20	1.93	(Sunenergy, 2018)
Boa Energia	1.43	1.97	1.69	(Boa energia, 2018)

The cost structure also can vary significantly depending on the inverter option. From Figure 6 one can see that, relative to the weighted scenario, opting for micro inverters leads to an average installed cost increase of 0.33$/$W_{DC}$, an 11.8% increase in overall cost, most of it due to micro inverters being approximately 2.6 times more expensive than the string option. The opposite is true for string inverters, reflected in a -0.14$/$W_{DC}$, or -5% cost decrease over the weighted scenario.

Another way residential PV costs can vary is whether the installation is a retrofit or new construction.

On one hand, systems in new construction tend to be quite small, have a much higher incidence of premium efficiency modules and BIPV, and are frequently installed in new housing developments with multiple solar homes, benefiting from economies of scale, reduced unit costs resulting from bulk purchases and

[6] Using IEA (2017) implicit assumption of 1€=1.1045$ exchange rate for 2016

[7] This might be for several reasons, including price decreases between 2016 and 2018, reported costs by the companies being below real installed cost, or simply the small sample analyzed.

economies of scope, with shared costs of certain labor and materials shared between multiple PV installations.

Following an analysis of residential installations in California in 2016 (Barbose & Darghouth, 2016), these countervailing tendencies play out in favor of new installations, with economies of scope and scale offering substantial savings on PV system pricing, and new systems consistently priced below the retrofit systems. Irrespective of technical characteristics, new construction systems offer a median cost differential of 0.5$/W (-11.36%) over their retrofit equivalents in 2015, this difference widening to 0.8$/W (-16.67%) if considering premium efficiency installations only.

Looking specifically at the differences between module efficiencies, one finds that premium module installations have cost benefits deriving from reduced number of modules to reach a certain system size (and related decrease in racking and mounting hardware, foundation, BoS, overhead and labor costs (Fu et al.,2017), outweighing the average 0.35$/W increase in hard costs over standard efficiency (Barbose & Darghouth, 2016), resulting in a median cost decrease of 0.6$/W (-13.33%) for residential premium installations.

Installed system costs for TF applications can be found in Horowitz et al. (2017), and, for CdTe technology (which will be used as the reference TF technology for this analysis, see section II2.1.1.1), they are in the range of 1.3$/$W_{DC}$ ([6]1.18€/W), of which 0.4€/W_{DC} is the TF module cost[8].

From these comparisons, and admitting they are representative of a worldwide phenomenon, one can infer that the corresponding reductions in installed system prices for Portugal would be the ones in Table 4

Table 4 - Calculated Installed cost metrics for PV in Portugal in 2016

PT Installed System Cost [€/W]						
Standard; Source: IEA (2017)				**Premium and New Construction**; Source: Barbose & Darghouth (2016)		
Total Installed System Cost in 2016	Module Cost (45.37%)	Inverter Cost (16.01%)	BoS Cost (16.01%)	Premium vs. Standard (-13.33%)	New Construction vs. Retrofit (-11.36%)	Premium and New Construction vs. Median (-16.67%)
2.2	1.00	0.35	0.35	1.91	1.95	1.83
Thinfilm; Source: Heinstein, et al.(2013) & Horowitz, et al. (2017)				**Inverters**; Source: Fu, et al. (2017)		
Total Thinfilm installed system cost		Thinfilm module cost		Weighted scenario (IEA, 2017)	Microinverter vs. mixed case (+11.8%)	String inverter vs. mixed case (-5%)
1.18		0.40		2.2	2.46	2.09

4.2. Cost of BIPV systems

The sustained price decrease in PV modules discussed above led to a corresponding decrease in the price of BIPV solutions (Yang & Zou, 2016). However, in the case of BIPV solutions, the costs of vary wildly depending on size, location, customer type, BIPV type and technical specifications. The cost components, like for standard PV systems, can be broken down into 4: manufacture of the PV module, transport, installation (mainly BoS costs) and maintenance (mainly inverter replacement cost). The potential cost

[8] Thin film modules are between 20% to 33% the cost/m^2 of standard c-Si modules (Heinstein et al., 2013). Knowing the cost/W (Table 4), average area and STC nameplate capacity for standard c-Si modules (see Table 7 in section II2.1.1.1), allows the estimation of a cost/m^2 of 152.7€/m^2 for c-Si, thus an average of 40.46€/m^2 for TF modules (26.5% the cost/m^2 of standard c-Si modules); from the area and STC values for TF in Table 7 one can then derive the cost/W of 0.4€/W_{DC} for TF modules

advantage of BIPV over PV mainly stems from eliminating some module-mounting hardware and the cost offset from substituting traditional building materials, which still results in installed prices of BIPV systems being higher than traditional PV (James et al.,2011).

In their summary of existing BIPV projects worldwide, Yang & Zou (2016) analyzed the few studies that exist breaking down these cost components but found them to differ so widely in their estimates as to be of little use. The most they could state is that the price of the module is between 43 to 77% of the total, BoS costs around 15% and maintenance around 10%, with the rest being attributed to transport, monitoring and installation (approximately 2 to 5% marginal extra installation cost over conventional cladding materials (Eiffert P. , 2003).

As an example of this variation, estimates for façade BIPV cost increase over traditional materials range from 33%[9] more (Koinegg et al., 2013) to 75% more[10] (ISSOL, 2016). These comparisons are very limited in their usefulness, as barely any information about system design, upfront costs and life cycle costs and benefits is provided. Importantly, the omission of avoided costs (stemming from self-generation) and sales to the grid (in the case of excess production) make these estimates poor indicators. Yang & Zou (2016) also found insignificant correlation between the lump sum costs involved and energy transferring capacity of BIPV solutions, in good part due to the wide cost variations in these solutions. To further complicate matters, economic viability of BIPV systems should not be assessed on a stand-alone basis but should account for reduced externalities (namely reduction in transmission losses and land use), and potential increases in operational costs of the distribution grid from the intermittent behavior of distributed generation. From the conducted research only one report was found systematically comparing BIPV installed costs with their BAPV alternative and quantifying the material cost offsets of replacing building materials (James et al., 2011), but it is specific to the US market and suffers from some of the deficiencies previously stated. What can be said is that, given that they are usually more expensive than the standard alternatives, the long-term electricity bill reductions must be accounted for to truly reflect the final cost of the solutions. More research should be conducted to derive comprehensive cost profiles for different BIPV solutions.

I.5. Support schemes and legal framework for PV and BIPV systems

There is a slew of government sponsored measures which can significantly impact the economics and thus the diffusion of PV and BIPV technology. Of these, the most important are Feed-in-Tariffs (FiT), which remunerate producers for power sold to the electricity grid at a predefined price and guaranteed for a fixed period (IEA, 2017). They can be divided into two types: Gross FiT and Net Fit (Yang & Zou, 2016).

Gross FiT systems allow for the sale of all the electricity produced into the grid, usually at a higher price than regular retail rates. The solar power system is connected in such a way that all the solar power produced is fed through the electricity meter before any in-house consumption and injected into the grid (GCSPS, 2011). The buildings´ consumption is drawn from the grid as usual, and the net gain for the

[9] Koinegg et al. (2013) estimate BIPV façade materials at 800$/m^2 vs. ceramic or glass alternatives at around 600$/m^2

[10] ISSOL (2016) states a 150$/m^2 cost increase for inserting PV technology in traditional isolated double glazing, priced at 200$/m^2

producer/end-user will be the total energy produced at the FiT rate subtracted by the total electricity consumed at the retail rate. These FiT are usually the most cost effective for PV systems, even though they impose a strain on the local grid, which can drive up grid operation costs.

Net FiT systems only allow the sale of surplus power into the grid, with the solar power system connected in such a way that the power produced feeds directly into the switchboard and is used in the building. If the consumption at any given instant is above the solar power being produced, the difference is drawn from the grid as usual. If the solar power produced exceeds the consumption at any given time, then that surplus is sent back through the electricity meter and onto the grid (GCSPS, 2011). Net FiT systems are preferable from a systems-wide perspective, as they only inject into the grid in case of surplus production, greatly reducing grid strain and system costs, even though they usually lower cost effectiveness of the PV system and the revenue for the end user (Yang & Zou, 2016). Net FiT systems can be broken down into net metering and net billing policies, whose main difference is the valuation of energy fed into the grid. Net metering monthly payments depend on the total energy injected on the grid (excess generation being the difference between the system´s total monthly generation and total monthly load, usually with value pegged to the retail electricity rate); net billing assesses the excess generation with higher granularity (excess generation being the sum of hourly (or sub-hourly) differences between generation and load) and sometimes assumes hourly rates unrelated to the retail electricity rate. The value of excess generation can have a significant impact on the design and economic valuation of distributed energy systems, and currently a wide variety of policies are in place worldwide that integrate elements of net billing, net metering or gross FiT (or hybrids of these policies), sometimes with inconsistencies in the terms used to define them, making detailed analysis of tariff structures necessary in order to understand underlying policy objectives and outcomes (Couture et al., 2015).

Beyond the use of FiTs, governments have resorted mainly to renewable energy credits and tax credits. The former provides end users with a cash payment based on the type and size of the system installed, reducing upfront costs and effectively providing a rebate on the cost of the system. The latter allow for an increased rate of depreciation on the asset, lowering loan repayments, reducing property taxes and sales taxes, thus impacting more on the long-term costs of the system (Yang & Zou, 2016). Very little BIPV specific FiT systems are in place currently, with most of these incentives being geared toward the more established large-scale PV and rooftop BAPV solar systems.

5.1. Support schemes and legal framework in Portugal

Historically, the world´s PV market drivers, have been mainly from direct subsidies, tax breaks, or FiT (IEA, 2017), of which Portugal is no exception, with its support mechanisms based on FiT, tax benefits and small level of investment subsidies (IEA, 2016a). The currently applicable law is the DL 153/2014 (DR, 2014), amending previously published decrees to bring the FiTs in line with the new reality of renewable generation, and to stimulate the self-consumption sector. A detailed overview of the UP regime is presented in Appendix I, and the step-by-step process for the licensing and installation of UPAC and UPP can be found in Solar (2017) and Solar (2017b).

II Conceptual Model

With one of the stated aims of the study being the determination of urban technical and economic potential of residential PV solutions, the structure proposed by Freitas et al. (2015) for assessment of solar potential can be adapted as follows:

- Input Data
  - 3DGIS/CIM model of the study area (see section II.3.1)
  - Irradiance, shading and meteorological model for the study area (see section II.3.2)
- Interface
  - User query and manipulation of the 3D model and irradiance data (see section II.4.1)
  - Software Interface Development (see section II.4.2)
  - Online platform (see section II.4.2)
- PV Technical, Production and Economic Performance Simulator
  - PV system design parameters (see section II.2.1)
  - Technical and Production performance modeling (see section II.2.1.3)
  - Economic performance modeling (see section II.2.2)

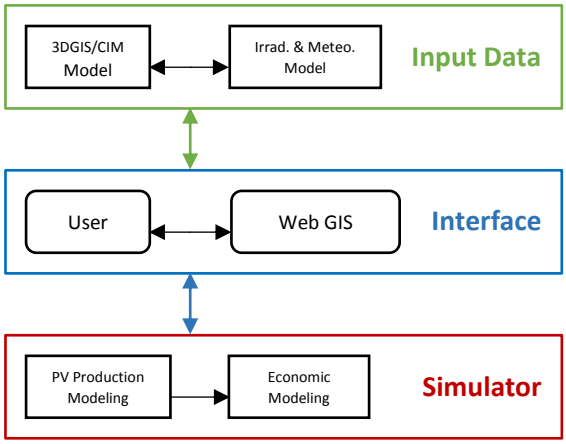

Figure 7 – Conceptual model structure

This approach is schematically represented in Figure 7. In the next sections an overview of each of these steps is provided, characterizing the choice of software, inputs and calculations for the production and economic modeling (see section II.1 and II.2), the external input data (see section II.3), and final solutions for the implementation of the interface and simulator (see section II.4 and II.5).

II.1. PV Technical, Production and Economic Performance Model

As previously stated, the technical and economic performance of a user designed PV system must be evaluated, so the main criteria for the software choice focused on the ability to run detailed simulations that accounted for the complexity of PV panel performance and the economic variables that impact its profitability.

Following the review in section I.3, NREL´s SAM software development suite was chosen (version 2017.1.17 was used throughout this dissertation). Since, for the purposes of this study, both the irradiance and 3D representation were handled by other researchers and are viewed as ready-to-use inputs for this analysis, focus will be drawn on the PV system production and economic performance. Details on the system specifications and SAM Development Kit can be found in Appendix II.

1.1. Technical & Production Performance Model – PVWatts and PVSAM

Within SAM, two approaches are used for flat plate PV modeling, respectively named PVWatts and Detailed Flat Plate PV model (PVSAM), thoroughly compared in Blair & Dobos (2013).

PVWatts (referred to in the SSC as *pvwatts*), besides being available within SAM, is also a tool freely available online, and estimates the energy production and cost of energy of grid-connected PV energy systems throughout the world. It allows homeowners, small building owners, installers and manufacturers to easily develop reasonable estimates of the performance of potential PV installations. For selected locations or user provided weather files, it calculates the solar radiation incident on the PV array and the PV cell temperature for every hour of the day, and with simple input design details (e.g. nameplate sizing, DC to AC ratio, orientation and tracking), it calculates plane-of-array irradiation, module temperature, applies the PVFORM model for DC and AC output (corrected for different temperature coefficients dependent on PV panel type), shading losses, angular incidence losses and estimated production losses (accounted for by an aggregate derate factor). PVWatts has long been the default production-modeling tool of the US PV industry and its strength lies in its simplicity by dropping a significant level of user control and parametrization (Yates & Hibberd, 2010). Because of the simplifications and assumptions behind PVWatts, the results from a simulation should be interpreted as a representative estimate for a similar system, operating yearlong under typical weather conditions. According to Dobos, A.P. (2014), for long term typical meteorological data, errors may be as high as +/-10% for annual energy totals and +/- 30% for monthly totals. For a specific year, actual performance can deviate from the long-term average up to +/-20% for annual energy and +/- 40% for monthly values.

PVSAM (referred to in the SSC as *pvsam*) is a more advanced PV production model developed by NREL and Sandia Laboratories, only available within SAM, requiring a highly detailed input of system parameters and providing extended simulation options for the various steps of a PV module production assessment. This includes: i) weather file (from a database or user-supplied) with albedo specifications and choice of sky diffuse model to be employed; ii) system design parameters, including sizing, configuration of modules, inverters and subarrays, mounting options, tracking, orientation and voltage mismatch calculation; iii) multiple calculation methods for DC power production (CEC, Sandia and Single Diode models, with temperature correction method); iv) AC power output with the Sandia inverter model or the Part Load Curve model (or specific modules and inverters from the CEC database); v) composite derate factors pre and post-inverter to account for system losses (including explicitly modeled losses due to irradiance, DC and AC wiring, tracking error, transformer and curtailment); and vi) shading losses for every hour of every month with a 3D external shade calculator (accounting for self-shading and backtracking effects).

The differences in the approach that each model employs are made explicit by going over the number of input and output variables being fed in and out of each model, which one can analyze in detail through the SDK Tool. From Table 5 one can see *pvsam* requires a lot more inputs from the user, necessitating a knowledge base much wider and limiting its potential use by a larger audience.

Table 5 - Number of Input & Output Variables in Each PV Model

	pvsam	pvwattsv1	pvwatts5
# of Input Variables	356	33	18
# of Output Variables	273	29	35

As an example, while *pvwatts* uses system capacity (commonly referred to as nominal plate capacity) as a direct input into the calculations, *pvsam* explicitly asks the user to design the PV system, requiring module type, number of modules, modules per string (or array) and then number of strings in parallel, just to calculate the power rating of the DC system input.

If that were to be implemented for this analysis, it would mean that for every rooftop or façade, just to determine system capacity, one would have to calculate the total area available for installation, from there derive the number of PV modules that could be placed (dependent on module type and installation constraints, type of building structure, and other factors) and specify the layout of such a system.

Comparing the results of *pvsam* and *pvwatts* modules, Blair & Dobos (2013) found them to predict total monthly AC output values to within 2% of each other (if using an updated derate factor in PVWatts, see section II.2.1.1.1). When compared to measured output of c-Si PV arrays (mono and polycrystalline), both PVSAM and PVWatts presented modeled results within reasonable agreement (within 5 and 11% of the measured output respectively). However, this wasn´t the case for thin film modules, which showed significant disagreement between models and differences nearing 14% being observed, which indicates the need for caution when using the output for thin film simulations.

Given the spirit of this research, and the widespread use of *pvwatts* even by some of the most popular PV performance platforms, *pvwatts* was chosen as the technical and production performance model for this dissertation.

1.2. Economic Performance Model

In addition to its production-modeling capabilities, SAM puts an emphasis on analyzing the financials involved in PV project development, providing multiple financial models to estimate project cash flow. While developed with the US market in mind, these models capture the essentials of the cash flow analysis required for any energy project, namely the value of the electricity generated, cost of installation, operation and maintenance incentives, taxes and financing structure. They can be used to calculate multiple financial metrics, including the LCOE, electricity costs with and without the system, savings, debt payments, NPV, payback period and IRR. The main types of projects represented are residential and commercial projects (that displace power purchases from the grid and buy and sell electricity at retail rates) and PPA projects (usually utility scale), that sell electricity at wholesale rates to meet IRR requirements. For the purposes of this analysis, the interest will be on the residential financial model, with the assumptions that the project buys and sells electricity, can be financed by a mix of loan or cash payment, and that the project recovers its costs by displacing consumption from the grid and selling electricity to it, with metrics calculated at the

project level assuming a single entity develops, owns and operates the project. Following up on the structure laid out in section I3.3, determination of a load profile, produced energy value and a cashflow analysis is required, calculated by SAM´s inbuilt modules, respectively referred to in the SSC as *belpe* (building electricity load profile estimator), *utilityrate5* and *cashloan*.

The hourly load profile for one year can be estimated in two ways, either by providing hourly load shape for a whole year (if available), and then scaling it to monthly utility bill consumption, or by using the inbuilt *belpe* module, and providing monthly aggregate consumptions for one year and basic building energy parameters such as building square footage, occupancy, type and number of appliances and temperature settings, coupled with weather parameters from a weather file. The *belpe* module is an adaptation of a reduced order, simplified heat balance thermal network RC model (specifically, a 3R3C), whose details can be found in Gilman, P. (2018).

The produced energy value module (*utilityrate5*), assumes all energy produced by the system goes towards reducing the building´s electricity consumption, and its settings determine how SAM calculates the monthly electricity bill and the savings from the energy produced by the system. Rate structure features that can be modeled include: i) monthly fixed or minimum charges; ii) time of use (TOU, dependent on time of consumption), and tiered (dependent on total monthly consumption) energy rates (in €/kwh); iii) fixed, TOU or tiered demand rates (in €/kW, dependent on contracted capacity); and iv) annual rate escalation to simulate price increases from the retailer in year 2 onwards, in addition to inflation. Excess generation compensation can be accounted for by net metering, net billing and FiT structures[11], whose calculation methods represent the majority of typical incentive policies around the world. The electricity bill calculation does not affect LCOE (LCOE only accounts for the cost of installing and operating the system, not the cost of energy supply to the building), but it does affect the project´s NPV, Payback period and net savings. The output of this model is the yearly value of the energy produced by the system over its lifetime, and as such it requires the specification of other technical and financial parameters such as analysis period, inflation rate, degradation rate, load escalation and rate escalation that reflect yearly changes in the inputs for its calculations.

The after tax cash flow is calculated with the *cashloan* module, which besides the load and electricity rate calculations of the previous modules, takes the following as inputs: i) system costs, including installation and operation and maintenance costs for the system; ii) financial parameters, including loan (type, rate, period and debt percentage), inflation, discount, tax, and insurance rates; and iii) incentives (tax credits and cash incentives). The outputs from the *cashloan* module includes the LCOE, which accounts for the installation and operation costs of energy production (inclusive of tax, debt costs, and incentives), the NPV of the after-tax cash flow, and the payback period.

[11] These three incentive structures are described in SAM slightly differently than in section I.5, another indication of the inconsistencies surrounding these definitions (as mentioned in Couture et al., 2015) depending on the country, regulation and jurisdiction. In this case, net-metering assumes excess generation to be difference between total monthly cumulative production minus load, net-billing assumes it to be the sum of hourly differences between generation and load and FiT just assumes all energy is sold at a sell rate (FiT) and all energy consumed is bought at a buy rate.

II.2. Architecture

In this section the specific requirements for the application of the models chosen in sections I.1.1 & I.1.2 (see sections II.2.1 and II.2.2) are detailed.

2.1. PV Watts

2.1.1. PVWatts Versions

Having opted for the *pvwatts* module to run the PV performance simulations, it was noted early on that the latest update to the PVWatts module (*pvwattsv5*) does not take user defined POA irradiance values, only allowing for the input of weather data (DNI and DHI) and calculating its own POA values using the Perez algorithm. That was brought to the attention of the SAM development team, who stated that it was an oversight and would be included in future versions of the *pvwattsv5* module (see SDK Forum, 2017), and suggested using the *pvsamv1* module for the computations, which as noted in section II.1.1, would place undue burden on the user.

The workaround was to use the older *pvwattsv1* compute module, which does take user defined POA values and adheres to the same modeling structure as *pvwattsv5*, with some key differences (an overview of which can be found in Dobos, A.P. 2014). The result is that *pvwattsv5* when compared to *pvwattsv1* for fixed tilt systems, predicts between 9.8% and 10.9% more annual AC energy output and, when both are compared to measured data, *pvwattsv5* on average under predicts output by a mere 1.8%, while for *pvwattsv1* that value is 11.9%, and close to 18% in the case of thin film technology (Dobos A. P., 2014).

To try and compensate for this and bring the output of *pvwattsv1* as close to the updated *pvwattsv5*, a thorough examination of the changes between the versions was undertaken (see section II.2.1.1.1) in order to alter the input parameters accordingly and try to reflect, as best as possible, the *pvwattsv5* performance and assumptions while running the *pvwattsv1* compute module.

2.1.1.1. Key adaptations between PVWatts Version 1 and Version 5

The adaptations to the approach of using *pvwattsv1* (v1) that were made to best reflect the *pvwattsv5* (v5) assumptions and improvements are as stated below (numbered 1 through 10) and stem from the relevant differences between the two versions, as stated in Dobos (2014):

1) Option to select Standard, Premium or Thin film PV module type

In *pvwattsv5* the user can select 3 different types of PV modules, enabling the distinction between common technology options without posing undue technical burden on the end user. This is a useful and necessary feature for this dissertation and required access to the CEC Database (available as a *.csv* file in the *libraries* folder which can be found within the folder created upon installation of the Desktop version of SAM v. 2017.1.17) in order to replicate as best as possible the categories used in *pvwattsv5,* derived by NREL by analyzing the same database of 11.000 modules, and presented in Table 6.

Table 6 - Assumptions for different module types (Dobos A. P., 2014)

Module Type	Efficiency	Cover Type	Temperature Coefficient
Standard	~15%	Glass	-0.47 %/ºC
Premium	~19%	Anti-reflective	-0.35 %/ºC
Thin Film	~10%	Glass	-0.20 %/ºC

The standard option represents typical poly or mono-crystalline silicon modules, with efficiencies in the range of 14-17%, is appropriate for typical preliminary analyses and is most like *pvwattsv1* assumptions. The premium option is appropriate for modeling high efficiency (~18-20%) monocrystalline silicon modules that have anti-reflective coatings and lower temperature coefficients. The thin film option assumes a low efficiency (~11 %), and a significantly lower temperature coefficient (even tough in thin film modules there is a wide variation in temperature coefficients between models), which is representative of most installed thin film modules as of 2013.

A statistical analysis of the CEC database was undertaken to try and replicate the categories used in v5, and from them derive the remaining technical specifications, besides the ones in Table 6, required as input values in v1 (e.g. NOCT and DC nameplate rating), but not explicitly discriminated in v5. A more recent (if uneditable) version of the CEC PV module database is available online (CEC, 2018), but using it was abandoned as that would lead to results that would´ve been at odds with the ones underlying the v5 assumptions (whose analysis was based on the older CEC database supplied with SAM v. 2017.1.17).

The first step was, for each module type, to apply the criteria stated throughout Dobos, A.P. (2014), attempting to recreate the values presented in Table 6. As this did not give the intended results, the assumption is that other unstated criteria were used, and they are not known. To circumvent this, additional filters were applied to the CEC database (18102 modules in total) in order to approximate as best as possible the values on Table 6, and in so doing trying to recreate the possible filters that the SAM development team applied as well when developing these categories for PVWatts, resulting in the values in Table 7. The filters, for each category, were as follows:

- For the standard module, all multi and monocrystalline c-Si modules with efficiency between 14% and 17% (both included) were considered (total of 12447 modules).
- For the premium module all monocrystalline modules with efficiency between 18% and 20% (both included), and temperature coefficients above -0.37%/ºC were considered (total of 62 modules). Even tough Dobos, A.P. (2014) only mentions monocrystalline modules and efficiency constraints, the CEC database contains many PV modules that correspond to those parameters (total of 410), but their average temperature coefficients are much lower than the -0.35%/ºC in Table 6. By constraining the temperature coefficient range to be above -0.37%/ºC, a shortlist of 62 modules was reached whose average temperature coefficient was -0.35%/ºC, and as such this sample was taken to be the most representative of the sample used by the SAM development team.
- For the thin film modules, all CdTe modules with efficiency between 9% and 11% were considered (total of 10 modules). In the CEC database there are many types of PV modules commonly considered as thin film technologies. They are Amorphous Silicon (a-Si, 1-a-Si, 2-a-Si, 3-a-Si, a-Si/nc in the CEC database), Cadmium Telluride (CdTe in the database), Copper-Indium-Gallium-Selenide (CIGS in the database) and Copper Indium and Selenium (CIS in the Database). However, if one were to average out the temperature coefficients of all these technologies, the value is closer to -0.33%/ºC, a far cry from -0.2%/ºC in Table 6. If selecting only thin film modules

with BIPV status in the database, an even worse average temperature coefficient of -0.45%/ºC is attained. As is stated in Dobos, A.P. (2014), the values on Table 6 are representative of the most common installed thin film technologies and, as stated in section I.2, due to the wide variability of temperature coefficients between different TF technologies, it should come as no surprise that an average of all TF modules irrespective of technology would return such unrepresentative values. According to the research, the predominant TF technology is CdTe, and for all 54 CdTe modules in the database the average temperature coefficient is much higher, at -0.25%/ºC. If that subset is constrained to only include efficiencies between 9 and 11% (both included), the average temperature coefficient is -0.196%/ºC and the average efficiency of 10%, very much in accordance with the values in Table 6. This small sample of 10 modules (all from the same manufacturer, FS Solar) was taken as representative of one of the main advantages of thin film over other module types (better temperature coefficient) and was used for this dissertation.

Having chosen which modules for each category from the database to include, calculation of the remaining parameters necessary as input to *pvwattsv1* was undertaken, resulting in the values in Table 7.

Table 7 - Results of CEC database analysis for input variables into pvwattsv1

	# of modules	Avg. Efficiency	Cover Type	Avg. Temperature Coefficient (φ) [%/°C]	Avg. Area [m^2]	Avg. DC nameplate rating (STC) [Wp]	Avg. NOCT [°C]
Standard c-Si	12447	15.28%	Glass	-0.458	1.736	265.646	46.6
Premium c-Si	62	19.07%	Anti-reflective Glass	-0.347	1.639	312.832	46.3
Thinfilm CdTe	10	10.11%	Glass	-0.196	0.720	72.766	45.1

An analysis of typical c-Si (standard and premium combined) and TF panel dimensions was done as well (Table 8), a required input for the determination of useable area for PV deployment (see section II.3.2)

Table 8 – Average dimensions by PV panel category

	Avg. Area [m^2]	Avg Width [m]	AvgLength [m]
PV Modules (Weighted for Premium and Standard)	1.75	0.99	1.75
Thinfilm Modules	0.72	0.6	1.20

2) Option to specify a DC-to-AC nameplate sizing ratio

When designing a PV system, one of the design parameters is the DC-to-AC sizing ratio, which is the ratio between nameplate capacities of DC power output of the PV module and the AC output of the inverter (also known as Inverter Load Ratio, ILR). For example, a system sized with and ILR of 1.2 would have, for a PV array rated at 1200kW DC output, an inverter with 1000kW AC rating. As a result, when DC power output from the array is above 1000kW, the inverter will "clip" the power by increasing the module´s operating DC voltage, moving the operation to a lower current point along the array´s current-voltage (I-V) curve, moving the array off of its maximum power point (MPP), thus reducing DC power to a level the inverter can handle, and resulting in losses. This may sound counterintuitive but, over life cycle of operation this oversizing of the DC input in relation to the inverter´s capacity can yield significant economic returns.

Whilst before, due to very high cost of PV modules, the main incentive was to maximize AC energy production out of each module, resulting in the adoption of ILR=1, the fall of module prices has changed project financials in such a way that currently ILRs of 1.1 to 1.3 are the standard. Depending on project location, and design specific loss factors (e.g. tilt, angle, orientation, mounting method, DC wiring losses, mismatch and soiling), the losses of clipping output during peak sun hours can be compensated by achieving higher DC loads during the beginning and end of day. In short, the massive reduction in costs of PV modules coupled with the improved performance of inverters at low load fractions has changed economics in such a way that the relatively small number of hours in which peak output is achieved resulting in clipping is compensated by having a bigger output from an oversized array in hours of low irradiance, leading to small but noticeable improvements in performance. For a more thorough explanation on why this is, see Fiorelli & Zuercher-Martinson (2013) and Grana (2016).

In *pvwattsv1* the ILR is defaulted to 1.0, with no option to change it, reflecting the standard system sizing practices at the time of its release. In *pvwattsv5*, it is defaulted to 1.2 (standard practice today), but can be changed by the user, simulating different oversizing and its results on specific project economics. To quantify the differences in performance, from an ILR of 1.0 to 1.2, two simulations for PV production in Lisbon were run using *pvwattsv5*, changing only the DC-to-AC ratio between simulations. The INETI 2005 EPW weather file for Lisbon and the default settings for PVWatts simulation in SAM Desktop were used, not accounting for any shading or availability curtailment.

The differences in production over a year were negligible (ILR=1.2 producing +0.13% annual energy than the ILR=1.0), and so the *pvwattsv1* limitation of not allowing for a user-defined ILR was considered of little importance. The impact on financials will also be quite negligible, for the installation cost of a slightly smaller or larger inverter is practically the same, and the acquisition cost differences between them are negligible when diluted over the life cycle of operation.

3) Module model no longer includes a quadratic correction at low light levels.

In *pvwattsv1*, for irradiance levels below 125W/m^2, a quadratic correction to the DC power output calculation is made, decreasing the output at those levels, a behavior observed in PV systems at the time of its release, and no longer observed in modern systems. For this reason, this correction was dropped in *pvwattsv5.* As the calculation method for *pvwattsv1* is not editable*,* and the irradiance level below which there is a correction cannot be set to 0, using *pvwattsv1* must be done keeping in mind that, for hours with low irradiances, the results will underestimate the real DC production of the array.

4) Total system losses are specified as a percentage, with a default of 14%, replacing the DC-to-AC derate factor used in *pvwattsv1*.

In *pvwattsv1*, a derate factor is applied ($\xi_{sys} = [0,1]$) to represent aggregate losses, the default being 0.77, and includes losses due to nameplate DC ratings errors, inverter efficiency at maximum power, voltage mismatch, diodes and connections, DC and AC wiring, soiling, system availability, shading, tracking error and aging. All of the losses included in ξ_{sys}, except for the inverter efficiency loss (η_{inv}), apply to DC power

output (P_{dc}), meaning that derated DC output (P'_{dc}) is given by equation (2),and the losses from inverter efficiency are modeled separately in the AC power calculation in the inverter module.

$$P'_{dc} = P_{dc} \times \frac{\xi_{sys}}{\eta_{inv}} \quad (2)$$

In *pvwattsv5* a system loss percentage approach was to model loss of power output, bringing PVWatts closer to common industry practice and making it easier for the user to understand. Compared to *pvwattsv1*, *pvwattsv5* percentage losses excludes all inverter losses, which are modeled separately (inverter and AC wiring losses), and include light degradation losses, the total resulting DC loss ($L_{total}(\%)$) being defaulted to 14%, assuming 3% losses for shading (both are standard values used in the industry (see PVGIS assumptions in European Comission (2017)), for further reference on the loss assumptions consult Marion et al., (2005).

Because the irradiation values in this model already account for shading losses, this must be corrected for. Keeping all other percentual values for losses unaltered (see Table 6 in Dobos, A.P., 2014) and removing the assumed 3% losses due to shading, one reaches a 11.42% total resulting DC loss (using equation (9) in Dobos, A.P., 2014).

As the user will not have the option to change the losses on the system, thie model assumes $L_{total}(\%)$ equals 11.42% and converts it to a DC derate-factor (ξ_{dc}), attempting to bring *pvwattsv1* simulation results closer to more recent system performance assumptions (Equation (3)).

$$\xi_{dc} = 1 - \frac{L_{total}(\%)}{100} = 0.8858 \quad (3)$$

Because the ξ_{sys} in *pvwattsv1* includes the inverter efficiency, defaulted to 96%, the resulting corrected derate factor is given by Equation (4)

$$\xi_{sys} = \xi_{dc} \times \eta_{inv} = 0.85 \quad (4)$$

From V1 to V5, a 10.4% increase in performance is thusly assumed due solely to improved input assumptions and not accounting for shading losses (if shading was included, the improvement would be 7.14%). $\xi_{sys} = 0.85$ will be the default for the model, helping to partially correct the systematic underestimation of performance of *pvwattsv1* (see section II.2.1.1).

5) Inverter efficiency curve is revised and nominal inverter efficiency can be entered by the user.

The default reference inverter efficiency increases from 0.92 to 0.96 from V1 to V5, so 0.96 will be used in this model. The revised and updated inverter efficiency curve for the inverter module (see Dobos, A.P., 2014) is based on the analysis of the CEC inverter performance data, accounting for inverters post-2010. The main difference is a better performance of the inverter at lower load fractions, which increases system performance, relative to *pvwattsv1*, by about 1 or 2%. Seeing as the inverter curve is not alterable, an underestimation of production of AC power of up to 2% must be assumed from using the *pvwattsv1.*

6) Nominal Operating Cell Temperature Correction due to installation characteristics.

In *pvwattsv5* the NOCT is converted to INOCT, adjusted based on installation characteristics. This input is then used to derive the operating cell temperature (T_{cell}) at each timestep by using a first-principles heat transfer energy balance model developed by Fuentes (Fuentes, 1987), which also accounts for POA

irradiance (in this case user defined), wind speed corrected for installation height and dry bulb temperature (values from the weather file). *pvwattsv1* uses the Fuentes model as well, but with a default INOCT of 45ºC, suitable for fixed open rack and tracking systems at an installed height of 5m to correct for wind speed effect on cell temperature[12]. However, this model is for roof mounted and façade systems, which typically have a more restricted air flow around the modules, resulting in typically higher INOCT. A 49ºC INOCT for roof mounted and façade systems will be assumed (default value assumed in *pvwattsv5* for roof mounted installations with a 10cm standoff (Dobos A. P., 2014)), to approximate the performance losses associated with reduced airflow and consequent increased INOCT. There is no possibility to change the defaulted installation height of 5m to reflect the real height of the PV module, which could be easily derived from the 3DGIS/CIM dataset. Thus, an error in the windspeed correction is to be assumed in the thermal model of *pvwattsv1*.

7) Variable temperature coefficients between different modules

The temperature coefficient was defaulted in *pvwattsv1* at -0.5%/ºC, a representative value of the standard PV module. Temperature coefficients vary significantly depending on PV module type, and as such, for each module type selected, and derived from the analysis of the database described above, this model will use the corresponding average temperature coefficients, highlighting the differences in thermal performance of the panels.

8) Module cover correction for angle of incidence and anti-reflective glass

By default, in *pvwattsv1* angular response correction, to account for reflection on panels, was only applied for incidence angles above 50º (Dobos A. P., 2013), calculating transmitted irradiance (I_{tr}) using the Sandia PV Array Performance Model polynomial correction by reducing incident POA irradiance (I_{poa}) given the angle of incidence (α) and beam normal irradiance (I_b) (see Equations (5) and (6)). In *pvwattsv5* however, a physical model is used, explicitly modeling the reflection, transmittance and absorption of a module cover with Snell´s law, Fresnel´s Equation and Bouger´s law respectively (Dobos A. P., 2014), allowing for the modeling of typical differences between standard glass and antireflective glass (a key difference between standard and premium modules).

Searching in the SSC SDKtool one can find the option in *pvwattsv1* to run a beta version of a correction for antireflective glass coating, that works by replacing the 5 coefficients of the Sandia PV Array Performance Model (see SDK Forum, 2017b), as can be seen in Table 9.

Table 9 – Module Cover Polynomial Coefficients (Dobos, A.P., 2013 and SDK Forum, 2017b)

	b_0	b_1	b_2	b_3	b_4	b_5
Standard Glass	1.0000	-2.438E-03	-3.103E-04	-1.246E-05	-2.112E-07	-1.359E-09
Anti-reflective Glass	1.0002	-2.13E-04	3.63416E-05	-2.175E-06	5.2796E-08	-4.4351E-10

$$f = b_0 + b_1\alpha + b_2\alpha^2 + b_3\alpha^3 + b_4\alpha^4 + b_5\alpha^5 \quad (5)$$

$$I_{tr} = I_{poa} - (1 - f) \times I_b \times \cos\alpha \quad (6)$$

[12] An experimental version of cell temperature correction is available in *pvwattsv1*, but only for concentrating photovoltaic collectors, and thus not applicable for flat plate PV panels (SDK Forum, 2017b)

This correction was applied in this model, and the details of the steps taken to input the correct values of I_b and α are documented in section II.2.1.2.

9) Ground coverage ratio

PVWatts uses a separate algorithm to calculate the fraction of each row that is shaded by adjacent rows of panels, based on the GCR, and reduces the beam and diffuse irradiance incident on each row accordingly (details on this algorithm can be found in Gilman, P., ,2015). According to the SDK tool in *pvwattsv1*, the GCR is considered 0.3, revised to 0.4 in *pvwattsv5*, and optimal values are considered between 0.3 and 0.6 (Dobos A. P., 2014). As mentioned in section II.3.2, this model will be assuming a GCR of 1 for rooftops and façades and installation parallel to the surface (angle with the surface = 0º), precluding the possibility of self-shading, which results in the GCR algorithm making no reductions to the incident irradiance values. In Gagnon et al., (2016), a GCR 0f 0.98 is recommended for tilted roofs, to reflect spacing between each module for racking clamps[13]. However, as it is beyond the scope of dissertation to assess to correct spacing distance between modules and given the very small difference to the assumed GCR of 1, this model will not use this recommended value.

10) Albedo

Tough only impacting the PVWatts POA calculation algorithm (overridden in this model as pre-calculated POA irradiation values will be part of the input), the albedo assumptions between versions have changed, both versions assuming from 0.2 for all hours, except when snow is present, in which case *pvwattsv1* changed the albedo to 0.6 to account for higher reflected radiation. In both versions, the albedo specified in the weather file (if present) will be used and override the default value.

2.1.2. PV system input parameters

In this section, close attention will be paid to the standard solar resource and model inputs, and the changes, default values and additions made to these inputs for the purposes of this model.

2.1.2.1. Solar Resource

For *pvwattsv1* simulations, hourly data for one year of two components of solar irradiance is required (beam, or direct normal irradiance (DNI in W/m^2) and diffuse horizontal irradiance (DHI in W/m^2), as well as ambient dry bulb temperature[14] in Celsius, and windspeed at 10 m in m/s, with each hour timestamped with the year, month, day and hour corresponding to the data line so the sun´s position can be accurately calculated (Dobos A. , 2013). As input weather file, it can take a standard Energy Plus Weather (EPW) data file format, converted to *.csv*, with the header information stating the Latitude and Longitude in degrees, Time Zone (hours offset from Greenwich Mean Time) and Site Elevation in meters above sea level. User calculated

[13] 1.27cm of spacing obtained from a SnapNrack Series 100 UL installation manual, a SunFix Plus Installation Guide, and an IronRidge Roof Mountain System Design Guide

[14] Temperature of air measured by a thermometer freely exposed to the air, but shielded from radiation and moisture (NOAA, 2018)

POA irradiance can also be an input and must be added to the last column of the file with the column name POA (see Figure 8).

Source	Location ID	City	State	Country	Latitude	Longitude	Time Zone	Elevation			1			
EPW	85360	Lisboa		PRT	38.73	-9.15	0	71						
Year	Month	Day	Hour	GHI	DNI	DHI	Tdry	Twet	RH	Pres	Wspd	Wdir	Albedo	POA
2005	1	1	7	13	0	8	10.2	9.8	97	1006.16	4.1	20	-999	0
2005	1	1	8	57	69.7043	38	10.7	10	95	1006.16	5	22	-999	28.59925
2005	1	1	9	138	489.6678	91	11.6	10.3	92	1006.16	4.9	32	-999	289.5736
2005	1	1	10	331	683.2176	127	12.6	10.6	87	1006.16	5.1	21	-999	496.7356
2005	1	1	11	269	788.4778	168	13.8	10.9	83	1006.16	4.8	27	-999	637.383
2005	1	1	12	289	836.6233	171	14.7	11.1	79	1006.16	5.6	359	-999	694.2065
2005	1	1	13	217	840.0047	141	15.3	11.2	77	1006.16	6	31	-999	663.4289
2005	1	1	14	152	799.4641	100	15.4	11.3	76	1006.16	6.2	20	-999	552.5526
2005	1	1	15	79	704.6849	52	15	11.1	78	1006.16	6.6	5	-999	380.9383

Figure 8 – Example of INETI 2005 Lisbon EPW file converted to .csv with added user calculated POA values

2.1.2.2. Model Inputs

The minimal inputs required by *pvwattsv1* are the system size (in kW DC), the system derate (as a fraction), the array tracking mode (Fixed, 1-Axis or 2-Axis), the panel tilt angle (in degrees) and the panel azimuth angle (in degrees). This list was extended and modified, to include points 1) through 16).

1) POA

For each panel being simulated, the POA irradiance ($I_{poa,E+}$) calculated in EnergyPlus (under the name *Surface Outside Face Incident Solar Radiation Rate per Area [W/m2](Hourly))* will be appended to the EPW weather file, and *enable_user_poa* variable in *pvwattsv1* will be set to 1 (see section II.5.1.2), forcing PVWatts to take the user-provided incident irradiance values as its inputs (in W/m^2), overriding the built-in Perez irradiance model

2) DNI

In a standard implementation of *pvwattsv1*, the DNI would serve to calculate the POA irradiance and the module cover correction as input to the beam irradiance (I_b) calculation (equation (7), see Dobos, A., (2013).

$$I_b = DNI \times \cos(\alpha) \tag{7}$$

Because the user supplies the POA irradiance, one only needs to guarantee the correct DNI is inputted into the model for the module cover correction. Because EnergyPlus reported results do not include DNI on each panel, but do include both the beam normal irradiance ($I_{b,E+}$) and the co-sine of the angle of incidence ($\cos \alpha_{E+}$) (respectively named in EnergyPlus as *Surface Outside Face Incident Beam Solar Radiation Rate per Area [W/m2](Hourly) & Surface Outside Face Beam Solar Incident Angle Cosine Value [](Hourly)*), the DNI incident on each panel (accounting for shading and reflectance) can be derived, calculated according to equation (8) and appended to the EPW weather file for each panel, replacing the site DNI column already present. DNI_{E+} accounts for site correction, adjusting the EPW DNI values and correcting for the longitude and latitude of the actual location being modeled (Alvalade), and for shadows and other complex urban irradiation phenomena.

$$DNI_{E+} = \frac{I_{b,E+}}{\cos \alpha_{E+}} \tag{8}$$

3) Module type

As mentioned in section II.2.1.1.1, the option to select a Standard, Premium or Thin film PV panel will be given to the user (module type 0,1 and 2 respectively), with the corresponding changes in system inputs as

stated in Table 7, unless the panel is on a façade, in which case only the Thin film option will be made available.

4) Surface Type

Tough not directly editable by the user, each panel has an attributed surface type (either *Cobertura* or *Fachada* (Rooftop or façade) under the header *Local* in the ArcGIS attribute table), which will be passed on to the model, only allowing for thin film PV modules on façades

5) Nameplate capacity

For each module type being modeled, the Average DC nameplate ratings (P_{dc0} in kW DC) of Table 7 will be used. For standard or premium modules, in simulations that do not include micro inverters, the aggregate nameplate capacity ($\sum P_{dc0}$) is given by equation (9), and depends solely on the number of PV panels (n) and the average nameplate capacity (P_{dc0}) derived from Table 7.

$$\sum P_{dc0} = \frac{n \times P_{dc0}}{1000} \ [kW] \tag{9}$$

For reasons stated below, different approaches to determining the nameplate capacity for the simulation are taken, depending on whether the simulation is for a system with micro inverters or if it includes Thin film modules. In the case of thin film modules, for reasons stated in section II.3.2, they have a variable area. To derive the aggregate nameplate capacity for one or multiple thin film modules ($\sum P_{dc0,TF}$) requires the total number of CEC database equivalent TF panels (n_{TF}) (dependent on the total area of TF being modeled ($Total\ Area_{TF}$) and the reference Area for TF panels in the CEC database analysis($Area_{CEC,TF}$)) and the average DC nameplate rating of the CEC database analysis ($P_{dc0,TF}$), as seen in equations (10) and (11). $Area_{CEC,TF}$ and $P_{dc0,TF}$ can be obtained in Table 7 and $Total\ Area_{TF}$ is an input into the simulation, dependent on which TF panels have been selected for simulation.

$$\sum P_{dc0,TF} = \frac{n_{TF} \times P_{dc0,TF}}{1000} \ [kW] \tag{10}$$

$$n_{TF} = \frac{Total\ Area_{TF}}{Area_{CEC,TF}} \tag{11}$$

In the case of micro inverter simulations, for reasons initially approached in section II.4.2 and further detailed in section II.5.1.2, panels will be simulated individually and not aggregately. Because of this, for standard and premium modules, the nameplate capacity is simply given by equation (12), and for thin film modules, by equation (10), where n_{TF} given by equation (13), solely dependent on the area of the single TF panel being modeled.

$$P_{dc0} = \frac{P_{dc0}}{1000} \ [kW] \tag{12}$$

$$n_{TF} = \frac{Area_{TF,i}}{Area_{CEC,TF}} \tag{13}$$

6) Number of panels

Tough not a direct input, the number of panels (n) selected for simulation will be used throughout the simulation

7) System Derate

As previously stated in point 4) section II.2.1.1.1, the user will be prompted to specify a total DC system loss ($L_{total}(\%)$) as a percentage (defaulted to 11.42%), which is then converted to a DC derate factor (ξ_{dc}), converted to a *pvwattsv1* system derate (ξ_{sys}) as a function of user defined inverter efficiency (η_{inv})

8) Inverter efficiency

This variable (η_{inv}) will be editable by the user, and defaulted to 96%, the standard used in SAM and representative of typical inverters

9) Inverter Type

The user will select *String, Micro*, or *No Option*, which will impact the calculation method (see section II.5.1.2) and the installed system costs (see section II.2.2.1.3.1). The default will be set to *Micro*, as in partially shaded environments they tend to perform better (see section I2.2)

10) Track mode

Will be set to 0, representing fixed systems, and cannot be changed by the user

11) Tilt

Will be set by the chosen panel´s attribute table from ArcGIS (β, *Slope_Angle* in ArcGIS), in this case 30º for roofs and 90º for façades

12) Azimuth

Will be set by the chosen panel´s attribute table from ArcGIS (γ, *Azimuth_Angle* in ArcGIS), where North = 0º

13) Temperature coefficient

For each module type being modeled, the Average Temperature Coefficient (φ, in %/ºC) of Table 7 will be used

14) Antireflective Glass

In case the module type selected is a *Premium*, this value will be set to 1, allowing for reflection losses correction of anti-reflective glass, as seen in point 8) of section II.2.1.1.1

15) INOCT

Will be set to 49ºC (see point 5) section II.2.1.1.1), and cannot be changed by the user

16) GCR

Will be set to 1 (see point 9) section II.2.1.1.1), and cannot be changed by the user

2.1.3. Technical and Production performance simulation

In this section, a detailed review of the various steps within *pvwattsv1* to assess the technical performance and production of PV panels is made. At the outset, before any calculations are run through PVWatts, two different simulation approaches will be run depending on the type of inverter chosen and its relation to shaded PV module behavior.

Shading, which has been removed from the losses calculation because it is accounted for in the input $I_{poa,E+}$ and DNI_{E+}irradiation, is explicitly assumed in PVWatts to affect panels uniformly (Gilman P. , 2015). That is, within a PV panel, a partially shaded module behaves in the same way as if the whole module were to

be uniformly shaded, the same applying to a partially shaded array (which is incorrect, as partially shaded modules can be disproportionately affected by shade, as was referred to in section I.2). Because of this, when an array (with multiple panels) is being simulated, the option of using micro inverters or a string inverter will have implications in the assumptions about possible power output.

As in the case of string inverters the production can be capped by the lowest voltage panel in the string of the array, the total AC production of the array ($P_{ac,array}$) will be obtained by a single simulation for an array (SIM_{array}), with panels numbered 1 through n, of a system with nameplate capacity (P_{dc0}) resulting from the sum of all panels´ nameplate capacities (P_{dc0_n}) as given by equation (14), and the hourly (i) POA irradiance value to be considered (I_{poa_i}) at each time step will be the minimum POA irradiance incident on any of the panels at any given time ($I_{poa_{i,n}}$), as given by equation (15) representing thusly the production cap set by the lowest producing panel at any given moment.

$$P_{dc0} = \sum_{1}^{n} P_{dc0_n} \tag{14}$$

$$I_{poa_i} = \min(I_{poa_{i,n}}) \tag{15}$$

In the case of micro inverters, as shading affects panels independently of each other, this model shall run n number of simulations separately (SIM_n) to assess the production for each panel n with its respective nameplate capacity (P_{dc0_n}) and hourly irradiation ($I_{poa_{i,n}}$), returning an AC output per panel ($P_{ac,n}$). The sum of these individual AC outputs will be the $P_{ac,array}$, as given by equation (16)

$$P_{ac,array} = \sum_{1}^{n} P_{ac,n} \tag{16}$$

Not specifying an inverter option, this model will use the same calculation method as for string inverters, but an average hourly POA irradiation value on each panel will be assumed (equation (17)). This means any results from a simulation without specifying the inverter type will be only representative of average systems, not accounting for losses from voltage mismatch between panels due to partial shading of the array, nor taking full advantage of different POA irradiation on multiple panels.

$$I_{poa_i} = \text{avg}(I_{poa_{i,n}}) \tag{17}$$

Following this introduction, the next section details the *pvwattsv1* module, which individually calculates steps 1 through 8.

1) Sun Position

For each hour, based on the weather file´s longitude and latitude coordinates, and the year, month day and hour, *pvwattsv1* calculates the sun´s position at the midpoint of the hour, to determine the solar zenith (θ_{sun} in degrees) and the solar azimuth (γ_{sun} in degrees), by using the Michalsky (1988) algorithm (unless calculating for sunrise or sunset, in which case the midpoint between the sunrise/sunset and the end/beginning of the hour is used). Because *pvwattsv1* does not allow the insertion of user defined angle of incidence (α), and its determination requires the calculation of the sun´s position, this step cannot be

overridden. In this model it is thusly calculated twice, once in EnergyPlus, to calculate the POA irradiance and DNI irradiance, and once within *pvwattsv1*. EnergyPlus uses a more recent calculation algorithm (Meeus, J., 2000) but as Michalsky´s algorithm has been shown to be accurate to within 0.01º until the year 2050 (Michalsky, 1988), and assuming EnergyPlus is no less accurate, there is no reason to believe the θ_{sun} and γ_{sun} calculations will differ significantly from EnergyPlus calculations.

2) Tracking

Angle-of-incidence, or AOI (α in degrees) calculations for fixed systems are based on standard geometrical calculations (equation (18)), and require knowing the solar zenith (θ_{sun}), the solar azimuth (γ_{sun}), the surface tilt (β in degrees) and the surface azimuth (γ in degrees). While θ_{sun} and γ_{sun} are calculated in step 1), β and γ are directly imported from ArcGIS for each panel being simulated (see points 11) and 12) of section II.2.1.2.2).

$$\alpha_{fixed} = \cos^{-1}[\sin(\theta_{sun})\cos(\gamma - \gamma_{sun})\sin(\beta) + \cos(\theta_{sun})\cos(\beta)] \quad (18)$$

The calculated $\alpha_{pvwatts}$ may differ slightly from the calculation in EnergyPlus (α_{E+}), for different algorithms are used (as was seen in the previous point, the sun position calculations are independent).

3) Plane-of-Array Irradiance

As seen in point 1) of section II.2.1.2.2, for each panel this model will use EnergyPlus´ calculated *Incident* solar radiation ($I_{poa,E+}$ in W/m^2), for all 8760 hours of the year, overriding the imbedded POA calculation of *pvwattsv1*. It is important to bear in mind how the beam component (I_b) of POA (I_{poa}) (see equation (19)) is calculated within *pvwattsv1* (equation (20)), as it is relevant in the next step.

$$I_{poa} = I_b + I_{d,sky} + I_{d,ground} \quad (19)$$

$$I_b = DNI \times \cos(\alpha), if \ \cos(\alpha) > 0; \ otherwise \ I_b = 0 \quad (20)$$

4) Module cover

Angular response correction to calculate transmitted irradiance (I_{tr} in W/m^2) is done according to Equation (6) (see point 8) section II.2.1.1.1), with the Sandia polynomial coefficients dependent on the module type, as mentioned in point 14) section II.2.1.2.2.

Because it is not possible to input $I_{b,E+}$ directly into *pvwattsv1*, nor $\cos(\alpha_{E+})$ or α_{E+}, it was decided to only supply the DNI incident on the panel (see point 2) in section II.2.1.2.2) and let *pvwattsv1* recalculate I_b internally according to equation (20), which may lead to errors. As mentioned in point 2) of the current section, calculated AOI from *pvwattsv1* ($\alpha_{pvwatts}$) can be different from the AOI calculated in EnergyPlus (α_{E+}). Because the model calculates the input DNI according to equation (21), and then *pvwattsv1* converts it to irradiance beam component (I_b) by way of equation (22), the resulting $I_{b,pvwatts}$ may be different from the previously calculated $I_{b,E+}$.

$$DNI_{E+} = \frac{I_{b,E+}}{\cos\alpha_{E+}} \quad (21)$$

$$I_{b,pvwatts} = DNI_{E+} \times \cos(\alpha_{pvwatts}) \quad (22)$$

As both *pvwatts* and *EnergyPlus* use the Perez algorithm to determine the I_b, both are using the same weather data set and using very similar (if not identical) solar coordinate calculations, whatever differences there may be between $I_{b,pvwatts}$ and $I_{b,E+}$ are certainly negligible.

5) Thermal Model

As discussed in point 6) section II.2.1.1.1, the Fuentes model is used to calculate the operating cell temperature (T_{cell} in ºC) with INOCT of 49ºC, to correct for mounting configuration, and no correction for windspeed from installation height is assumed.

6) Module model

The *pvwattsv1* implements an adaptation of version 3.3 of the PVFORM model (see section II.1.1, Menicucci, D., 1986 and Menicucci & Fernandez, 1988). Following the adaptations in section II.2.1.1.1, it computes de hourly DC power from the array (P_{dc}, in kWh/h) by taking, for each module type, the corresponding Average DC nameplate rating at STC (P_{dc0}, in kW) and Average Temperature Coefficient (φ in %/ºC) (see Table 7), as well as the reference cell temperature at STC ($T_{ref} = 25$ºC) and the previously calculated operating cell temperature (T_{cell}) and transmitted irradiance (I_{tr} in W/m^2), according to equation (23). As previously mentioned in point 3) of section II.2.1.1.1, for low irradiance ($I_{tr} \leq 125\ W/m^2$) a quadratic correction is assumed, as seen in equation (24).

$$P_{dc} = \frac{I_{tr}}{1000} P_{dc0} \left(1 + \varphi\left(T_{cell} - T_{ref}\right)\right) \qquad for\ I_{tr} > 125\ W/m^2 \tag{23}$$

$$P_{dc} = \frac{0.008 \times {I_{tr}}^2}{1000} P_{dc0} \left(1 + \varphi\left(T_{cell} - T_{ref}\right)\right) \quad for\ I_{tr} \leq 125\ W/m^2 \tag{24}$$

7) System Derate

The system derate (ξ_{sys},), arising from point 4) in section II.2.1.1.1, will be given by equation (25), dependent on the total assigned DC loss ($L_{total}(\%)$) and the inverter efficiency loss (η_{inv}). As the system losses to the DC output (ξ_{dc}) do not include AC losses, it is defined with equation (26). The application of the DC derate factor to the P_{dc} through equation (27) yields the derated DC power output (P'_{dc}), which is passed to the inverter model.

$$\xi_{sys} = (1 - \frac{L_{total}(\%)}{100}) \times \eta_{inv} \tag{25}$$

$$\xi_{dc} = \frac{\xi_{sys}}{\eta_{inv}} \tag{26}$$

$$P'_{dc} = P_{dc} \times \xi_{dc} \tag{27}$$

8) Inverter Model

The *pvwattsv1* implements an adaptation of version 3.3 of the PVFORM model to compute AC power from the inverter system and, as stated in point 2) of section II.2.1.1.1 it assumes a DC-to-AC ratio of 1 (equation (28)) for the nameplate AC rating of the inverter (P_{ac0}). The effective DC input power rating of the inverter ($P_{inv,dc0}$) is calculated from the P_{ac0} and η_{inv} through equation (29), and the load fraction of operation of the inverter (f) is calculated with the P'_{dc} and $P_{inv,dc0}$ with equation (30).

$$P_{ac0} = P_{dc0} \tag{28}$$

$$P_{inv,dc0} = \frac{P_{ac0}}{\eta_{inv}} \quad (29)$$

$$f = \frac{P'_{dc}}{P_{inv,dc0}} \quad (30)$$

The inverter conversion efficiency at operating conditions (η_{op}) is calculated through an empirically derived third order polynomial formula for load fractions between 10% and 100% (equation (31)) and assumes linear change for loads below 10% (equation (32)), being capped at 0.925.

$$\eta_{op} = 0.774 + 0.663f - 0.952f^2 + 0.426f^3 \quad for\ 0.1 \leq f \leq 1 \quad (31)$$

$$\eta_{op} = -0.015 + 8.46f \quad for\ 0 < f < 0.1 \quad (32)$$

The final AC power output (P_{ac}) is calculated in equation (33), by applying η_{op} to the P'_{dc}, corrected by a ratio of the simulation´s inverter effiency at full load (η_{inv}) and the reference inverter efficiency (0.91) used to derive the part load efficiency curves of equations (31) and (32) (see Menicucci, D., 1986 and Menicucci & Fernandez, 1988). For $f > 1$, the P_{ac} is clipped to the maximum AC power rating (P_{ac0}).

$$P_{ac} = P'_{dc} \times \eta_{op} \times \frac{\eta_{inv}}{0.91} \quad (33)$$

2.2. SAM Economic Model

The economic model uses three distinct computation modules: *belpe, utilityrates5* and *cashloan.* Section II.2.2.1 describes each module´s input parameters, and how they were arrived at, and section II2.2.2 describes in detail the calculations within each module.

2.2.1. Economic Model Input Parameters

2.2.1.1. Belpe

The ideal load profile for the model would be one based on real hourly load measurements. An attempt to obtain this was made by contacting EDP (Portugal´s leading power retailer and distribution grid operator), but there was no reply to this request. There are many studies concerning load forecasting methods, and if available, they should be applied to calculate a representative load curve (see for example Rodrigues et al., 2014 & Rodrigues et al., 2016), using detailed building energy simulation tools such as *EnergyPlus* or *TRNSYS*. For this model, the inbuilt *belpe* module was used which estimates this hourly consumption load profile following the guidelines laid out in Hendron & Engenbrecht (2010), taking as its inputs the building´s square footage, occupancy, type and number of appliances and temperature settings, coupled with weather parameters from a weather file and monthly aggregate consumptions for one year (corresponding to the utility bill consumptions for each month).

The building details were extracted from CityEngine (see section II.3), and are synthesized in Table 10, corresponding to *nº10, Rua José d´Esaguy, Lisbon*, which as will be seen in section III, will be the basis for this case study (but these variables will remain editable by the user for other simulations). Because only residential use will be considered (see section II.2.2.1.3.2), the 4 ground floor shops will be assumed to be

Table 10 - Building information

nº10, Rua José d´Esaguy	
Implantation Area (m^2)	232.1
Nº of Floors	4
Nº of Apartments (1st to 3rd floor)	6
Nº of Shops (Ground floor)	4
A_{apt}	116.05
n_{apt}	8

equivalent to two apartments in terms of energy consumption (total number of apartments in the building (n_{apt}) will be considered 8); as there are two apartments per floor, the area for each apartment (A_{apt}) will be considered half of the implantation area[15], the total area A_{total} being given by equation (34).

$$A_{total} = n_{apt} \times A_{apt} \quad (34)$$

Energy Retrofitted option is selected, assuming the building has been updated with passive energy saving measures, which defaults the building envelope construction parameters to the most recent (see Gilman, P., 2018) replacing the parameters dependent on the *Year Built* variable (making it a useless input). All appliances are excluded (value defaulted to 0 for heating system, cooling system, stove, refrigerator, dishwasher, washing machine, dryer and miscellaneous electrical loads), as the average hourly load curve produced by *belpe* without the electrical appliances more closely resembles the Portuguese reference case (Figure 9). The temperature settings are such that heating and cooling systems are activated when temperature drops below 20ºC or goes above 25ºC respectively (heating and cooling setpoints). The weather file used will be the same as for the *pvwattsv1* module, the INETI Synthetic data for Portugal - 2005 Lisbon EPW file, but for this module the values used will be the original ones for Lisbon and not the panel and site-specific irradiation values calculated by *EnergyPlus*.

For the occupancy (O_{apt}), the latest census data indicates 2.6 inhabitants/household in 2011[16] (PORDATA, 2011), and this will be the value used (tough it is editable by the user), with constant occupancy throughout the year, with total building occupancy (O_{total}) given by equation (35).

$$O_{total} = n_{apt} \times O_{apt} \quad (35)$$

A survey conducted by the European Commission of a sample of 92 representative households in Portugal (ENERTECH, 2002), revealed that in 2002, the average annual electricity consumption per household in Portugal was 28 kWh/year/m² (referred to in the model as C_{area}) and 1142 kWh/year/person (referred to in the model as C_{occ}). Because these values are quite outdated, they were updated with the growth rate in domestic electricity consumption reported in the platform PORDATA (2016), for the years between 2002 and 2016, of 16.02%[17], resulting in C_{area} = 32.49

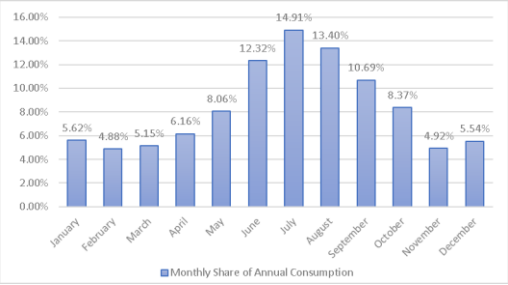

Figure 10 - SAM Belpe Default Monthly Load Distribution Curve

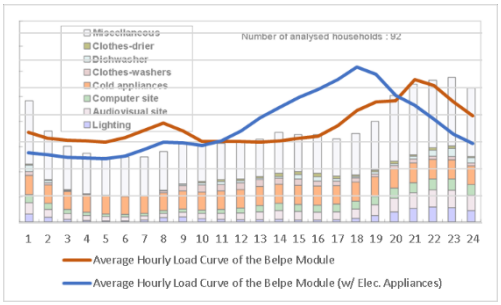

Figure 9 – SAM Belpe Module Average Hourly Load Curve Overlaid the ENERTECH (2002) curve for Portuguese Households

[15] Which overestimates the area of the apartment by including the collective and service areas, and balconies. Coincidentally, the resulting A_{apt} is similar to the 116.6 m² average household size in the sample used in ENERTECH (2002) (see below in this section)

[16] Less than the 2001 census (2.8 inhabitants/household (PORDATA, 2011)), and consistent with the ENERTECH (2002) sample of 2002 with a 2.92 inhabitants/household average

[17] PORDATA (2016) indicates a per capita consumption of 1,092.4 kWh/capita in 2002 and 1,267.4kWh/capita in 2016

kWh/year/m² or C_{occ} = 1,324.95 kWh/year/person in 2016, which will be the values used to estimate total annual consumption for the model, depending on the area and number of occupants in the household. This annual consumption will be allocated to each month (providing the required monthly consumption input for the model) by using SAM prebuilt monthly load distribution curve, normalized in Figure 10, which conforms to the expectations in a Mediterranean climate, with mild temperatures in winter and high ones in summer, resulting in higher loads during the summer from cooling demand (IDAE, 2011). The *belpe* module returns a structure of the average hourly load curve[18] quite similar to the empirically derived curve from Portuguese households found in ENERTECH (2002), as can be seen in Figure 9, so the *belpe* module can be used with moderate confidence that its results will not stray too far from a Portuguese reference case.

2.2.1.2. Utilityrate5

To estimate the utility bill annual savings, the *utilityrate5* module is used. For the buy rate of the *utilityrate5* module, two of EDP Comercial´s (Portuguese electricity retail leader) structures will be used: a fixed structure and a bi-hourly, daily cycle TOU structure[19], synthesized in Table 11, with the user given the option to select one of them, and the contracted capacity to the retailer (EDP Comercial, 2018). There is no differentiation between weeks, weekends, months and no tiers, therefore the weekday and weekend schedules are the same and the rates only vary according to TOU in the bi-hourly structure, with off-peak rates corresponding to the hours between 10PM and 8AM (EDP Comercial, 2018b). For the purposes of this model, the bi-hourly cycle is assumed, with contracted capacity per household of 6.9kVA, and the user supplied VAT is applied to these buy rates, representing the buildings total electricity bill.

Table 11 – Buy-rate structure input (EDP Comercial, 2018)

€/KWh (direct debit + electronic invoicing)			
Contracted Capacity (kVA)	Simple	Bi-hourly (Daily Cycle)	
		Peak	Off-peak
3.45	0.1538	0.2007	0.0958
4.6	0.1573	0.2008	0.0959
5.75	0.1585	0.2009	0.0959
6.9	0.1587	0.2008	0.0959
10.35	0.1588	0.2008	0.0959
13.8	0.16	0.201	0.0961
17.25	0.1609	0.2014	0.0965
20.7	0.1616	0.2013	0.0964

Source: EDP Comercial (2018)

The fixed demand rate is not accounted for, as it is assumed that the installation of the system will not change the contracted capacity to the retailer, thus no savings can accrue from that change. There are also no monthly or annual minimum charges, and no variable demand charges (the Portuguese residential retail market does not have that option). It is assumed that there is no annual escalation rate, therefore any yearly increase in buy-rate comes only from the assumed level of inflation (see section II.2.2.1.3)

The sell rate is determined by the DL 153/2014 (see section I5.1), given by equation (36), and variable sell rates are enabled in the module (*enable_en_ts_sell_rate* =1).

$$R_{UPAC,m} = E_{supplied,m} \times OMIE_m \times 0.9 \quad [€/kWh] \tag{36}$$

$R_{UPAC,m}$ is the monthly remuneration from grid sales in month m; $E_{supplied,m}$ is the energy sold in month m; $OMIE_m$ is the sale rate resulting from the simple arithmetic mean of the daily settlement prices in month m for the Portuguese spot market in OMIE (Table 12)

[18] Excluding electrical appliances
[19] Assuming direct debit and electronic invoicing

For the purposes of this model, an analysis of the average Baseload OMIE monthly settlement prices in Portugal for each month between 2011 and 2017 (OMIP, 2018) was conducted, returning the monthly averages of Table 12, which will be used as the monthly sell rates ($OMIE_m$) for all energy sold to the grid over the lifetime of the system. All buy and sell rates and charges are considered in year 1 euros.

Table 12 – OMIE Monthly Average Settlement Prices for Portugal between 2011 & 2017 (OMIP, 2018)

	Jan	Feb	Mar	Apr	May	Jun	Jul	Aug	Sep	Oct	Nov	Dec
Pt Baseload Average 2011-2017 [OMIEm, €/MWh]	47.56	40.51	37.19	35.21	42.36	48.61	49.97	49.30	51.62	53.14	49.66	53.74

Because the case study will be a UPAC, the metering structure should be set to 2, corresponding to a single bidirectional meter, with no monthly rollover in credits, representing the compensation calculation of net-billing, with cumulative hourly excess credited to current month bill at sell rate (i.e. the system only buys the difference in each time step between the load and the system production at buy rate, and only sells if system production is above load in that hour, at the appropriate sell rate)[20].

No load escalation is assumed for the whole simulation, and system output hourly calculations are only run for the first year, with all other years scaled according to the input parameters. As the power of PV modules tends to decrease slowly with age a degradation (D) must be assumed. According to Jordan & Kurtz (2013), PV modules typically lose about 0.5% of power per year of operation, with 1% being considered a conservative value (Yates & Hibberd, 2010). The analysis of residential project PV studies (Table 14) reveals a middle of the road assumption of 0.75% to be quite standard, and that is what will be used in the model. The analysis period is 25 years as specified in section II.2.2.1.3.2.

2.2.1.3. Cashloan module

The *cashloan* module takes as its inputs, besides the yearly production, load and utility bill savings calculations of the previous modules, the following: i) system costs, including installation, operation and maintenance costs for the system; ii) financial parameters, including loan (type, rate, period and share) and, inflation, discount. tax, and insurance rates, and iii) incentives

2.2.1.3.1. System Costs

System costs are comprised of installation and operational costs. For the project installation costs, only the Total Installed Cost is a direct input of the model, and is accounted for in Year 0 of the project cash flow, and in SAM it is the sum of direct (modules, inverters, BoS, installation labor, installer margin and overhead) and indirect (permitting, engineering and development, grid interconnection, land purchase, sales tax rate) capital costs. Operational and Maintenance (O&M) costs represent running project costs, which can be recurring or specific to a single year.

[20] Technically there shouldn´t be any difference between the net-metering (metering structure 1) and net-billing (metering structure 2) valuations as per the excess generation calculation methods defined in SAM; both calculate the excess generation monthly, with the only difference being the net-metering calculates the difference of the cumulative monthly load and production, and the net billing calculates the monthly sum of the hourly differences between load and production. Since the sell rate is the same for every hour of each month, the result should be the same. However, the net metering calculation in SAM assumes the excess generation to be sold at next months´ sell rate, which is unrepresentative of the Portuguese system, and thus net billing with current month sell rate (structure 2) was chosen.

Following the analysis in section I3.3.1, Table 13 was obtained detailing the estimates of total installed system costs/W_{DC} in Portugal (C_{inst}), dependent on the user´s module and inverter choices, and new or retrofit construction, and will serve as input into the model[21]. It includes all the above stated direct costs plus permitting and grid interconnection indirect costs. It does not however consider land costs or engineering costs, for given the residential nature of the project, this model assumes the former to be a sunk cost, and the latter to be null given the standard and modular nature of these types of installations[22]. All installed system costs will be majored by the default VAT rate (r_{VAT}), in Portugal of 23% (which can be edited by the user) and multiplied by the aggregate system nameplate capacity ($\sum P_{dc0}$).

Table 13 – Input of Total Installed System Cost in Portugal (€/W_{DC})

	Standard Total Installed System Cost in Portugal (1)	2.2 €/W_{DC}					
	€/W_{DC}	Standard		Premium		Thinfilm	
Inverter Choice	No Option	2.2	(1)	1.91	(2)	1.18	(3)
	String Inverter	2.09	(4)	1.82	(2)&(4)	1.12	(3)&(4)
	Microinverter	2.46	(4)	2.14	(2)&(4)	1.32	(3)&(4)
	€/W_{DC}	Standard		Premium		Thinfilm	
New Construction	+ No Option Inverter	1.95	(2)	1.83	(2)	1.02	(2)&(3)
	+ String Inverter	1.85	(2)&(4)	1.74	(2)&(4)	0.97	(2)&(3)
	+ Microinverter	2.18	(2)&(4)	2.05	(2)&(4)	1.14	(2)&(3)

Sources: (1) IEA (2017);(2) Barbose, G., & Darghouth, N. (2016);(3) Horowitz et al. (2017); (4) Fu et al., (2017)

O&M costs represent annual expenditures on equipment and services that occur throughout the lifetime of the project and are reported in the cash flow in years 1 and later. Estimates for O&M costs ($C_{O\&M}$) vary considerably between studies (see Table 14) and this model adopts the Fu et al., (2017) estimate of 21$/kW$_{DC}$ ([6]19.01€/W$_{DC}$).

For component replacement cost, as seen in section I2.2, micro inverters typically have a warranty beyond lifetime of the project this model will assume they require no replacement. For the string inverters, which typically last about 15 years before replacement, this model will assume replacement halfway through the lifetime of the project[23], and the cost associated with it (C_{string}) is 16.01% of total installed cost (0.35€/W$_{DC}$, see Table 2), and will affect all simulations for the "No Option" or "String" inverter choices. The registration fees (C_{reg}) from Appendix I will be reflected in the initial installation cost, dependent on the capacity of the installation, and assuming it is connected to the grid for sale of excess generation.

Table 14 – LCOE and Cashflow Analysis Variable Definitions and Assumptions (Fu et al., 2017, Pereira et al., 2016b, Lazard, 2017)

LCOE and Cashflow Analysis Assumptions - Residential PV	NREL (Fu, et al.,2017))	Lazzard, 2017	Pereira, Joyce, & Reis, 2016b
n - system lifetime [years]	30	20	25
r - real discount rate [%] [4]	6.9 (Equity Discount Rate)	12 (Equity Discount Rate)	6.5
It – Initial investment at t=1, or replacement cost in specific year (CAPEX)	I_{t1}=2.8$/W (for Residential Sector) ;I_{t15}=0.13$/W (Inverter Replacement mid life of project)	I_{t1}=[3.125-3.56]$/W (for Residential Sector)	I_{t1}=[2.3-2.9]€/W (for Residential Sector) ;I_{t13}=0.3*I_{t1} (Inverter Replacement mid life of project)
Mt – Operation and Maintenance costs (OPEX) in year t	21$/kW-yr	[20-25]$/kW-yr	1% of I_{t1}
Bt – Auxiliary power cost in year t	N/A	N/A	≠0 in case of Sun-tracking systems; =0 for fixed systems
Yearly Energy Degradation	0.75%/year	N/A	0.7%/year
Inflation Rate [%]	2.50%	N/A	N/A
Debt Fraction [%]	40%	60%	N/A
Debt Interest Rate [%]	4.80%	8%	N/A

[21] It was assumed that for façade systems with TF technology, the installed system cost is independent from inverter or construction type.
[22] This assumption is questionable for the TF systems, but was nonetheless a simplification that was assumed for this model
[23] The same assumption is valid for the "No Option" inverter

2.2.1.3.2. Financial Parameters

SAM provides the option for standard loan and mortgage loan types, the latter with tax deductible loan interest payments. A standard loan type will be assumed for this project as, since 2012, it is no longer possible to tax deduct mortgage loan interest payments in Portugal (Diário de Notícias, 2017).

For renewable energy financing, multiple banks in Portugal give out loans, with the possibility to finance up to 100% of the invoiced amount, with flexible loan terms ranging from 1 to 10 years (Martins, F.M., 2016).Following a summary analysis of the Portuguese renewable loan market (Maia, 2017), the annual nominal interest rate[24] (r_{loan}) ranges from 1.88 to 3.25%. A conservative value of 3% will be assumed, with a loan term (t_{loan}) of 7 years. These values will be editable by the user, and a useful link to evaluate specific financing conditions can be found in Comparajá.pt (2018). The debt fraction (f_{debt}) for the study will be assumed at 50% but can also be changed.

The analysis period for the project will be 25 years, a standard value, as reflected in Table 14. The default Inflation rate (r_{inf}) that will be assumed for the analysis period will be the forecast from the Banco de Portugal for the period 2018-2020 of 1.5% (Banco de Portugal, 2018), extended to the remaining analysis period, with a possibility for the user to specify an alternate inflation rate.

The real discount rate (r_{real}), which is a measure of the time value of money, will be required to calculate the discounted present value of cash flows. For many projects, the minimum real discount rate assumed is the cost of equity, reflecting the minimum expected returns for the investment of equity, at a minimum risk. However, this supposes that the investor is comparing multiple investment alternatives and opting for the most efficient capital allocation mechanism from a pool of choices. This is not the situation that is being modelled in this project, as other considerations, beyond financial ones, are taken into account, namely environmental, political and sociological, so the underlying assumption is that the investor will attempt to guarantee that the project will not lose money and will not be trying to maximize gains. Thus, the weighted average cost of capital (WACC) is a better metric to use as a real discount rate, as it reflects the actual cost of financing the project, considering weighted cost of equity and debt, and the resulting financial metrics from the cashflow analysis assume only a reasonable (and not maximized) return is required for the project. The default real discount rate for the project will be the WACC, but because discount rates are very subjective, and depend heavily on the risk and investment profile of the investor, this will be editable by the user to reflect his own return expectancies.

In the WACC calculation, the cost of debt is equal to the loan rate, and the cost of equity will be equal to the expected inflation rate, reflecting the assumption that the investor only wishes to ensure the invested equity returns at least as much as inflation over the investment period, and he is not considering any alternative investments. The nominal discount rate (r_{nom}), used to calculate the NPV, is the result of adjustment of the real discount rate to account for inflation.

[24] *Taxa anual nominal*, TAN

For the purposes of this analysis, the default income tax (r_{IRS}) will be of 35% corresponding to the middle income tier in the *Escalões de IRS 2018* (Economias, 2018). It will, however, be editable by the user to reflect his own income bracket and taxation. In case the tenants of the building are a mix of commercial and non-commercial entities (respectively taxable under IRC and IRS), the resulting gains from installing the system should be divided among the tenants by the share of the condominium, and taxed under the respective tax code (Inforestilo , 2015). The assumption will be that the building is entirely residential, which is conservative, as the IRS is higher than the IRC.

The current VAT in Portugal (IVA) is of 23%, which will be the default value used for the analysis but can also be edited by the user. The VAT will be applicable on all costs of the project, including total initial installation cost and O&M costs, and buy rates from the electrical grid. There is a required liability insurance for any project registered on SERUP (see Appendix I), and this one-shot cost will be assumed to be included in the total installed costs.

On the subject of tax incentives, a few considerations are required (see section I5.1). In case the investor is a company, subject to IRC, there is an accelerated depreciation schedule available resulting in a tax break. Also, for buildings exclusively used for renewable energy production, an IMI tax break is made available. Under the Lei 32/2012, concerning urban rehabilitation, a series of tax benefits can be obtained. In this residential analysis, the former two tax breaks are not applicable (the assumption being that the building under analysis is purely residential, with no commercial entities). The latter tax incentive, because it requires a very complex analysis imposing knowledgeable consideration of a range of topics outside the scope of this dissertation, will not be considered. From the above one concludes that there will be no incentives for PV deployment modeled in this analysis.

The salvage value for the project at the end of its lifetime is assumed to be zero, and thus will not be modeled.

2.2.2. Economic Performance Simulation

The economic performance simulation is done in a three-step sequence, starting with the hourly load profile estimation with *belpe*, estimating the value of the energy produced with *utilityrate5*, and finally analyzing the cashflow with *cashloan*.

2.2.2.1. Belpe

The following is a simplified explanation of the calculations carried out within the *belpe* module, as its details are both complex and beyond the scope of this dissertation. For a complete guide to the *belpe* computations, refer to Gilman, P. (2018).

For this model´s purposes, the only additional calculation besides the inbuilt *belpe* module concerns the monthly load inputs into the *belpe* module. Following the input values mentioned in section II.2.2.1.1, the total annual energy consumption of the building ($C_{building}$) will be given by the average value of equations (37) and (38). The resulting annual $C_{building}$ is distributed by each month according to the percentages in Figure 10, and these values serve as the inputs into the *belpe* module.

$$C_{building} = A_{total} \times C_{area} \quad (37)$$

$$C_{building} = O_{total} \times C_{occ} \quad (38)$$

The building is modeled as a single zone with a square floorplan with its user-supplied A_{total} evenly divided over the number of stories designated by the user. Annual lighting and plug loads are calculated according to O_{total} and the electrical appliances included.

The *belpe* module runs a 3R3C energy balance model, with the electrical loads for the building (modeled as a simple box) being calculated according to Figure 11. After initializing the module with all its input variables, the ambient temperature (T_{amb}) is converted to sol-air temperature, and the resulting outer surface temperatures are averaged to get T_{S-A}.

The building envelope is modeled with a resistance R_{env} and capacitance C_{env}, enabling calculation of heat transfer to the interior walls of the space with temperature T_{surf}, to which the solar and radiative thermal gains $Q_{sol} + Q_{rad}$ (from radiation through widows and occupants and equipment) are applied.

The convective heat transfer between the interior surfaces and the zone air temperature are modeled via a resistance to represent convection coefficient h_{surf}, and air capacitance C_{air}; convective heat transfer between T_{air} and the zone's thermal mass is also modeled with resistance h_{surf}, and with capacitance C_{mass} and temperature T_{mass}. The convective thermal gains ($Q_{conv} + Q_{inf}$) from infiltration, occupants and other equipment are applied directly to T_{air}, and the HVAC equipment's operation is directly governed by the zone air temperature, with a simple control algorithm. 3 differential equations for each temperature node in Figure 11 are solved with a first order implicit Euler method for an hourly time-step, returning the interior temperature, which is then plugged into the HVAC operation to calculate its electricity consumption, leading to a recalculation of the temperatures and a resulting HVAC load to which all other equipment loads are added[25]. The last step of the calculation involves scaling the calculated loads according to the monthly electricity use data provided by the user. All months without HVAC loads are simply scaled with the monthly scale factor, and all months with HVAC loads are scaled with the smallest of the monthly load scale factors, and then just the HVAC loads are scaled with a load factor that results in a total monthly consumption equal to the one provided by the user[26]. The resulting 8760 values represent the hourly energy load for the building (L).

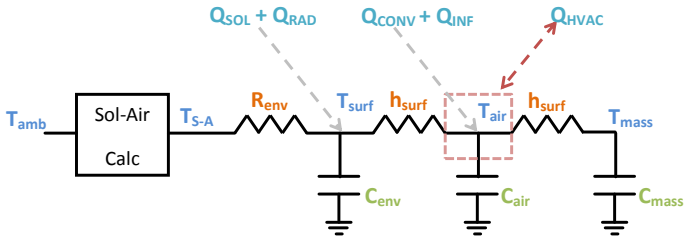

Figure 11 – 3R3C Energy Balance Model (Gilman P. , 2018)

[25] The building's annual lighting and plug loads are selected for residential buildings and based on the number of occupants as well as the user's input regarding appliance and equipment electrical use. These annual loads are assigned based on Hendron & Engenbrecht (2010)

[26] Reasons for this are expanded upon in Gilman, P. (2018) and relate to differences between *belpe* and EnergyPlus HVAC load predictions

2.2.2.2. Utilityrate5

The *utilityrate5* module calculates the yearly electricity bill with and without the system, assuming a similar rate structure, and the difference between the two is the corresponding yearly savings which serve as inputs into the *cashloan* module. For the UPAC simulation the metering option 2 is used, corresponding to a net billing model, where cumulative hourly excesses are credited to current month´s bill at the sell rate. It assumes a bidirectional meter with no monthly rollover in credits, in which excess power in each hour is sold to the grid at the appropriate sell rate and grid power only supplies the portion of the load in each hour that the system cannot supply, at the appropriate buy rate for that hour. Any credit remaining at the end of December is credited to the December electricity bill

For year 1, at each time step i, AC power output (P_{ac}) and load (L) are compared with equation (39)(76), to determine, for each hour, whether and how much electricity the system is drawing from the grid ($L_i > P_{ac,i}$), or selling to it ($L_i < P_{ac,i}$).

$$G_i = P_{ac,i} - L_i \tag{39}$$

When $G_i > 0$, the value is multiplied by the appropriate monthly sell rate ($r_{sell,i}$) for that hour according to Table 12Table 11, resulting in an hourly income ($S_i = G_i \; if \; G_i > 0$). When $G_i < 0$, the value is multiplied by the appropriate buy rate ($r_{buy,i} \times (1 + r_{VAT})$) according to Table 11[27], resulting in an hourly expense ($E_i = G_i \; if \; G_i < 0$).

The yearly electricity cost with the system (C_{sys}) is given by equation (40). In case the value is negative it represents a cash payment to the system owner.

$$C_{sys} = \sum_1^{8760} (-1 * E_i) - \sum_1^{8760} S_i \tag{40}$$

The yearly electricity cost without the system (C) is given by equation (41)(40).

$$C = \sum_1^{8760} (L_i \times r_{buy,i} \times (1 + r_{VAT})) \tag{41}$$

The annual energy value (E_{val}) is the difference between C and C_{sys}, as given by equation (42), represents the annual savings resulting from usage of the system, and is the value that serves as input into the *cashloan* module for year 1.

$$E_{val,1} = C_1 - C_{sys,1} \tag{42}$$

For all subsequent years (n) in the analysis period (for this model´s purposes, years 2 through 25) the user selected inflation rate (I) is applied to r_{sell} and r_{buy} and the degradation rate (D) is applied to the $P_{ac,i}$, according to equations (43) (44) and (45), and $E_{val,n}$ is calculated for each year, completing the array of system inputs required for the *cashloan* module.

$$r_{sell,i,n+1} = (1 + I) \times r_{sell,i,n} \tag{43}$$

$$r_{buy,i,n+1} = (1 + I) \times r_{buy,i,n} \tag{44}$$

$$L_{i,n+1} = (1 - D) \times L_{i,n} \tag{45}$$

[27] In case the user-specified contracted capacity is below 3.45kVA, 3.45kVA is assumed. Any values of user-specified contracted capacity within the intervals on Table 11 will default to the capacity on the lower bound of that interval

2.2.2.3. Cashloan

The *cashloan* module takes as inputs the array of energy valuations for each year in the analysis period ($E_{val,j}$) and performs a cashflow analysis with the inputs specified in section II.2.2.1.3. Early testing of this calculation module for the residential PV system produced unexpected results, and further research into the calculation methods of the module produced insights as to why: the high degree of complexity of the U.S. tax code in relation to property and insurance tax deductions, the cross interaction between state and federal tax systems, coupled with the multiple tax credits and direct cash incentives and how they are valued for tax purposes are all incorporated into the module´s calculations, and, as the modules themselves are a "black-box"[28], this calculation cannot be changed. This conclusion was arrived at by using the "Send to Excel with Equations" function (in the results page for a simulation within SAM Desktop) and parsing through the excel file thus generated. This meant that many of the calculations are unrepresentative of Portuguese tax calculations and that some of the intended configurations that are required to run this model (e.g. string inverter replacement cost at half-way through system lifetime) are impossible to configure. Thus, the option was made to replace the *cashloan* computation module with its equivalent but reformulated spreadsheet calculator, removing all redundant or irrelevant calculations for the simulation in a Portuguese setting. This brought the added benefit of making it easier, in future improvements to the model, to easily incorporate other tax provisions, namely those specified under Lei 32/2012 and Lei 82-D/2014 (as mentioned in section I5.1).

Following the analysis of section I3.3.1 total installed system costs were determined. They are dependent on the inverter type chosen, module type and retrofit or new construction, and the values attributed according to Table 13. The total installed system cost (C_{total}) will be a function of system size (equation (14)), VAT and the registration costs (C_{reg}) from Appendix I, and given by equation (46)(75).

$$C_{total} = (C_{inst} \times (1 + r_{VAT}) \times P_{dc0}) + C_{reg} \quad (46)$$

Total debt (C_{debt}) and total equity (C_{equity}) are given by equations (47) and (48).

$$C_{debt} = C_{total} \times f_{debt} \quad (47)$$

$$C_{equity} = C_{total} \times (1 - f_{debt}) \quad (48)$$

For each operating year (n) in the analysis period ($0 \leq n \leq 25$), the calculations will take as inputs the annual energy value ($E_{val,n}$) from the *utilityrate5* module, and the annual operating costs ($C_{oper,n}$) given by equation (49), dependent on capacity costs ($C_{cap,n}$) and variable costs ($C_{var,n}$), given by equations (50) & (51). Operating costs will be reflected throughout all years in the analysis, with component replacement cost (for the case of string inverters) being added halfway through the lifetime of the project.

$$C_{oper,n} = C_{cap,n} + C_{var,n} \quad (49)$$

$$C_{cap,n} = (C_{O\&M} \times (1 + r_{VAT}) \times P_{dc0}) \times (1 + r_{inf})^{(n-1)} \quad (50)$$

$$C_{var,13} = \left(C_{string} \times (1 + r_{VAT}) \times P_{dc0}\right) \times (1 + r_{inf})^{(13-1)} \quad (51)$$

$$if\ inverter \neq microinverter, otherwise\ C_{var,n} = 0$$

[28] Meaning the user can only specify inputs and generate outputs, not actually configure the calculation algorithm itself.

Annual debt payments ($C_{loan,n}$) depend on the loan rate (r_{loan}) and term (t_{loan}), debt balance ($D_{bal,n}$), interest (I_n) and principal (P_n) payments, calculated according to equations (52) to (55), for all $0 < n \leq t_{loan}$.

$$C_{loan,n} = I_n + P_n = \frac{r_{loan} \times C_{debt}}{(1-(1+r_{loan})^{-n}} \quad (52)$$

$$\begin{cases} D_{bal,1} = C_{debt} \\ D_{bal,n+1} = D_{bal,n} - P_n \end{cases} \quad (53)$$

$$I_n = D_{bal,n} \times r_{loan} \quad (54)$$

$$P_n = C_{loan,n} - I_n \quad (55)$$

The pre-tax cashflow for each year (CF_n) is is given by equation (56):

$$\begin{cases} CF_0 = -C_{equity} \\ CF_n = -(C_{oper,n} + C_{loan,n}) \end{cases} \quad (56)$$

The income tax (r_{IRS}) will be applicable to the taxable income generated by the system by selling power to the grid and will be assumed constant throughout the lifetime of the project. Taxable yearly income ($C_{tax,n}$) occurs only if there´s a cash payment to the system owner in year n (see equation (42)), and results in a yearly tax collection (Tax_n) given by equation (58).

$$C_{tax,n} = E_{val,n} \quad , if\ n > 0 \ \cap \ E_{val,n} < 0 \quad (57)$$

$$Tax_n = C_{tax,n} \times r_{IRS} \quad (58)$$

The taxes are added to the pre-tax cashflow to calculate the after tax annual costs ($C_{AT,n}$), as per equation (59)

$$\begin{cases} C_{AT,0} = CF_0 = -C_{equity} \\ C_{AT,n} = CF_n + Tax_n \end{cases} \quad (59)$$

The after tax cashflow, net of financing ($CF_{AT,n}$) is the after tax annual costs plus the value of the enrgy generated by the system ($E_{val,n}$), and is given by equation (60). For payback period calculations, the project cashflows are required (cashflows excluding the financing cashflows, $CF_{P,n}$), and include the total installed system cost and the loan payments, as given by equation (61)

$$\begin{cases} CF_{AT,0} = C_{AT,0} = -C_{equity} \\ CF_{AT,n} = C_{AT,n} + E_{val,n} \end{cases} \quad (60)$$

$$\begin{cases} CF_{P,0} = -C_{total} \\ CF_{P,n} = CF_{AT,n} + I_n + P_n \end{cases} \quad (61)$$

With the cashflow calculations, one can derive the payback period by first calculating the cumulative cashflows (CF_{cum}) for each year as per equation

$$\begin{cases} CF_{cum,0} = CF_{P,0} \\ CF_{cum,n} = CF_{cum,n-1} + CF_{P,n} \end{cases} \quad (62)$$

For year n where $CF_{cum,n} > 0$ (the last year in the payback period, k), the fraction of that year that is within the payback period (f_{PB}) is given by equation (63), and the payback period is calculated with equation (64).

$$f_{PB} = \frac{CF_{cum,k-1}}{CF_{P,k}} \tag{63}$$

$$PB = (k-1) + f_{PB} \tag{64}$$

The net present value (NPV) is the present value of $CF_{AT,n}$ at the nominal discount rate (r_{nom}), as seen in equation (65). As discussed in section II.2.2.1.3.2, the r_{nom} is dependent on the real discount rate (r_{real}), which in turn is equal to the weighted average cost of capital ($WACC$) assuming the cost of equity is equal to the inflation rate (r_{inf}), given by equations (66) and (67).

$$NPV = -C_{equity} + \sum_{n=1}^{n} \frac{CF_{AT,n}}{(1+r_{nom})^n} \tag{65}$$

$$r_{nom} = ((r_{real}+1) \times (r_{inf}+1)) \times 100 \tag{66}$$

$$r_{real} = WACC = r_{inf} \times (1 - f_{debt}) + r_{loan} \times (f_{debt}) \tag{67}$$

The project internal rate of return (IRR_P) is the rate of return that makes the NPV of all project cash flows equal to zero (solving equation (68) for IRR_P)). The equity IRR (IRR_E) only uses after tax cash flow, net of financing (solving equation (69) for IRR_E).

$$0 = -C_{total} + \sum_{n=1}^{n} \frac{CF_{P,n}}{(1+IRR_P))^n} \tag{68}$$

$$0 = -C_{equity} + \sum_{n=1}^{n} \frac{CF_{AT,n}}{(1+IRR_E))^n} \tag{69}$$

The levelized cost of energy can be nominal or real, the former being a current dollar value, and the latter constant dollar, inflation-adjusted value. $LCOE_{real}$ is more appropriate for long-term analyses (see equation (70), adapted from equation (1)), accounting for inflation over the project life, while $LCOE_{nom}$, in current dollars, is more appropriate for short-term comparisons (see equation (71), adapted from equation (1)). Both $LCOE$ are a function of after-tax project costs ($C_{AT,n}$) and annual energy produced (Q_n), which for year 1 is equal to the array AC energy output calculated by *pvwattsv1* ($P_{ac,array}$, see equation (16)), and is subsequently decreased each year by the specified degradation rate (D), according to equation (72).

$$LCOE_{real} = -C_{equity} - \frac{\sum_{n=1}^{n} \frac{C_{AT,n}}{(1+r_{nom})^n}}{\sum_{n=1}^{n} \frac{Q_n}{(1+r_{real})^n}} \tag{70}$$

$$LCOE_{nom} = -C_{equity} - \frac{\sum_{n=1}^{n} \frac{C_{AT,n}}{(1+r_{nom})^n}}{\sum_{n=1}^{n} \frac{Q_n}{(1+r_{nom})^n}} \tag{71}$$

$$\begin{cases} Q_1 = P_{ac,array} \\ Q_n = Q_{n-1} \times (1-D) \end{cases} \tag{72}$$

II.3. Input Data

The starting point for the analysis will be a 3DGIS/CIM model of solar radiation exposure in Lisbon´s Alvalade neighborhood, based on the work of Machete, R. (2016) and Silva, J.P. (2016) providing the necessary data on solar resource availability, quality and physical availability of area for deployment. Figure 12 presents the flowchart with the necessary steps to obtain the input data for the simulator.

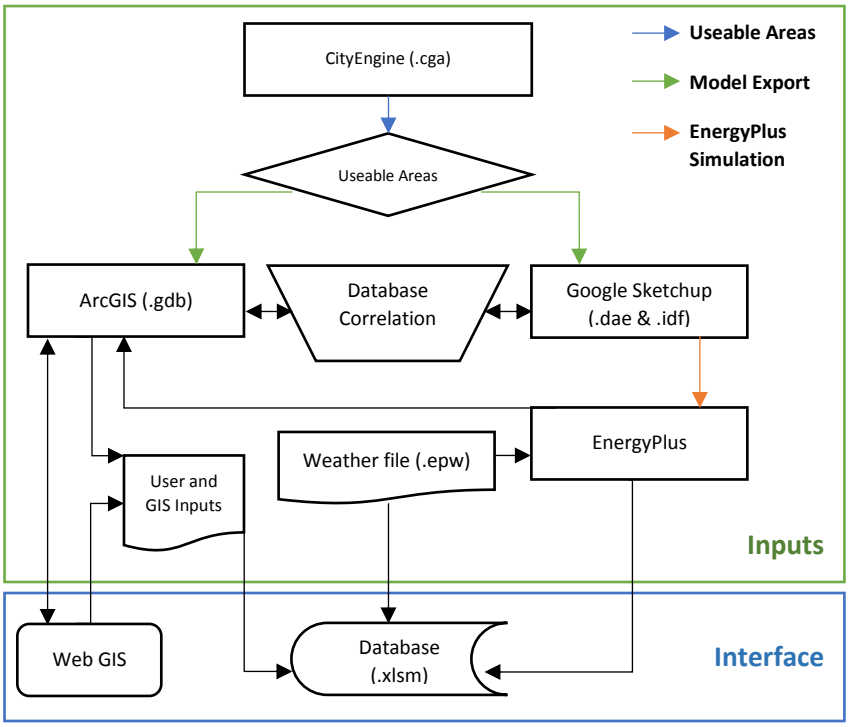

Figure 12 - Flowchart for Simulator Input Generation

3.1. 3D-GIS/CIM cityscape model

For the purposes of this study, topographical data derived from Silva, J.P., (2016) will be used. A 3D model of the Alvalade neighborhood in Lisbon was developed resorting to a computer-generated architecture (CGA) algorithm to model complex city morphology from a given set of georeferenced data on building footprints and architectural rules, to automatically create an urban landscape that captures the essence of the area in question. The model was created in CityEngine and based on the buildings´ footprints and running code with a CGA rule file, a volumetric representation of the neighborhood was achieved at LoD2. The option to use this data set instead of real 3-D models of the neighborhood allows us to circumvent one the main obstacles of urban solar potential analysis, which is getting adequate 3D models of the urban landscape. This is a requirement to correctly capture the complex lighting and shading interplay at work in the urban fabric, which significantly impacts the solar energy availability and thus the solar electricity production.

Using CGA also allows for the adaptation of the model to any potential city environment with a distinct and repeatable morphology, requiring only minimal GIS data sets on the planimetry, altimetry and surface features of the area (more easily available than full fleshed 3-D models) and a set of basic architectural instructions to spawn the 3-D city model.

Not using real 3-D data will ultimately limit the real-world application of any results derived from this study, but it is a trade-off between accuracy of the results and the applicability of the methods described to a wider set of locations.

The choice of the study area, the Alvalade neighborhood, was made considering the diverse factors that can impact the technological and economic performance of urban implemented PV solutions. As noted by Chow et al. (2016), the more diverse a range of characteristics of a study area, the more suitable it is for evaluating the PV potential of distributed generation. As a densely populated and mainly residential area, with buildings of different morphology, age, height and function is an ideal candidate for analysis.

3.2. Irradiation, Shading and Meteorological Data

Irradiation data was derived by the methodology in Machete, R., (2016), building on the model of Silva, J.P., (2016), to compute the incident solar radiation on the study area, accounting for shading and area availability at the urban level. This application will give us a detailed solar irradiance map overlaid on the urban fabric of the Alvalade neighborhood.

In the original implementation presented in Machete (2016), the Kumar radiation model is used, with solar coordinate values from 2011. This model is validated for clear-sky conditions only, and takes into account extraterrestrial solar flux, sun position in the sky at all times during the day, surface coordinates for the study area, the influence of the air mass between the earth´s surface and outer space and the presence of water vapor and aerosols in the atmosphere (Kumar et al., 1997). It was a methodology developed to assess solar radiation in remote areas where ground measurement is particularly hard and is especially suited to model solar exposure gradients between different areas.

The methodology has since been modified by the same researcher, overcoming some of its limitations (e.g. it did not calculate diffuse radiation and was computing solely for summer and winter solstice) and irradiation and shading are now computed using EnergyPlus software and the INETI TMY 2005 meteorological data set.

The main steps used to obtain the solar radiation on the panels were: 1) determination of useable area for deployment and division of the surfaces in the model in CityEngine; 2) exporting the resulting model to ArcGIS (GIS database file, *.gdb* format) and to Google Sketchup (Collada file, *.dae* format); 3) converting from *.dae* to *.idf* file within Google Sketchup; 4) export the *.idf* file, jointly with the weather file, to EnergyPlus, and run the irradiance and shading simulations; 5) append the results from these simulations to the attribute table of the *.gdb* file created in step ii).

1) Useable areas and division of surfaces

Useable area for PV deployment was determined by further subdividing façade and rooftop building elements according to specific dimensional constraints. Because of the high LoD (LoD2) of the CityEngine 3DGIS/CIM model, possible areas of the rooftops and façades for PV deployment are easily identifiable, and all areas identified as tiles on the roof and plaster on the façade were divided with the split function.

The division of the model´s useable surfaces into surfaces representative of the PV Panels dimensions (so irradiation calculations can be done on those surfaces in step 4)) is determined by the area occupied by each PV panel on the surfaces, which depends on their dimensions, the GCR and the required service areas.

The determination of PV panel dimensions was done according to average PV and TF panel size (calculation details in II.2.1.1.1), and was approached in two distinct ways, depending on whether roofs or façades are being considered. For roofs, as c-Si PV panels are being modeled, an area of influence for each point of 1.75m^2 (see section II.2.1.1.1, Table 8), with width and height constraints of 1mx1.75m, replicating the average dimensions of c-Si panels. For façades, a similar approach was used, but focusing on the area of influence (0.72m^2, see section II.2.1.1.1, Table 8) unconstrained by the width and height of TF panels. This is because façades present much more geometric and material limitations on useable area than roofs and TF panels are dimensionally much more variable than c-Si panels, implying an adequate fit for any surface dimension can easily be found in the market.

The GCR was assumed to be 1 for both cases, as panels will be assumed parallel to their respective surfaces and packed together (in practice this would be near impossible as the modular and standard sizes of the panels coupled with the irregular geometry, areas and building materials of rooftops plus regulatory constraints limit total use of available rooftop area). On roofs with a 30º tilt, this assumption is close to their optimal tilt for the 38º latitude of Lisbon (Breyer & Schmid, 2010), and previous research has shown the impact of suboptimal tilt angle in favor of higher GCR tends to provide higher yields (Culligan & Botkin, 2007). In the case of flat roofs (which aren´t modeled by this simulation) this assumption would not hold, as the installer would have to tilt the panels at a different angle than their surface (closer to the latitude angle of Lisbon[29]), and the resulting GCR would be below 1. For façades, no tilting was assumed as a that would not be a viable option from a regulatory, construction and architectural point of view.

No service areas were considered as it was unlikely that PV panels on roofs or façades would completely cover the respective surfaces, thus leaving available area for all maintenance and access.

With the above constraints, the split function was applied to obtain the individual building surfaces (Figure 13). As a consequence of the above mentioned, the individual surfaces created on the façades to represent each TF module vary considerably in shape and in area, while the those created on the rooftops all follow strict area and dimensional constraints.

```
Seccao -->
      split(y) {~0.6 : split(x){~1.2 :Painel_Normal}*}*
      report("Local","Fachada")

Seccao_telhado -->
      split(y) {1.7535 : split(x){0.99:Painel_Normal}*}*
      report("Local","Cobertura")
```

Figure 13 - CGA Code for Determining PV Deployment Area

2) Exporting the model

The 3DGIS/CIM with the individual building surfaces has to be exported from CityEngine in two formats, one for ArcGIS (*.gdb*) and the other for Google Sketchup (*.dae*)

The export to ArcGIS is done in *.gdb* format, with all the relevant model attributes, and some extra attributes by altering the CGA code (Figure 14) to report the panel ID, Azimuth, Zenith, Slope, Area, Width and Height, which are lost in the *.dae* export and are irrelevant for EnergyPlus calculations.

```
report("ID",uid)
report("Azimuth_Angle",geometry.angle(azimuth))
report("Zenith_Angle",geometry.angle(zenith))
report("Slope_Angle",geometry.angle(maxSlope))
report("Area",geometry.area)
report("size_X",scope.sx)
report("size_Y",scope.sy)
```

Figure 14 – Extra code for the CGA rule file for export to ArcGIS

[29] The optimal angle for south oriented BIPV systems in the northern hemisphere has been shown to coincide with the latitude angle in 98.6% of studied regions (Cheng, Jimenez, & Lee, 2009)

The export to Google SketchUp is done in *.dae* format (Collada file type), a more visual format, readable by Google Sketchup, but that loses some of the attributes of the panels, including the Object ID, which is necessary to maintain the relationship between the two databases. Only 2 blocks surrounding the chosen building are exported for the analysis, with the building itself exported in LoD2, divided in panels (as detailed building surfaces), and the surrounding blocks in LoD1 (as a shading group).

3) Conversion of *.dae* file to *.idf* file format in Google Sketchup

To create a file format that EnergyPlus can read, the Collada file was converted to *.idf* by using the Legacy Open Studio toolbar extension in Google Sketchup. The *.idf* file created has information relating to the site location, surfaces, materials, and other relevant attributes for the EnergyPlus calculations, and generates a new set of attributes for the building surfaces (e.g. new Object IDs), totally unrelated to the original Object IDs exported from CityEngine to ArcGIS. Because of this, each panel in Google Sketchup had to be visually inspected and compared to its representation in ArcGIS, a new column in the attribute table of the ArcGIS file was created, and for each panel in the *.gdb* attribute table, the corresponding code generated in the *.idf* file was manually inserted. Without this step, no results from any calculation in EnergyPlus could be used, as they would refer to panels whose object IDs had no correspondence in the ArcGIS attribute table.

4) EnergyPlus irradiance and shading simulation

The *.idf* file, jointly with the chosen weather file (INETI Synthetic data for Portugal - 2005 Lisbon EPW file, whose details can be found in INETI (2015) are exported to EnergyPlus for irradiance and shading simulations over all hours (8760) of one year. The IDF editor is used to configure which variables to report and how the *.idf* file should be handled by EnergyPlus, and the EP launch is used to run the simulation on each building surface (i.e. PV panel). EnergyPlus uses the Perez, R., (1990) algorithm to determine the direct and diffuse components of irradiance (with anisotropic skies described as an isotropic dome with circumsolar and horizon brightening components) and the inbuilt shading module (EnergyPlus, 2018) to account for shadows cast by the shading group. No vegetation is considered as the area under study does not have shading by vegetation.

The relevant outputs from the EnergyPlus simulation are site specific (i.e. Alvalade Neighborhood) and panel specific. The site specific data includes all Environment data, correcting the weather file´s irradiation values to account for the location of the Alvalade neighborhood relative to the coordinates in the weather file, namely hourly *Site Diffuse Solar Radiation Rate per Area* (GHI_{Alv}, in W/m^2, with a 1.42% reduction in total annual GHI vs. the weather file), hourly *Site Direct Solar Radiation Rate per Area* (DNI_{Alv}, in W/m^2, with a 2.47% reduction in total annual DNI vs. the weather file), hourly *Site Solar Azimuth Angle* ($\gamma_{sun,E+}$ in degrees) and hourly *Site Solar Altitude Angle* (inverse of the zenith, $\omega_{sun,E+} = 90° - \gamma_{sun,E+}$, in degrees).

Panel specific data includes hourly values, for every panel, of the *Surface Outside Face Incident Sky Diffuse Solar Radiation Rate per Area* ($I_{d,sky,E+}$ in W/m^2), *Surface Outside Face Incident Ground Diffuse Solar Radiation Rate per Area* ($I_{d,ground,E+}$ in W/m^2), *Surface Outside Face Incident Beam Solar Radiation Rate per Area* ($I_{b,E+}$ in W/m^2), and the sum of these three components, the *Surface Outside Face Incident Solar Radiation Rate per Area* ($I_{poa,E+}$ in W/m^2). It also includes hourly and panel specific values for the *Surface*

Outside Face Beam Solar Incident Angle Cosine Value ($\cos(\alpha_{E+})$) which as was seen in section II.2.1.3 can be used to derive the individual panel´s DNI_{E+} (see equation (21))

All these outputs come in a *.csv* file with a single sheet, which was converted to a more legible format, with each variable in a sheet, to make it more easily imported back to ArcGIS. To import the results into ArcGIS, one must simply create a table with the Object ID in a column and fill the remaining columns with the results per panel the user wishes to import.

Because the PV panel model takes information from the attribute table of the ArcGIS file, the calculation results of EnergyPlus and the Lisbon EPW 2005 weather file, an additional Excel *.xlsm* file ($Basetable.xlsm$) was created that joins these three databases, and will form the backbone for all PV panel simulations (hereby referenced as the *database*). It includes all relevant POA ($I_{poa,E+}$), DNI (DNI_{E+} , derived from equation (21)), Weather and Panel attributes data. To make the database file lighter, all redundant information was eliminated, namely the sheets with $I_{d,sky,E+}$, $I_{d,ground,E+}$, $I_{b,E+}$ and $\cos(\alpha_{E+})$, reducing the file size to 30% of the original size.

II.4. Interface

To connect the inputs of the previous section and the PV simulator, an interface had to be designed, to allow the two-way communication across software platforms and between the user and the simulator. Figure 15 presents the flowchart for the Interface structure.

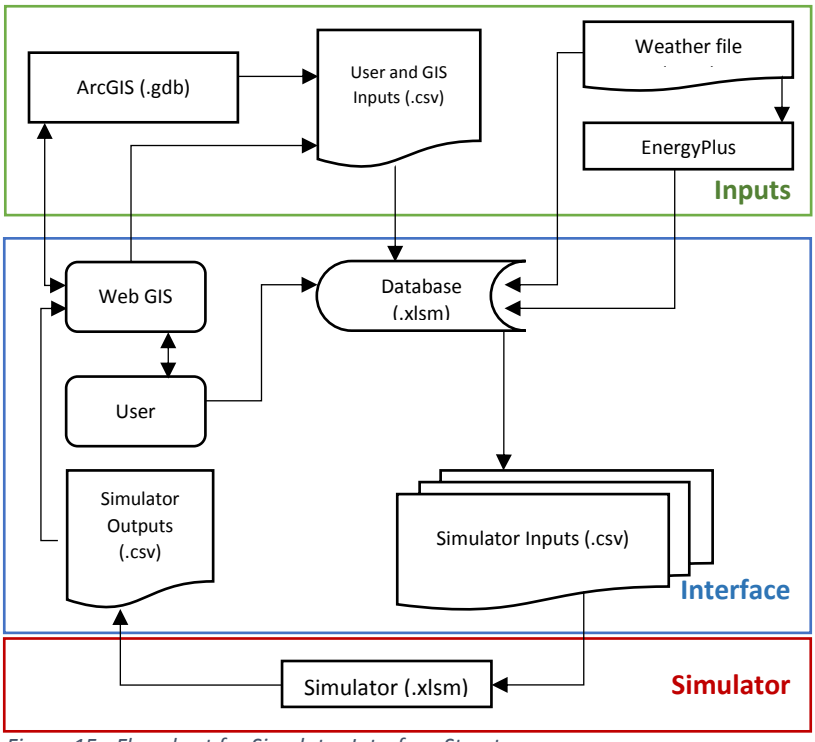

Figure 15 - Flowchart for Simulator Interface Structure

4.1. User query and manipulation of the 3D model and irradiance data

The query and manipulation of the data will be done via a webGIS interface available on the internet, which will enable the user to interact with the 3D-GIS model within ArcGIS, select and design the PV system and run the simulation (see Figure 16). The GIS and irradiance data shall be displayed on a 3D model within the web GIS platform, with appropriately defined access policies for the manipulation of the model by the user. While visualizing the buildings´ morphology and its irradiation levels, the user will be prompted to design his PV system by selecting pre-determined building surfaces (see section II.3.2) and defining on a standardized form the variables relevant to the technical (e.g. module type, system losses, inverter type and efficiency) and financial performance (e.g. financing structure, occupancy, utility bill details). This process can be automated by Python code within the webGIS platform, to generate a *.csv* file (*Input_ArcGIS.csv*, see Figure 17) which feeds into the *database* (*Basetable.xlsm)*, subsequently running the simulator routine and returning its results.

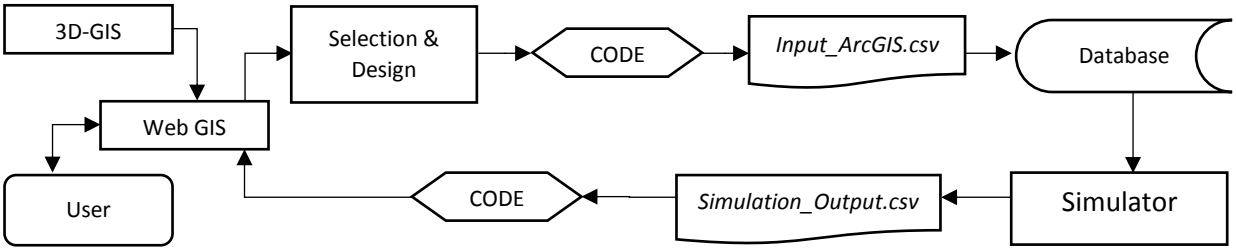

Figure 16 – Flowchart for design of User and Simulator Interface

OBJECTID	Module Type	System Losses	Inverter Efficiency	Inverter	Nº Pers/Household	Average Surface Area/Household	Nº Stories	Nº Households	Cycle	Contracted Capacity	New Construction	VAT	Debt Fraction	Loan Interest	Loan Term	IRS	Inflation	Discount Rate
64	Standard	11.42	0.96	No Option	2.6	116.05	4	8	Bi-hourly	6.9	0	0.23	0.5	0.03	7	0.35	0.015	
65																		
66																		

Figure 17 – Input_ArcGIS.csv file structure

4.2. Software interface development

This chosen panels´ attributes in *Input_ArcGIS.csv* are imported and compared against the *Basetable.xlsm* database created in section II.3.2, retrieving for each panel it´s hourly irradiation data (DNI and POA) and attributes such as placement (rooftop or façade), tilt, azimuth and area. A maximum of 100 simultaneous panels was assumed for the model, enabling the simulation of a very large systems for residential uses. All the relevant data is grouped together, and depending on whether the user selected No Option, String or Micro inverter, is treated differently, with the workbook running predetermined calculations.

For “No Option” inverter, the hourly average irradiation for all the selected panels is calculated (equations (73) and (74)), assuming the irradiation is homogeneous over all the panels selected and for the “String” inverter, the hourly minimum irradiation incident on all the selected panels is calculated (equations (75) and (76)), simulating the voltage cap losses deriving from partial shading of a module on a string in a series circuit. For both these inverter choices, a single weather and irradiation file is generated by running a macro,

for a group of PV panels with same tilt, azimuth, placement, and a total area resulting from the sum of the individual panels´ areas, and they are simulated within PVWatts as a single aggregate entity.

$$I_{poa,i} = avg\ (I_{poa,ij}) \quad (73)$$

$$DNI_i = avg\ (\ DNI_{ij}) \quad (74)$$

$$I_{poa,i} = min\ (I_{poa,ij}) \quad (75)$$

$$DNI_i = min\ (\ DNI_{ij}) \quad (76)$$

i = number of hours (1 to 8760); j = panel identification

However, for the "Micro" inverter option, because of the ability to generate electricity independently of the output of nearby PV panels, specific weather and irradiation files must be created for each panel, and each panel´s output gauged independently and then summed. This requires the creation of weather and irradiation files of equal number to the PV panels being modeled (which is also done automatically with a macro), and the individual simulation of each panel in PVWatts, which is more time consuming but the only way to account for the panels´ differentiated solar exposures.[30]

The outputs of the macro within the workbook consist of two file types: i) a *.csv* weather file (*Weatherfile.csv,* in the automatically created folder *Weather_Sim DD-MM-YYYY hh-mm-ss*), consisting of a mix between Portugal - 2005 Lisbon EPW file and panel specific DNI and POA data (i.e. a standard *.epw* file, converted to *.csv* format[31] with specific formatting regarding column placement and appending of the POA data series, see Figure 8); ii) a *.csv* input file (Figure 18) with the technical and economic performance variable inputs for the simulation (*InputPVWatts.csv* in the automatically created folder *Input_Sim DD-MM-YYYY hh-mm-ss*) based on information from the user and the *database*. In the case of "Micro" inverter choice, the weather files are named *Micro_Panel_i.csv* and the input files *Micro_Panel_Inputi.csv* (i being the sequential number of the PV panel being modeled). The *InputPVWatts.csv* refers to module types as 0,1 and 2 (Standard, Premium and Thin film), inverter types as 0,1 and 2 (No Option, String and Micro) and Local (placement) as 0 and 1 (Rooftop and Façade).

Number Panels	Module Type	System Losses	Inverter Efficiency	Inverter	Tilt	Azimuth	Local	Total Area	Nº Pers/Household	Average Surface Area/Household	Nº Stories	Nº Households	Cycle	Contracted Capacity	New Construction	VAT	Debt Fraction	Loan Interest	Loan Term	IRS	Inflation	Discount Rate	OBJECTID
16	0	11.42	0.96	0	29.99998	247.8646	0	27.77544	2.6	116.05	4	8	1	6.9	0	0.23	0.5	0.03	7	0.35	0.015		64
																							65
																							66
																							67

Figure 18 – InputsPVWAtts.csv file structure

[30] The option to aggregate panels into a single system for the "No Option" and "String" inverter option has some drawbacks, namely only enabling the simulation of panels on the same plane, azimuth and placement. However, it is computationally much more efficient to simulate one single system made of many PV panels than to simulate each panel´s output individually and then sum them. This was the option taken for "Micro" inverter option, but only because no other way was found to account for the effect of different irradiations on the modules. Individual simulation of each panel would also be possible for the other two inverter options, so long as care is taken to account for the homogeneous irradiation assumption in "No Option" inverter (the hourly AC power resulting from the selected PV panels would be the hourly average AC power of all panels, multiplied by the number of panels) and the voltage mismatch assumption in the "String" inverter option (the hourly AC power resulting from the selected PV panels would be the hourly minimum AC power of the lowest producing panel on the string, multiplied by the number of panels).

[31] Before being used by the SSC, the *.epw* file must be converted to a compatible *.csv* format. This was done with a macro available within SAM desktop ("*Solar Resource File Converter*")

II.5. Simulator

The simulator of PV panel production and economic performance is made up of an Excel Macro-enabled workbook (*Simulator.xlsm*) designed to run macros for the production (*pvwattsv1*), load estimation (*belpe*) and economic output (*utilityrate5*) of a PV system, followed by a cashflow analysis. Figure 19 presents the flowchart for the simulator structure.

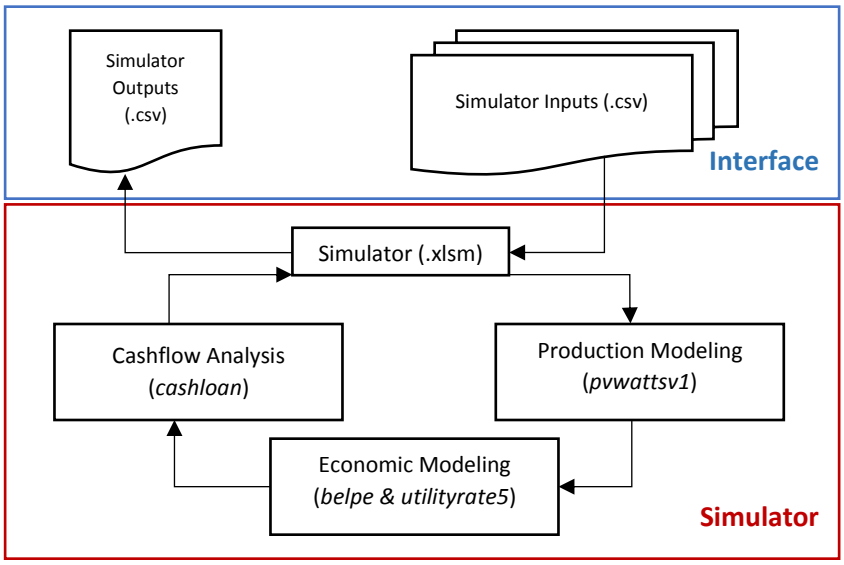

Figure 19 - Flowchart of Simulator Structure

5.1. Implementing PVWatts

The implementation of the PVWatts model was made through Excel macro written in VBA language (Visual Basic), since Excel looked like a suitable candidate to interact with both SAM´s SSC and ArcGIS applications, due to its universality and relative simplicity. In order to get us started with the correct scripting, function calls and syntax required to interact with the API to run the SSC, SAM Desktop application *Generate Code Option* was used on a standard simulation of a PVWatts case, using the default values provided in SAM.

Generating a VBA code returns 3 files: i) *.bas* file (basic file, *untitled.h*) where the actual code for that specific (yet untitled) simulation is written in BASIC language. The .bas file contains all the written code with the instructions to be run as a macro in VBA Excel; ii) *.h* file (header file, *sscapi.h*) which is the API (application programming interface) in C language. The .h file reads the instructions from the .bas file and communicates them to the SAM simulation core; iii) *.dll* file (dynamic library file, *ssc.dll*), which is the actual SAM Simulation Core´s dynamic library, where all calculations are made, and which works much the same way as an executable (.exe) file. Because the code will be edited, the .bas file will become irrelevant. However, the header and the library file must be kept as they are the simulation engine.

5.1.1. Pvwattsv5 subroutine as generated by default for PVWatts

The standard code generated by SAM for a PVWatts simulation includes the steps in Figure 20.

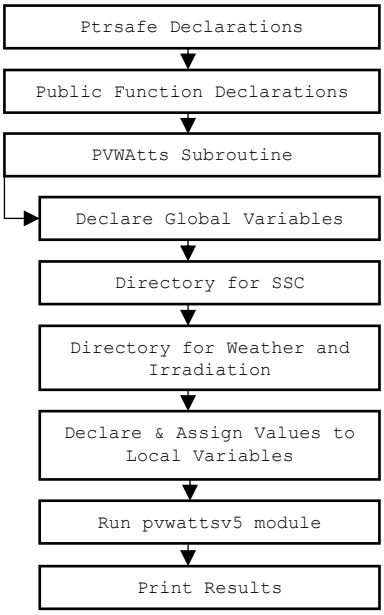

Figure 20 –Flowchart for Standard PVWatts simulation VBA code structure

Ptrsafe Declarations for all the functions used by the SSC is required, as these are functions created on a 32-bit system but will be compiled on a 64-bit machine (as the one used for these simulations). Existing Declare statements will not compile in 64-bit VBA until they have been marked as safe for 64-bit by using the Ptrsafe attribute (Microsoft, 2018).

Public Function Declarations are also required, as they are the functions used throughout the VBA code, executing the prebuilt data retrieval and management functions of the SSC in a VBA environment.

PVWatts Subroutine is the core of the simulation, with global variable declaration, assignment of the directories for the API (*.h*) and Library (*.dll*) files, and for the weather and irradiation data (SAM compatible *.csv* file), followed by local (simulation) variable declaration and value assignment. These steps are followed by computation of the *pvwattsv5* module and printing of its results.

In order to fully understand the VBA code, and to enable its editing, it is crucial to use the SSC SDK Tool to understand variable properties and the SSC Guide (Dobos & Gilman, 2017) to understand function declarations and their properties, as well as the overall code structure.

5.1.2. Adapting default subroutine for pvwattsv1

To fully automate the PV technical performance simulation, significant changes were made to the default code generated by SAM, to account for, among other things, user supplied inputs (including POA, not a standard feature of *pvwattsv1*) and the choice of inverters. The original code was incorporated into the *SAM VBA Simulator.xlsm* Excel workbook (the *simulator*), which will serve as the simulation interface and will run a Macro with the thoroughly edited VBA code for the simulation. Observing Figure 21, the initial steps in the VBA code remain the same, with Ptrsafe and Public Function Declarations. However, once inside the PVWatts subroutine and after declaring the Global Variables, the user is prompted to choose an input file ("*Select PV Panel Input for PVWatts Simulation*"), and should select *InputPVWatts.csv* (or *Micro_Panel_Input1.csv* in the case of Micro inverter), previously generated with the *database* (see section II.4.2). This step will copy the values from the input file into a sheet of the *simulator* (sheet *External_Inputs*). This is followed by a prompt to choose a weather and irradiation input file (*"Select Weather and Radiation Input for PVWatts Simulation")*, and the user should select *Weatherfile.csv* (or *Micro_Panel_1.csv* in the

case of a Microinverter system) previously created with the *database*. This step creates a variable with the directory location information for the relevant weather and irradiation file. Because of the different approaches to simulation, the model evaluates the input values and, in case the inverter type is Micro inverter, runs a specific approach to *pvwattsv1* (Micro Panel PVWatts Simulation, Figure 23). In case the "String" or "No Option" inverters have been selected, it runs the Standard PVWatts Simulation (Figure 22).

Before the simulation with the *pvwattsv1* module, the *simulator* workbook was designed to run calculations on the values imported from the input file and generate the correct values to be subsequently assigned to the variables within the *pvwattsv1* module. These calculations follow the determinations of section II.2.1.3 and the impacted local variables are : i) the nameplate capacity of the PV system; ii) module type; iii) derate factor; iv) inverter efficiency; v) tilt; vi) azimuth; vii) temperature coefficient; viii) anti-reflective glass enabler; ix) track mode; x) INOCT; and xi) GCR.

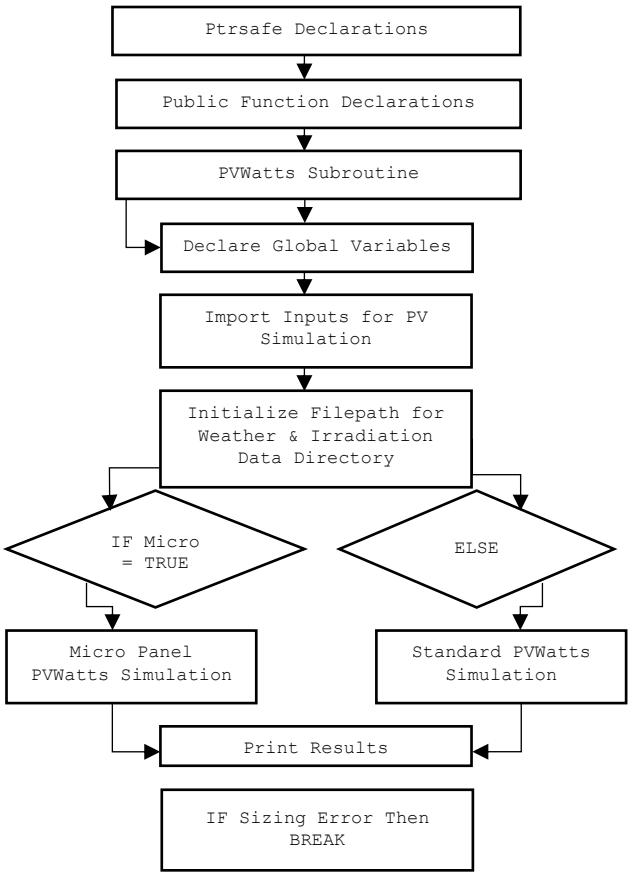

Figure 21 – Adapted Flowchart for PVWatts simulation VBA code structure

In the Standard PVWatts Simulation, the local variables are declared and initialized with the values as determined in the previous paragraph. Looking specifically at the user provided POA data, as it is not a standard feature of *pvwattsv1*, some extra steps had to be taken to initialize this array variable. Specific functions within the VBA code had to be created to access, parse and transform the range of POA data within the weather file into an array which *pvwattsv1* could use in its calculations[32].

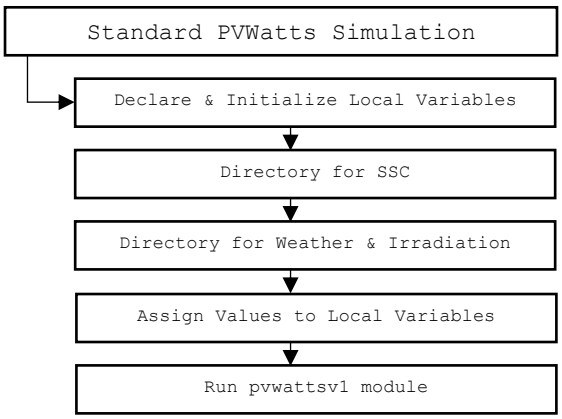

Figure 22 – Standard Flowchart for PVWatts Simulation VBA Code Structure

This step is followed by assignment of the directories for the API (*.h*) and Library (*.dll*) files, and assignment of the user provided directory location for the weather and irradiation data.

[32] Function `POA Array()` accesses the weather file, its values are copied to a multidimensional array of doubles with Function `getDataFromFile()`, and its values are parsed with Function `Slice_Array()` to return a single column array of doubles with 8760 values for POA irradiation

In the value assignment portion of the code, the *enable_user_poa* variable had to be set to 1, and all other variables are assigned the values as previously initialized. The *pvwattsv1* module can then be run, and its results can be printed in a workbook sheet ("*Outputs_pvwatts*"), including (but not limited to) the total Annual AC energy produced, the hourly DC energy produced, hourly AC energy produced, Total POA (user provided), Transmitted POA (corrected for angle of incidence) and Cell Temperature. For a full list of available output variables, consult the SSC SDK Tool.

The *pvwattsv1* module concludes by checking if the system nameplate capacity being modeled exceeds the total contracted capacity of the building[33] or the annual production exceeds the annual load calculated from the user inputs for the *belpe* module, as per the sizing rules laid out in DL 153/2014 (see Appendix I), displaying an error message in case that is true, stopping the code and prompting the user to restart with an adequately sized system or to review the parameters for the load calculation.

In the Micro Panel PVWatts Simulation, as mentioned in section II.4.2, each panel is simulated independently, and the resulting hourly AC power generated by each panel is summed in the end of the simulation to give the total system output. Due to this, the structure of the VBA code is significantly affected, and initially runs a Loop for each panel being simulated. This Loop starts Importing the input file for the panel being simulated (first *Micro_Panel_Input1.csv,* then *Micro_Panel_Input2.csv*, and so on), proceeding to determine the directory location information for the relevant weather and irradiation file (first *Micro_Panel_1.csv* then *Micro_Panel_2.csv* and so on) and assigning it to a variable.

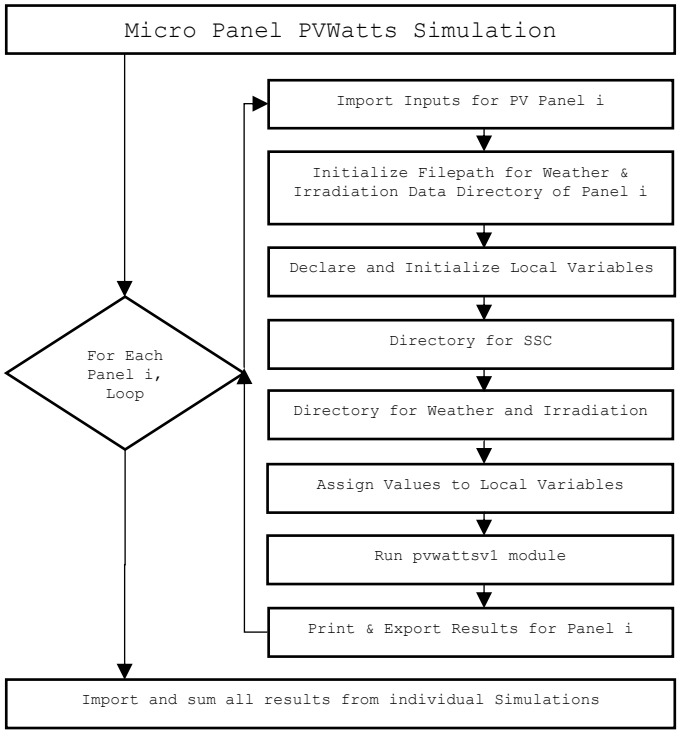

Figure 23 – Micro Panel PVWatts Simulation VBA Code Structure

Following this step, all subsequent steps are similar to the Standard PVWatts Simulation, with all local variables declared and initialized, directories for the API, Library and the weather and irradiation file assigned, and values assigned to the input variables of *pvwattsv1*. The module is run, and its results are printed in a workbook sheet ("*Outputs_pvwatts*").

However, as this involves looping through the panels, there is a need to store the results for each panel simulation. This is addressed by copying the results of each simulation *i* into a new *.csv* file

[33] Because the DC/AC ratio is 1 (see section II2.1.1.1), the system´s AC output is the same as its nameplate capacity, and thus the latter, jointly with the sum of all contracted capacities of each household within the building, can be used to gauge the compliance of the system sizing with the legal framework

(*Micro_Panel_PVWAttsOutputi.csv,* stored in automatically created folder *OutputPVWattsMicro DD-MM-YYYY hh-mm-ss*).

After running the complete loop through all selected panels, the macro retrieves the results from each simulation, copies them to the workbook sheet *OutputsPVWattsMicro* and then proceeds to sum all the hourly values for the AC produced power of each PV panel at each time step, printing the resulting total hourly AC energy production and total Annual AC energy production in the workbook sheet *OutputsPVWatts.*

5.2. Implementing the Economic Model

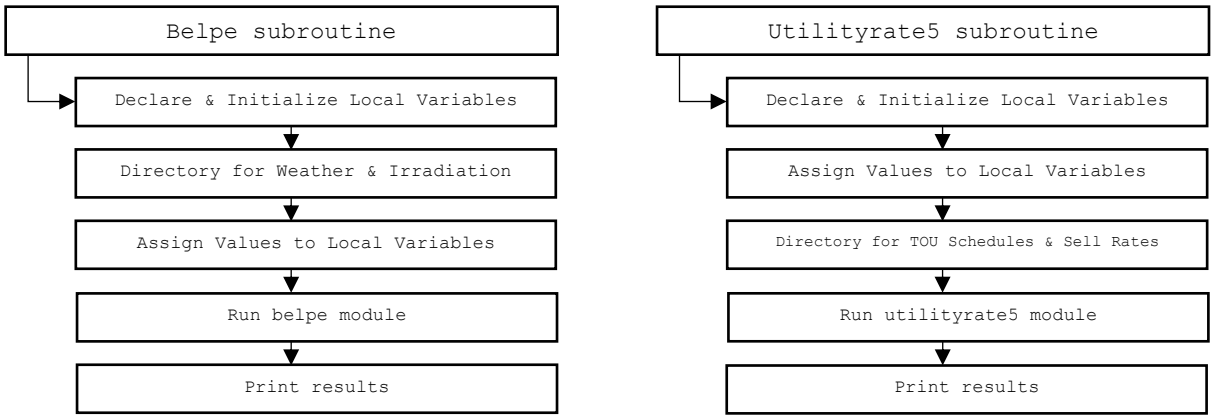

Figure 24 - Standard Flowchart for belpe and utility rate5 Simulation VBA Code Structure

Both the *belpe* and *utilityrate5* modules follow a very simple structure when implemented in VBA, synthesized in Figure 24

In the *utilityrate5* module, the weekend and weekday TOU schedules are implemented with a matrix (table in *.csv* format), with columns representing hours, rows months, and numbers representing the different TOU rates.

The *cashloan* spreadsheet calculator is set-up to transform the inputs mentioned in section II.2.2.1.3 and calculate step-by-step according to equations (46) to (72) in section II.2.2.2.3, returning the economic evaluation metrics.

After conclusion of all the calculations, the results are exported to a Folder named *Simulation Results_DD-MM-YYYY_hh-mm-ss* wich contains a *.csv* file ("*Simulation_Output_DD-MM-YYYY_hh-mm-ss.csv*"), in the correct format to be imported back into ArcGIS detailing the results for the user designed PV system, and a *.xls* file ("*Simulation_Graphs_DD-MM-YYYY_hh-mm-ss.csv*") with all the simulation numerical results and graphs.

5.3. VBA Code Interpretation

To facilitate the understanding of the VBA code underlying the model please refer to Appendix III on page xii for details and guidance.

III Case study

III.1. Case presentation

The case study for the model will be a residential UPAC on nº10 in Rua José d´Esaguy, with residential uses on all 4 floors and 2 apartments per floor, facing S68ºW (azimuth angle of 248º). The building was modeled in CGA, imported into ArcGIS, with useable areas for PV deployment and irradiation calculations done according to the methodology in section II.3. This resulted in 222 detailed building surfaces (76 on the rooftop and 146 on the façade) with irradiation calculated in each (Figure 26). Of these, 48 rooftop surfaces and 56 façade surfaces (Figure 27 and Figure 25) were selected as the basis for analysis.

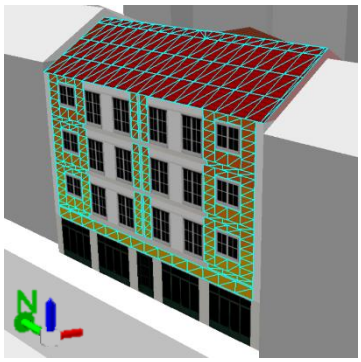

Figure 26 – Detailed building surfaces

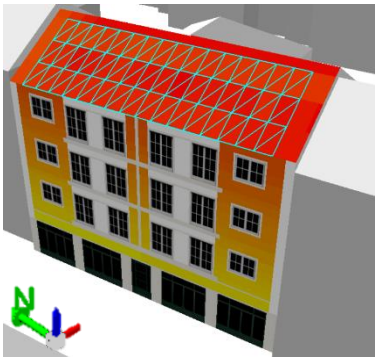

Figure 27 – Selected Rooftop Surfaces

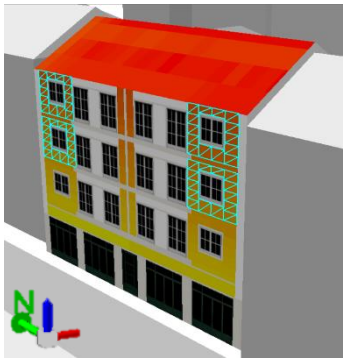

Figure 25 – Selected Façade Surfaces

This selection of panels and their respective object ID´s were exported to the *Input_ArcGIS.csv* file, and a first set of simulations with standard parameters was done to understand whether these selections were adequately sized to the consumption profile of the building. As it turns out, the inclusion of 48 premium panels on the rooftop, tough it does not violate the sizing guidelines of DL 153/2014, does produce economically unsuitable systems, as the peak generation is attained during non-peak load hours, meaning a very large amount of energy is being sold to the grid at a rate below the LCOE, negatively impacting all economic metrics, with high payback period and low IRR (Figure 30).

Reducing this to 16 panels (Figure 28) generates much better economic results (Figure 29), as only limited amounts of electricity are being sold to the grid (even for a premium, high yield installation), and this will be the selection used for all further rooftop simulations. In the case of the façade selection, the 56 selected panels yield adequate results (the low energy production due to the thin film technology, low area availability and low irradiation ensures that all energy is used by the building at all times, see Figure 31), so this will be the selection used for façade simulations.

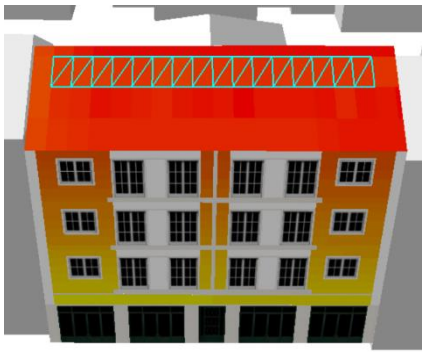

Figure 28 – Final Rooftop Panel Selection

Number Panels	48.00
Module Type	Premium
Total Installed Capacity (kW)	15.016
System Losses (%)	11.42
Inverter Efficiency	0.96
Inverter	String Inverter
Tilt	30.00
Azimuth	247.86
Local	Rooftop
Total Area (m2)	83.33
Nº Pers/Household	2.60
Average Surface Area/Household (m2)	116.05
Nº Stories	4.00
Nº Households	8.00
Cycle	Bi-hourly
Contracted Capacity (kVA)	6.90
New Construction	Retrofit
VAT (%)	23.00%
Debt Fraction (%)	50.00%
Loan Interest (%)	3.00%
Loan Term (Years)	7
IRS (%)	35.00%
Inflation (%/Year)	1.50%
Real Discount Rate (%/Year)	2.25%
Nominal Discount Rate (%/Year)	3.78%

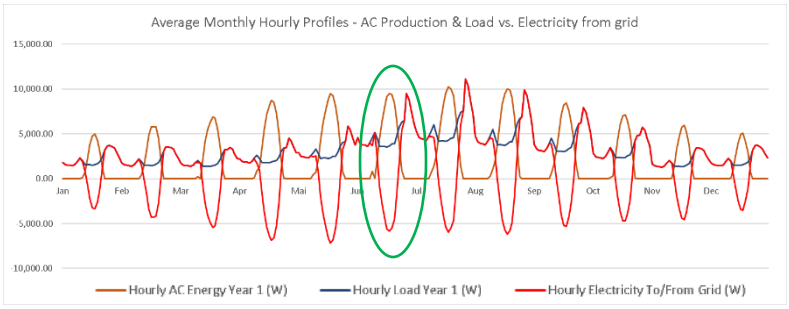

Annual Production Y1 (kWh)	18210.89	NPV (€)	3604.31
Annual Consumption (kWh)	28861.34	Payback Period (Years)	16.83
Electric Bill W/ System Y1 (€)	3290.54	Project IRR	4.55%
Electric Bill W/o System Y1 (€)	5700.5	Equity IRR	4.86%
Savings in Y1 (€)	2409.94	Real LCOE (€c/kWh)	14.03
Total Installed Cost (€)	33840.57	Nominal LCOE (€c/kWh)	16.55
Debt (€)	16920.29		

Figure 30 – Rooftop Premium Simulation with 48 panels

Number Panels	16.00
Module Type	Premium
Total Installed Capacity (kW)	5.005
System Losses (%)	11.42
Inverter Efficiency	0.96
Inverter	String Inverter
Tilt	30.00
Azimuth	247.86
Local	Rooftop
Total Area (m2)	27.78
Nº Pers/Household	2.60
Average Surface Area/Household (m2)	116.05
Nº Stories	4.00
Nº Households	8.00
Cycle	Bi-hourly
Contracted Capacity (kVA)	6.90
New Construction	Retrofit
VAT (%)	23.00%
Debt Fraction (%)	50.00%
Loan Interest (%)	3.00%
Loan Term (Years)	7
IRS (%)	35.00%
Inflation (%/Year)	1.50%
Real Discount Rate (%/Year)	2.25%
Nominal Discount Rate (%/Year)	3.78%

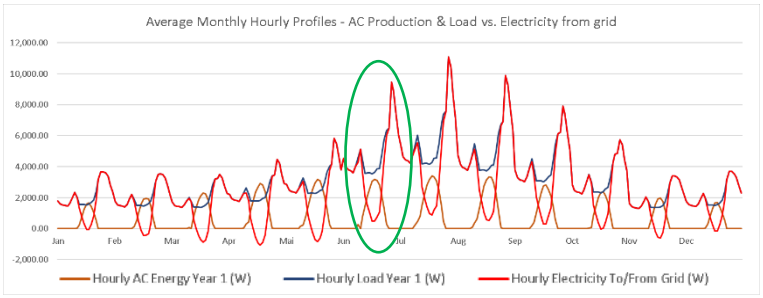

Annual Production Y1 (kWh)	6089.67	NPV (€)	11383.30
Annual Consumption (kWh)	28861.34	Payback Period (Years)	8.59
Electric Bill W/ System Y1 (€)	4343.35	Project IRR	10.90%
Electric Bill W/o System Y1 (€)	5700.5	Equity IRR	13.03%
Savings in Y1 (€)	1357.13	Real LCOE (€c/kWh)	14.17
Total Installed Cost (€)	11485.19	Nominal LCOE (€c/kWh)	16.72
Debt (€)	5742.6		

Figure 29 – Rooftop Premium Simulation with 16 panels

Number Panels	56.00
Module Type	Thinfilm
Total Installed Capacity (kW)	2.659
System Losses (%)	11.42
Inverter Efficiency	0.96
Inverter	String Inverter
Tilt	90.00
Azimuth	247.86
Local	Façade
Total Area (m2)	26.31
Nº Pers/Household	2.60
Average Surface Area/Household (m2)	116.05
Nº Stories	4.00
Nº Households	8.00
Cycle	Bi-hourly
Contracted Capacity (kVA)	6.90
New Construction	Retrofit
VAT (%)	23.00%
Debt Fraction (%)	50.00%
Loan Interest (%)	3.00%
Loan Term (Years)	7
IRS (%)	35.00%
Inflation (%/Year)	1.50%
Real Discount Rate (%/Year)	2.25%
Nominal Discount Rate (%/Year)	3.78%

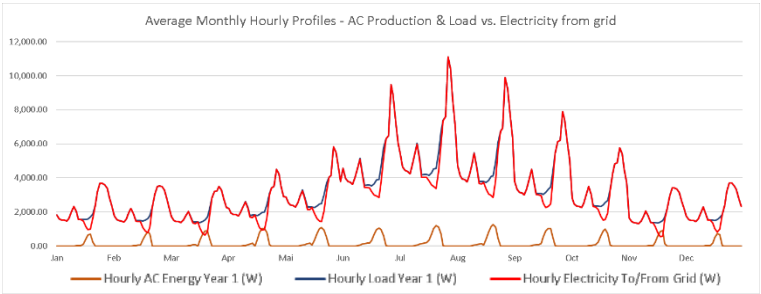

Annual Production Y1 (kWh)	1425.59	NPV (€)	976.92
Annual Consumption (kWh)	28861.34	Payback Period (Years)	15.56
Electric Bill W/ System Y1 (€)	5349.54	Project IRR	5.82%
Electric Bill W/o System Y1 (€)	5700.5	Equity IRR	6.43%
Savings in Y1 (€)	350.99	Real LCOE (€c/kWh)	23.03
Total Installed Cost (€)	3788.7	Nominal LCOE (€c/kWh)	27.16
Debt (€)	1894.35		

Figure 31 – Façade Thin film Simulation with 56 panels

III.2. Developments

To assess the impact of the different input variables on the system economic performance, a large set of comparative simulations was run for both rooftop and façade solutions, described in detail in Table 20 and Table 21 of Appendix IV.

For rooftop simulations, a reference simulation (PV1) was run, followed by 18 simulations where 12 different input variables are changed, and their impacts assessed on system performance. The variables are:

i) Module Type (PV2 and PV3, to assess impact of technology choice);
ii) Inverter Type (PV4 and PV5, to assess impact of inverter choice);
iii) Occupants (PV6, to simulate reduced electricity consumption);
iv) Energy Rate Cycle (PV7, to assess impact of flat buy rate over TOU rate);
v) New Construction (PV8, to assess impact of installation on new construction over retrofitting);
vi) VAT (PV9, assessing impact of a reduction in VAT);
vii) Debt Fraction (PV10 and PV11, simulating different debt loads´ impacts);
viii) Loan interest rate (PV12, to understand the impact of an increase in loan rate);
ix) Loan Term (PV13, quantifying the impact of increasing the loan term);
x) Inflation rate (PV14 and PV15, to assess the impact of higher and lower average inflation over the analysis period);
xi) Sell Rate (PV16 and PV17, to understand the impacts of increases and decreases in reference sell rate);
xii) Irradiation (PV18 and PV19, simulating higher and lower irradiation over the analysis period).

For façade simulations a similar approach was used, with the reference simulation being TF1. As only thin film solutions were considered viable on façades (see section II.2.1.2.2), Standard and Premium PV solutions were not assessed, resulting in the remaining 11 input variables being changed over 16 different simulations (TF2 through TF17).

III.3. Results and Discussion

Before diving into the results of the simulations (summarized in Table 22 and Table 23, in Appendix V) the following two considerations are deemed necessary. Firstly, in the initial sizing simulations laid out in section III.1, the rooftop system of 48 panels (Figure 30) performed very poorly because there is a systemic mismatch between the peak demand profile and the peak production profile. Even though both the sizing limitations of DL 153/2014 are respected and the system produces, in absolute terms, approximately half the energy consumed by its occupants, leading to a sizeable utility bill reduction, these aren´t enough to compensate the enormous investment and debt servicing costs which aren´t compensated by the extensive sale to the grid below the system´s LCOE during the peak production hours, the project only turning a positive cash flow in year 8 (Figure 32). The system is oversized because there is no way to store the energy produced for later demand, which calls for the inclusion of a battery to shift the peak production to match with the peak load. This would no doubt be an economically feasible system, and wouldn´t violate the sizing guidelines of DL 153/2014.

Figure 32 – Simulation Results of 48 Premium Rooftop Panels

Secondly, during the simulations, it became apparent that there is an ongoing issue with the User POA feature of *pvwattsv1*. On random hours, days and months, the user supplied POA irradiance does not get converted to incident POA irradiance within *pvwattsv1*, leading to the POA and resulting AC output being curtailed for those hours. This issue does not affect all months, never affects more than one hour per day, tough when it does, it is always the same hour of the day within the affected month (Figure 33). This is an error that cannot be corrected as the SDK´s calculations are a "black-box", but it´s also an error with seemingly negligible impact and whose end result is producing a lower energy output which is a conservative stance.

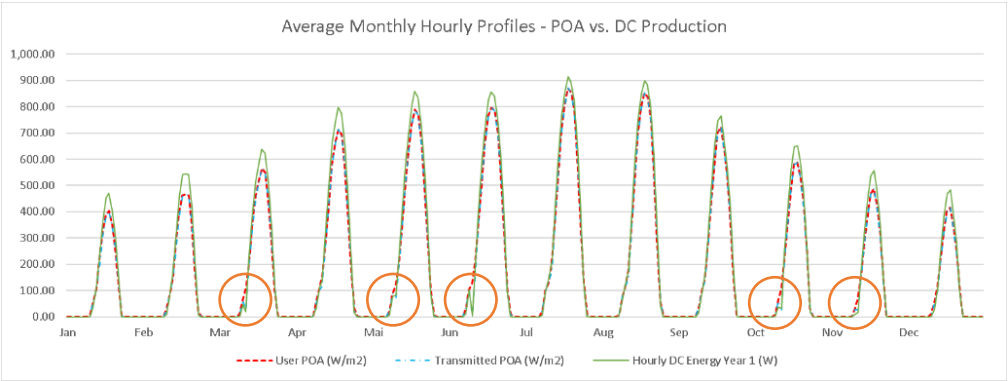

Figure 33 – Error processing user supplied POA values

3.1. Rooftop PV Systems

The reference Rooftop Simulation (PV1), which models a Standard system, with no inverter option and all remaining input variables set to their default value (see section II.2) yielded promising results (Figure 34). The annual savings on the electricity bill account for over 20% of the original utility bill, with a consequently high NPV of over 8k€ for an installation cost of 11.6k€. Positive cashflows are generated from year 1 onwards (except in year 13 with the cost of replacing the inverter), with a payback period of 9.9 years, reasonable if somewhat on the higher end of the spectrum, as in Europe, a maximum payback time for PV modules of less than 10 years is generally expected (Jelle, Breivik, & Rokenes, 2012). The real LCOE of 164€/MWh indicates that this system attains socket parity, as this cost is in line with or below the retail costs laid out in Table 11 (approximately 159€/MWh for a simple rate structure and between 96 and 200€/MWh for off-peak and peak consumption in a bi-hourly rate structure). In PV1, as a bi-hourly rate structure is modeled, the costs avoided correspond to the peak rate, with an average differential of 36€/MWh being the corresponding saving in all hours where the total production is consumed. The system is, however, still very far from grid parity, with the average wholesale costs in Portugal from Table 12 being in the range of 46€/MWh, less than a third the cost of the system. The equity IRR of 10.55% outperforms the average yield over the last ten years of gold (10.36%/year) and the SP500 (6.57%/year), and current Portuguese 7-year treasury bonds (1.38%/year), an indication that the system is a solid investment.

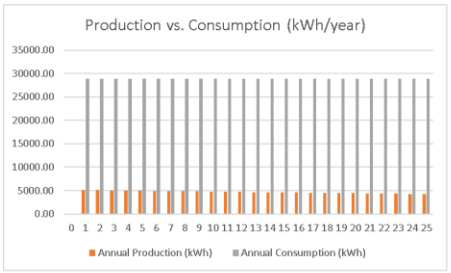

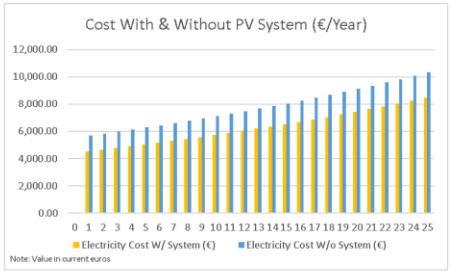

Results	PV1
Total Installed Capacity (kW)	4.25
Number Panels	16
Tilt (º)	30
Azimuth (º)	247.9
Local	Rooftop
Total Area (m2)	27.78
Annual Production Y1 (kWh)	5111.15
Annual Consumption (kWh)	28861.3
Electric Bill W/ System Y1 (€)	4519.71
Electric Bill W/o System Y1 (€)	5700.50
Savings in Y1 (€)	1180.80
Total Installed Cost (€)	11624.42
Debt (€)	5812.21
NPV (€)	8276.28
Payback Period (Years)	9.87
Project IRR (%)	9.06%
Equity IRR (%)	10.55%
Real LCOE (€c/kWh)	16.40
Nominal LCOE (€c/kWh)	19.35

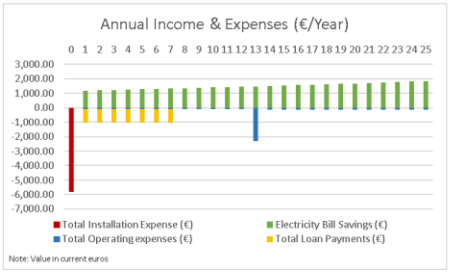

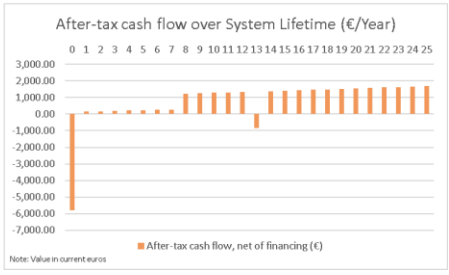

Figure 34 – Simulation Results for PV1

The module type variations yielded interesting results. For the premium module (PV2), a 20% increase in annual production easily compensated the approximately 4% increase in installed costs. This, coupled with higher electricity bill savings from higher production ensures a better economic performance than PV1 (NPV almost 3k€ more, payback almost a year earlier, equity IRR close to 2% above and a real LCOE decreased by 18€/MWh), fully justifying the initial higher investment. The thin film module (PV3) performed surprisingly well compared with PV1 (Figure 35), with the very low installation cost (less than 40%) compensating the lower energy yield (approximately 68% of PV1, a less significant reduction than might be expected, in part

due to the high performing nature of this technology under higher temperatures compensating it´s lower nameplate capacity). The electric bill savings are lower in absolute terms, but the overall economic performance is superior, with payback attained after just 5.2 years (strong and positive cashflows from year 1 onwards), a NPV increase of over 1k€, an astounding 25.8% equity IRR and a very low real LCOE of only 103€/MWh.

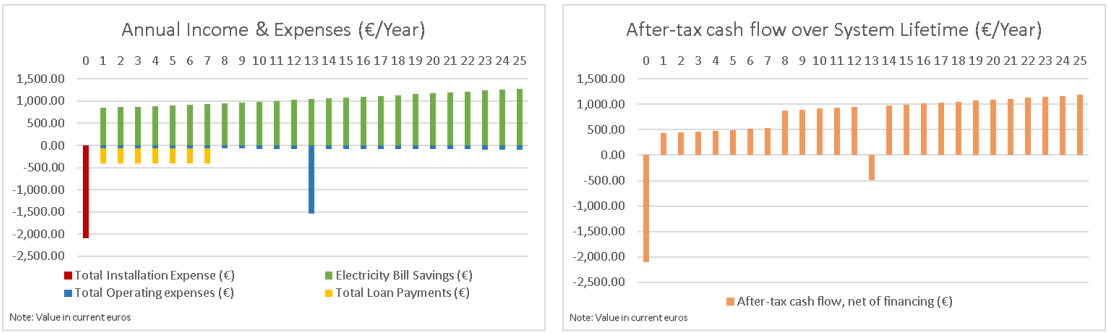

Figure 35 – Annual Income, Expenses and Cashflow for PV3

The inverter type variations for rooftop installations isolate the effect of initial cost and replacement cost differences in the technologies (string inverters and micro inverter, in PV4 and PV5 respectively), as AC production should be negligibly affected. Given the maximum difference between the highest and lowest yearly cumulative irradiation for the panels of the array is quite insignificant (only 21.624 W/m^2, or +1.4%/year), this mitigates the impact of the assumptions about inverter performance (see section II4.2). For the most part, production and annual energy savings behave as expected, with a marginally higher and lower yearly energy output (+0.02%/year and -0.85%/year for micro inverters and string inverters respectively) and correspondingly insignificant reductions and increases in utility bill savings (shaving off 0.22€/year for micro inverter system and lowering the savings by only 8.36€/year for a string system). The big difference is found in the initial installed cost, with the micro inverter system costing approximately 1.9k€ more to install than the string inverter alternative, which is not compensated by any significant improvement in performance, increasing the debt load (Figure 38 and Figure 37) and the payback period (one year later than PV1 reference, and 1.4 years later than the PV4 alternative). Even though the string system incurs a component replacement cost halfway through the lifetime of the system, it is not enough to dilute the initial cost advantage (Figure 36), resulting in a higher NPV and equity IRR than both the PV1 and PV5 systems. It can be said that the impact on economics of the inclusion of the micro inverter is generally negligible,

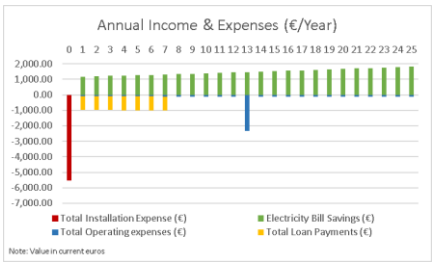

Figure 38 – Annual Income and Expenses in PV4

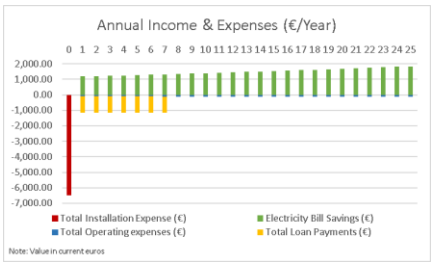

Figure 37 – Annual Income and Expenses in PV5

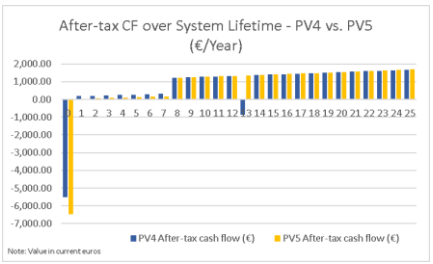

Figure 36 – Cash flow comparison of PV4 & PV5

while the inclusion of the string inverter, with its lower costs and similar performance, guarantees a better investment on evenly irradiated rooftops.

The load consumption decrease simulated by PV6 (close to -30%/year) aims to gauge the impact of an oversizing of the array for the building´s consumption profile, thus increasing the sales to the grid in the hours of peak production. As the design and financing conditions are strictly the same, the production, installed cost and resulting LCOE are unaltered. What does change are the yearly utility bill savings, with PV6 bringing in less savings (approximately -140€/year) than the higher consumption alternative (Figure 39) by way of reduction in the absolute savings from shifting from grid to system production and increase in sales to the grid at a rate below the LCOE. In the long run this ensures a better economic performance for PV1, with PV6 payback period over a year longer, a lower NPV by a margin of over 2k€ (27% reduction) and an equity IRR 1.8% below the PV1 reference case. This comparison reveals the importance of the correct sizing of the system relative to its expected consumption, both in absolute terms and in load shape profile.

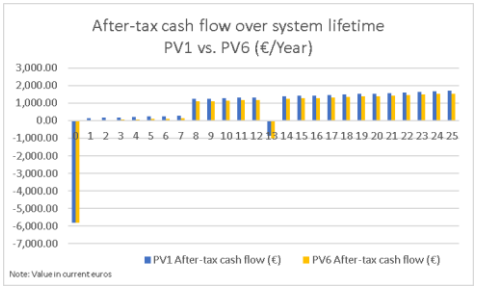

Figure 39 - Cash flow comparison of PV1 & PV6

The PV7 system compares the usage of a simple flat buy rate structure to the reference case´s TOU bi-hourly rate. Because the system, financing and consumption variables are unaltered, the resulting production, consumption, installed cost and LCOE remain unchanged. However, an interesting phenomenon occurs in the utility bill costs with and without the system, with the PV7 utility bill costs without the system being lower than the reference case by approximately -70€/year, but the reverse being true for the utility bill with the system, which increases in PV7 relative to PV1 by around +170€/year. In a building without the PV system, the difference in behavior is due to the fact that the modeled load shape (see Figure 9) concentrates consumptions around peak hours, and thus most of the consumption is priced at a higher buy rate in PV1 than PV7, giving an indication that this building´s electricity bill could be reduced by shifting to a flat-rate structure, or by altering the consumption habits to shift the load to the lowest priced hours. However, in a building with a PV system installed, the production which occurs during peak hours displaces higher priced electricity drawn from the grid in PV1 than in PV7, resulting in a lower utility bill for the bi-hourly rate structure. The impacts are quite significant, with the NPV of PV7 decreasing by 4.6k€ (over 50% reduction), being only cash flow positive after the loan is paid off (Figure 40), negatively impacting the payback period (increased by 4.5 years to a total of 14.4 years) and almost halving the equity IRR to 6.9%. This reveals the importance of evaluating the grid load demand shape resulting from the inclusion of a PV

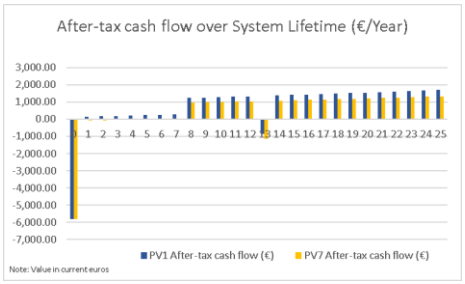

Figure 40 - Cash flow comparison of PV1 & PV7

system, and how that change can make a bi-hourly rate structure more attractive than the flat rate structure for buildings with PV systems installed.

The PV8 simulation comparison to PV1 provides insight into the isolated impact of decreased installation costs on the economic performance of the system (all production, consumption and electricity bill savings remaining the same). As could be expected from an 11.2% reduction in total installed system price, PV8 fares better on all economic metrics, with a 16% increase in NPV (additional 1.2k€), close to 2% increase in equity IRR, payback a year earlier and a lower real LCOE of 149.6€/MWh, confirming the advantages of installing PV systems on new developments over the retrofitting alternative.

In PV9, a reduction in VAT of 7% was simulated, revealing a negligible impact on the IRR and payback period of the system. This is because VAT reductions affect both the installed and operational costs, as well as the utility bill costs and the savings accrued from using the system, which cancel each other out. The NPV and LCOE are both lower in PV9 because the absolute cashflows are lower, thus their present value and their impact on cost of energy are lower as well. Because this approach affects income and expenses in the same way, the only way that it could work would be if VAT was only reduced for PV system components, making it closer in terms of impacts to the simulation in PV8.

Simulations PV10 through PV13 all represent changes to the financing structure of the project. In these simulations the payback period and project IRR, because they are independent of financing structure, remain unchanged, but the remaining economic indicators are all affected.

Simulations PV10 and PV11 represent the impact of the debt fraction on project economics. This directly impacts the WACC which in turn is used as the real discount rate. In PV10, the discount rate increase and higher load burden during the loan term (Figure 41) leads to a NPV decrease of around 14% and a real LCOE increase of approximately 5€/MWh when compared to PV1. However, equity IRR jumps to 14%, as the weight of the initial investment cost is removed from the after-tax cashflows (Figure 42), generating a more balanced cash flow profile over the investment period that only turns positive once the loan term is over. The reverse is true for PV11, with a lower discount rate inducing a 20% increase in NPV (over 1.6k€) and decrease in real LCOE of close to 10€/MWh, tough equity IRR is negatively impacted (equaling project IRR), lowering by almost 1.5% due to the high upfront costs (Figure 43), even though the cash flows are positive from year 1 onwards (except for the year of component replacement cost, see Figure 42). This analysis shows the importance of liquidity on project economics and how the absence of a loan can be economically advantageous.

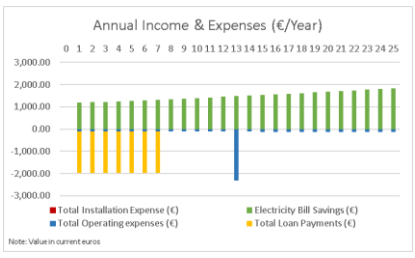

Figure 41 - Annual Income and Expenses in PV10

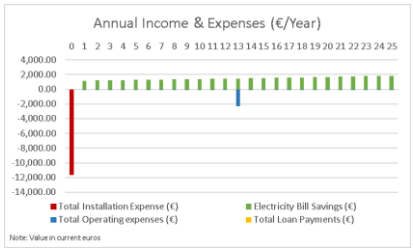

Figure 43 - Annual Income and Expenses in PV11

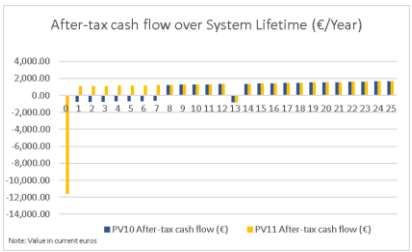

Figure 42 - Cash flow comparison of PV10 & PV11

The increased loan interest rate of simulation PV12 brings with it all the expected negative impacts, with higher debt servicing negatively impacting the NPV, equity IRR and real LCOE. A 2% increase in the loan rate decreases NPV by 28% (-2.3k€), decreases equity IRR by 0.5% and increases real LCOE by 17€/MWh. The impacts are similar to the impacts of increasing the debt fraction, only the equity IRR is diminished as, contrarily to PV10, the upfront capital is the same as for PV1, but the payment on that debt is percentually higher.

The reverse of PV12 is true in PV13, with the increased loan term leading to improvements in NPV, IRR and LCOE. This is due to the debt repayment costs being more spread out over the course of the project (Figure 44) and thus being discounted more steeply the further out they are (assuming that inflation rate over the lifetime of the project remains below the loan rate, and the latter remains unchanged, which is unlikely when negotiating the loan).

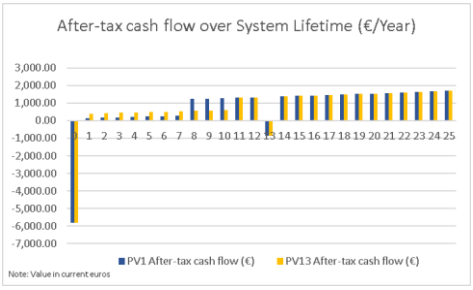

Figure 44 - Cash flow comparison of PV11 & PV13

The effect of inflation on project economics can be seen in simulations PV14 and PV15. For PV14, a 1% decrease in assumed inflation rate produces lower lifetime utility bill costs in current euros, and, because the WACC was assumed dependent on the inflation rate (see section II2.2.1.3.2) and no real discount rate is specified, the resulting nominal discount rate is decreased, thus the electricity bill savings are discounted less steeply. The result of this is an increase in NPV of approximately 14%, payback period increasing by 6 months (seeing as the electricity bill savings are smaller on account of lower inflation), equity IRR decreasing 1.35% and real LCOE adjusting slightly to 3€/MWh lower. The complete opposite is true for PV15, where a 1% increase in inflation has the mirrored effect of PV14. What can be said is that lowering the assumed inflation rate will negatively impact the IRR and payback period, whilst improving the LCOE and NPV, even tough, for the small variations modeled, the impacts were not very significant.

Simulations PV16 and PV17 provide insight into the effects of changing the sell rate of electricity injected onto the grid by +/- 25%. As caution was taken to appropriately size the system in order to lower sales to the grid (see section III.1) the impact of this variation will be small. Unsurprisingly, an increase in the sell rate improves electricity bill savings throughout the years, but so marginally as to be insignificant. The effects of an increased sell rate are positive on all economic indicators, improving NPV, lowering the payback period and improving the IRR, with no impact whatsoever on the LCOE (as that is solely dependent on the costs to install and maintain the system, and its electricity output). The reverse is true for PV17, and in both simulations the effect would be stronger were there to be more sales to the grid. However, as was previously alluded to, this would steer us away from an optimal and economically viable system overall, therefore the low sensitivity of the results to variations in sell rate provides evidence that the system is appropriately sized.

For simulations PV18 and PV19, the effect of increasing and decreasing the irradiation by +/-25% are modeled, with unsurprising results. A 25% increase in radiation leads to a 24.96% increase in electricity generated, at the exact same cost. This of course leads to more energy savings, improved NPV (55% increase, corresponding to +4.5k€), 3.4% increase in equity IRR and reductions in the real LCOE of about 33€/MWh and of the payback period by about 1.61 years. However, for the 25% decrease in irradiation, the impacts, though mirrored, are stronger than for PV18. The AC generation is reduced by 26.4% (possibly due to the low irradiance correction of equation (24)), resulting in lower energy savings, which turns the project into negative cash flows until the end of the loan term (Figure 45). A much lower NPV is achieved (reduced to 2.8k€, a third of PV1), the payback period increased to 15 years, IRR is reduced, and a massive increase occurs in real LCOE, which jumps to 228.8€/MWh, 58.8€/MWh higher than PV1. What this comparison shows is the high sensitivity of the results to the weather patterns and that variations in irradiation levels have a stronger impact on the downside than on the upside.

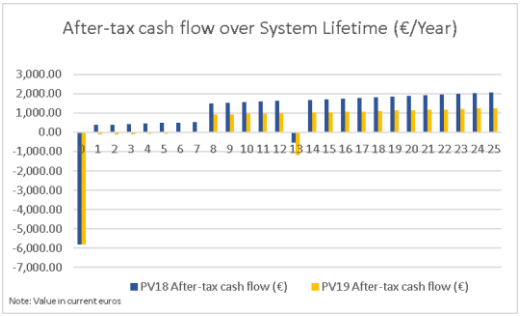

Figure 45- Cash flow comparison of PV18 & PV19

From this analysis one can conclude that an ideal rooftop system that aims to reduce the monthly utility bill would incorporate premium panels in a string array, would be sized adequately to the consumption, contract a bi-hourly rate from the retailer, use the least amount of debt possible, at the lowest rate and for the longest term, and with the highest irradiation possible throughout the lifetime of the project.

Knowing this, a new reference scenario was modeled (PV20), and changing the variables than are unknown at the outset of the project (occupancy for the lifetime of the project, inflation and irradiation), simulations PV21 and PV22 were run, representing an Optimistic and Pessimistic Scenarios respectively, subsequently compared to PV20 (Table 15).

The new reference scenario, with the system design parameters set to the best possible following the previous analysis, when compared to PV1, yields higher annual utility bill savings (increased by around 180€/year), a 25% increase in NPV to over 10k€, payback almost one year earlier, a lower real LCOE (134€/MWh, decreased by 30€/MWh) and a lower equity IRR (on account of total upfront costs in the absence of debt).The PV21, representing the high end of the spectrum, yields a NPV almost double that of PV20 (90% increase, corresponding to +9.3k€), payback within 7.6 years, an equity IRR increase of 2% and an astoundingly low real LCOE of 99€/MWh, putting it within the LCOE range of utility scale PV. PV22, representing the most pessimistic assumptions, gives a positive, if negligible, NPV of 1.1k€ (89% reduction against PV20), payback at the end of 15 years (still well within the lifetime of the system), a low but still sizeable equity IRR of 6% and a real LCOE of 198€/MWh, still below the retail peak buy rate. Even with the most pessimistic of assumptions, the correct choices in sizing and system design have far reaching impacts

on system performance and can practically guarantee, even in the worst conditions, a positive NPV and a decent return on equity.

Table 15 – New Reference, Optimistic and Pessimistic Rooftop Scenarios (PV20, PV21 & PV22)

Input Variations	PV20	PV21	PV22	Results	PV20	PV21	PV22
Module Type	Premium	Premium	Premium	Total Installed Capacity (kW)	5.01	5.01	5.01
System Losses	11.42%	11.42%	11.42%	Number Panels	16.00	16.00	16.00
Inverter Efficiency	96%	96%	96%	Tilt (º)	30.00	30.00	30.00
Inverter	String	String	String	Azimuth (º)	247.86	247.86	247.86
Nº Pers/Household	2.6	3	1	Local	Rooftop	Rooftop	Rooftop
Average Surface Area/Household (m2)	116.05	116.05	116.05	Total Area (m2)	27.78	27.78	27.78
Nº Stories	4	4	4				
Nº Households	8	8	8	Annual Production Y1 (kWh)	6089.67	7624.62	4483.68
Cycle	Bi-hourly	Bi-hourly	Bi-hourly	Annual Consumption (kWh)	28861.34	30981.26	20381.66
Household Contracted Capacity (kVA)	6.9	6.9	6.9	Electric Bill W/ System Y1 (€)	4343.35	4480.98	3086.09
New Construction	0	0	0	Electric Bill W/o System Y1 (€)	5700.50	6116.19	4042.38
VAT (%)	23%	23%	23%	Savings in Y1 (€)	1357.13	1635.25	956.30
Debt Fraction (%)	0%	0%	0%	Total Installed Cost (€)	11485.19	11485.19	11485.19
Loan Interest (%)	3%	3%	3%	Debt (€)	0.00	0.00	0.00
Loan Term (Years)	7	7	7	NPV (€)	10343.43	19631.28	1161.37
IRS (%)	35%	35%	35%	Payback Period (Years)	8.95	7.58	14.98
Inflation (%T)	1.5%	0.005	0.025	Project IRR (%)	9.75%	11.79%	5.99%
Discount Rate	WACC	WACC	WACC	Equity IRR (%)	9.75%	11.79%	5.99%
Sell Rate	Standard	Standard	Standard	Real LCOE (€c/kWh)	13.46	9.91	19.82
Irradiation (W/m2)	Energy+	Energy+ + 25%	Energy+ -25%	Nominal LCOE (€c/kWh)	15.97	10.53	25.83
				Higher than PV20	Lower Than PV20		

3.2. Façade PV Systems

The reference Façade Simulation (TF1), which models a thin film system, with no inverter option and all remaining input variables set to their realistic default value (see section II.2) returned the expected results, with a low production (accounting for only 13% of total annual consumption), annual savings on utility bill of around 7% of the original bill, resulting in a low NPV of 1.5k€ for a total initial investment of 3.9k€, a long payback period of 13.5 years, a reasonable equity IRR and a high real LCOE of 213€/MWh. This puts the system just outside the range of grid parity, even tough, for a small investment, the returns are eventually achieved, if slow to come (Figure 46).

The TF2 and TF3 simulations truly showcase the impact different inverter choices can have for unevenly irradiated arrays (the yearly cumulative irradiation difference between the highest and lowest irradiated panels in the array ascends to 169.892 W/m^2, or +21.7%/year). The resulting AC generation is more than doubled in the system with a micro inverter, whilst the system with string inverter only decreases its output by 10% relative to the reference TF1. This induces an increase in annual utility bill savings that more than makes up for the added cost of micro inverters. While TF2 has a worse economic performance than TF1, the values are comparable and within the same range. The same is not true for TF3, which boasts a 9.6k€ NPV (more than doubling the initial investment), a 5.9 year payback period, real LCOE of 94€/MWh and an equity IRR of 22.68%. The performance is in many ways similar to the thin film system modeled in PV3, the main difference being the need to include micro inverters in order to attain the desired potential performance out of this technology on façades.

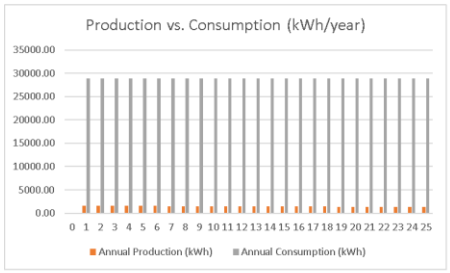

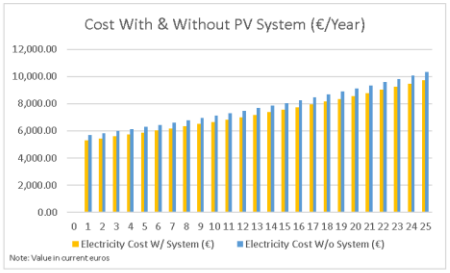

Results	TF1
Total Installed Capacity (kW)	2.66
Number Panels	56
Tilt (º)	90
Azimuth (º)	247.86
Local	Façade
Total Area (m2)	26.31
Annual Production Y1 (kWh)	1589.25
Annual Consumption (kWh)	28861.34
Electric Bill W/ System Y1 (€)	5309.49
Electric Bill W/o System Y1 (€)	5700.50
Savings in Y1 (€)	391.03
Total Installed Cost (€)	3981.63
Debt (€)	1990.82
NPV (€)	1553.84
Payback Period (Years)	13.5
Project IRR (%)	6.84%
Equity IRR (%)	7.72%
Real LCOE (€c/kWh)	21.34
Nominal LCOE (€c/kWh)	25.17

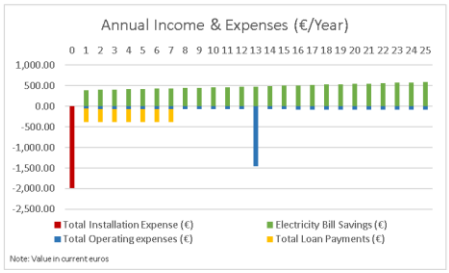

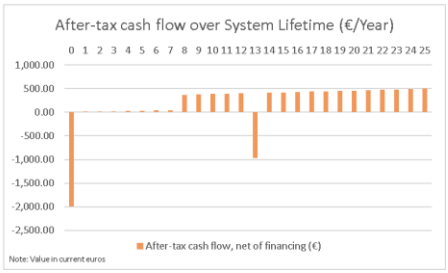

Figure 46 - Simulation Results for TF1

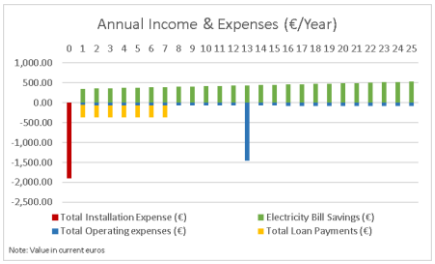

Figure 49 - Annual Income and Expenses in TF2

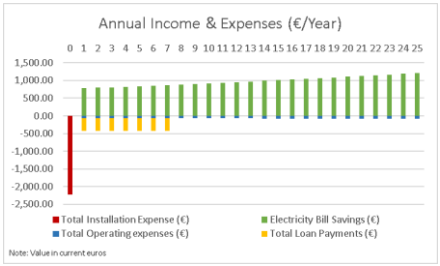

Figure 48 - Annual Income and Expenses in TF3

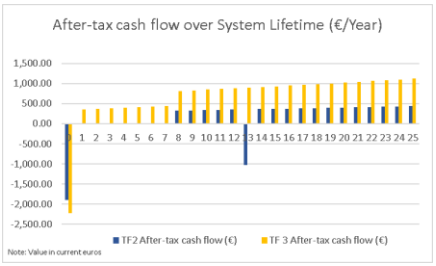

Figure 47 - Cash flow comparison of TF2 & TF3

The TF4 simulation represents a lower consumption load but does not translate to more sales of electricity to the grid as there are no hours where production exceeds consumption (see Figure 31). Thus, the decrease in NPV is solely due to the absolute decrease in utility bill savings, and the remaining negative impacts are less felt than the analogous situation modeled in PV6, with somewhat comparable economic assessment to TF1, meaning that TF façade systems´ economic performance is less sensitive to variability in consumption profiles on account of their small generation when compared to consumption.

The TF5 simulation of flat buy rate structure negatively impacts the annual energy savings, as all the energy produced by the system goes to replace grid withdrawals, that in this case are valued lower than TF1, since most of the consumption happens during peak hours. The impacts on the economics are significant, with an almost null NPV, payback period of 18.4 years and very low IRR, drawing attention to the importance of the TOU buy rate structure in the evaluation of these systems, particularly when grid injections seldom happen.

For simulations TF6 through to TF13, the behaviors of TF systems are very similar to their PV counterparts PV8 through to PV15. TF6 and TF7 (representing installation on new construction and a decrease in VAT), both manifest the decrease in installation costs positively impacting all economic metrics and the VAT

reduction of 7% proportionately decreasing the NPV and LCOE, leaving everything else unchanged. The changes to the financing variables (TF8, TF9, TF10 and TF11) and inflation (TF12 and TF13) affect economic indicators in similar fashion as for rooftop systems.

Because the façade system barely sells any energy to the grid, the TF14 and TF15 cases show no change whatsoever to any of the calculated economic variables, as there is, in fact, barely any change to the calculations of economic performance.

The TF16 and TF17 simulations for higher and lower irradiation levels manifest a similar behavior as rooftop systems, but more exacerbated. A 25% increase in irradiation leads to a 32% increase in AC output due to the comparatively better performance of TF cells under high temperatures than their c-Si counterparts. As a result, the NPV more than doubles in TF16, the equity IRR increases by 5.5%, the payback period decreases by more than 5 years and the LCOE drops to 161€/MWh. For TF17, the reverse is true, with very pronounced impact on the NPV (a negative value), payback period over 20 years, a negligible IRR and a LCOE over 300€/MWh. This analysis reveals the particularly sensitive nature of TF cells to operating conditions and the resulting impact on economic evaluation.

From these simulations one can infer that the ideal thin film façade system would include micro inverters, contract bi-hourly rate to the retailer, use the least amount of debt possible, at the lowest rate and for the longest term with the highest irradiation possible throughout the lifetime of the project. A new reference case taking this into account was created (TF18), and Optimistic and Pessimistic Scenarios were run to analyze the sensitivity of this ideal system to the most impacting and unpredictable variables of inflation and irradiation (TF19 and TF20).

Table 16 - New Reference, Optimistic and Pessimistic Façade Scenarios (TF18, TF19 & TF20)

Input Variations	TF18	TF19	TF20	**Results**	TF18	TF19	TF20
Module Type	Thinfilm	Thinfilm	Thinfilm	Total Installed Capacity (kW)	2.66	2.66	2.66
System Losses	11.42%	11.42%	11.42%	Number Panels	56.00	56.00	56.00
Inverter Efficiency	96%	96%	96%	Tilt (º)	90.00	90.00	90.00
Inverter	Micro	Micro	Micro	Azimuth (º)	247.86	247.86	247.86
Nº Pers/Household	2.6	2.6	2.6	Local	Façade	Façade	Façade
Average Surface Area/Household (m2)	116.05	116.05	116.05	Total Area (m2)	26.31	26.31	26.31
Nº Stories	4	4	4				
Nº Households	8	8	8	Annual Production Y1 (kWh)	3361.89	4434.72	2294.21
Cycle	Bi-hourly	Bi-hourly	Bi-hourly	Annual Consumption (kWh)	28861.34	28861.34	28861.34
Household Contracted Capacity (kVA)	6.9	6.9	6.9	Electric Bill W/ System Y1 (€)	4922.25	4720.94	5145.88
New Construction	0	0	0	Electric Bill W/o System Y1 (€)	5700.50	5700.50	5700.50
VAT (%)	23%	23%	23%	Savings in Y1 (€)	778.27	979.58	554.64
Debt Fraction (%)	0%	0%	0%	Total Installed Cost (€)	4436.95	4436.95	4436.95
Loan Interest (%)	3%	3%	3%	Debt (€)	0.00	0.00	0.00
Loan Term (Years)	7	7	7	NPV (€)	10839.02	18383.38	4414.34
IRS (%)	35%	35%	35%	Payback Period (Years)	5.91	4.72	8.23
Inflation (%T)	0.015	0.005	0.025	Project IRR (%)	17.59%	21.67%	12.49%
Discount Rate	WACC	WACC	WACC	Equity IRR (%)	17.59%	21.67%	12.49%
Sell Rate	Standard	Standard	Standard	Real LCOE (€c/kWh)	8.90	6.18	14.23
Irradiation (W/m2)	Energy+	Energy+ + 25%	Energy+ -25%	Nominal LCOE (€c/kWh)	10.56	6.56	18.54
				Higher than TF18	Lower Than TF18		

The new reference scenario TF18, when compared to TF3 (the only difference being the debt percentage considered) presents no changes in any of the production, consumption and savings calculations, with the payback period and project IRR unchanged as well as they are independent of financing structure. What can be seen is an improvement of approximately 13% NPV to close to 11k€, equity IRR converging to project IRR (as 0% debt is assumed) and a LCOE approximately 5€/MWh cheaper than that of TF3 at

89€/MWh (the lowest for all the reference cases simulated). This same system is modeled optimistically in TF19, resulting in an unsurprisingly high performing solution with over 18k€ NPV, payback before 5 years and a real LCOE on par with peak wholesale prices, bringing it, under these conditions, very close to grid parity. Finally, the TF20, representing the most pessimistic assumptions, still gives an acceptable performance level, even under these conditions, with all economic indicators far above the reference TF1 and TF2 scenarios, revealing the importance of adequate inverter choice in the system design phase of the project. This results in a system with a NPV above 4k€, the equity IRR above 12% and an acceptable payback period of 8.2 years, a testament to the resilience of a micro inverter façade TF system even under a pessimistic outlook. This comparative analysis supports the assessment in Heinstein et. al. (2013)., regarding the economic performance of TF technology in real life conditions being comparable to, or even better than, traditional c-Si technology due to the better thermal and shaded performance, and to the lower costs/m^2 outweighing the lower efficiency.

3.3. Rooftop and Façade PV Systems

As a final comparison, PV23 is a simulation for a PV system that includes the best performing rooftop and façade systems (PV20 and TF18) with all other variables remaining unchanged. The results are laid out in Table 17, and show that, even though the production and installed costs of PV23 are the sum of their constituents, the utility bill savings are not, a sign that a portion of the additional electricity produced by the façade is being squandered on grid sales. Compared to PV20 this results in a lower IRR (-0.7%), an extra 8 months in payback period, compensated by an increase in the NPV of approximately 2.5k€ (on account of higher utility bill savings) and a lower LCOE (the generation of TF panels diluting the cost of the more expensive premium panel AC generation) of only 117€/MWh, on the lower bound of the socket parity range. These results show that with an additional initial investment of only 4.4k€, the monthly utility bill savings can increase by 300€/month, the LCOE can drop by 17€/MWh, the NPV increase, and all this at the cost of a few months´ extension on the payback period and less than 1% reduction in IRR. The selection of a TF façade solution is thus a viable and desirable complement to a rooftop system, improving key financial performance metrics.

Table 17 - Best performing Rooftop, Façade and Rooftop+Façade Systems (PV20, TF18 &

Input Variations	PV20	TF18	PV23	Results	PV20	TF18	PV23
Module Type	Premium	Thinfilm	Premium+Thinfilm	Total Installed Capacity (kW)	5.01	2.66	7.67
System Losses	11.42%	11.42%	11.42%	Number Panels	16.00	56.00	72.00
Inverter Efficiency	96%	96%	96%	Tilt (º)	30.00	90.00	30&90º
Inverter	String	Micro	String+Micro	Azimuth (º)	247.86	247.86	247.86
Nº Pers/Household	2.6	2.6	2.6	Local	Rooftop	Façade	Roof + Façade
Average Surface Area/Ho	116.05	116.05	116.05	Total Area (m2)	27.78	26.31	54.08
Nº Stories	4	4	4				
Nº Households	8	8	8	Annual Production Y1 (kWh)	6089.67	3361.89	9504.76
Cycle	Bi-hourly	Bi-hourly	Bi-hourly	Annual Consumption (kWh)	28861.34	28861.34	28861.34
Household Contracted C	6.9	6.9	6.9	Electric Bill W/ System Y1 (€)	4343.35	4922.25	3950.56
New Construction	0	0	0	Electric Bill W/o System Y1 (€)	5700.50	5700.50	5700.5
VAT (%)	23%	23%	23%	Savings in Y1 (€)	1357.13	778.27	1749.9
Debt Fraction (%)	0%	0%	0%	Total Installed Cost (€)	11485.19	4436.95	15810.87
Loan Interest (%)	3%	3%	3%	Debt (€)	0.00	0.00	0
Loan Term (Years)	7	7	7	NPV (€)	10343.43	10839.02	12860.81
IRS (%)	35%	35%	35%	Payback Period (Years)	8.95	5.91	9.62
Inflation (%T)	1.5%	1.5%	1.5%	Project IRR (%)	9.75%	17.59%	9.07%
Discount Rate	WACC	WACC	WACC	Equity IRR (%)	9.75%	17.59%	9.07%
Sell Rate	Standard	Standard	Standard	Real LCOE (€c/kWh)	13.46	8.90	11.72
Irradiation (W/m2)	Energy+	Energy+	Energy+	Nominal LCOE (€c/kWh)	15.97	10.56	13.90
				Higher than PV20	Lower Than PV20		

IV Conclusions

IV.1. Limitations

The methodology adopted in this dissertation presents some limitations that should be addressed, some specific to the model itself, some more general to the systems being modeled.

1.1. Model Limitations

Using *pvwattsv1* will tend to underestimate AC output as is seen in section II1.1, particularly for thin film technology. Tough steps were taken to account for this, some limitations remain (see section II2.1.1.1 and III.1), so one should consider the AC output results to be underestimating the actual output achievable in any of these systems. This is a conservative position, as any results derived from these calculations will tend to underestimate the actual real-life output, which should improve economic returns above these estimations.

It is assumed that partially shaded modules behave in the same way as if the whole module were to be uniformly shaded (which is incorrect, as partially shaded modules can be disproportionately affected by shade, as referred to in section I.2). Attempting to correct for this, different approaches to modeling of systems with micro inverters and string inverters were carried out, but quality of results regarding real life measurements is unassessed.

The specific methodology for calculations with micro inverters is lacking, requiring a better handling of arrays for recursive calculations (e.g. the façade calculation of 56 panels takes close to 8½ hours to conclude). At the moment it is too computationally intensive and requires better programming skills to manipulate the large and numerous arrays[34]. On the other hand, calculations with *String* or *No Option* inverter selected are quite fast, and suitable for any areas where partial or uneven shading and/or irradiation is not a problem, such as unobstructed roofs or façades.

There is room to develop this method into a Python application (e.g. creating a tool within ArcGIS) to use the same modules in the SSC library, as the SDK includes a Python wrapper. If the methodology used for this dissertation is deemed suitable, then the only limitation to this would be the development required to guarantee the correct implementation of the methodology in a purely ArcGIS/CityEngine/WebGIS environment, bypassing the Excel/VBA that was used in this case.

This methodology cannot model flat roofs, as surface tilt was assumed to equal panel tilt, with GCR equal to 1, no self-shading, no tracking, and no backtracking algorithm. Subsequent research could account for flat roofs, by making explicit calculations with the self-shading behavior in mind.

The load calculation (*belpe*) module has undergone limited validation, looking at just one location and set of weather data. More validation cases should be run looking at different climates and rate structures to

[34] Because of this, the output of hourly values (e.g. DC energy Generated, AC Energy Generated, Cell temperature, POA, Transmitted POA, User POA, Load, Electricity to/from Grid) have been commented on the current version of the VBA code; they can be included, but substantially increases run time of the code. In case one wishes to generate graphs with hourly discretization of all system calculations, they must be uncommented.

ensure that it will reliably perform as desired (Gilman P. , 2018) and is representative of the consumption patterns of the building tenants.

1.2. General Limitations

There is currently no way to validate the production results with real life production, nor the economic outputs of the model, as to the best of the researcher's knowledge, there is no systematic campaign to collect and analyze real world residential PV production and economic performance in Lisbon.

Also, standalone PV systemstend to have a structural mismatch between production and consumption profiles without large scale storage, which limits the economic viability of larger PV systems. This should be a priority for research, to understand impact of load profiles changes and whether current storage solutions offer a cost competitive advantage for larger systems.

The results for thin film models on rooftops, tough promising, are theoretical in the sense that this technology is usually not implemented on rooftops, as it isn´t mature and the weathering solutions aren´t as developed as for c-Si technology (negatively impacting the warranties). It is a promising start, but thin film solutions aren´t yet ready for commercial widespread use on rooftops.

Integrating large quantities of BIPV into the grid would require a flexible grid, supporting infrastructure and a suite of enabling technologies (Gagnon, et. al, 2016), requiring capital investment on the grids for distributed generation, which is not accounted for in this study.

Environmental considerations such as carbon offset or energy payback time[35] are not addressed by this study, but, for a wide scale deployment of PV, these metrics are important to fully quantify the benefits of such a decision.

Finally, modern technology, unaccounted for in this work, may give much better return on investment in the future (e.g. MIT 3D PV cells, Super Thin films), so the research is ongoing, and the expectation is that results will improve in step with technological progress.

IV.2. Contributions

The objectives traced at the outset of this dissertation have been fully attained. A methodology to transform highly spatiotemporally detailed 3DGIS/CIM urban solar exposure data into useable economic assessment metrics of residential PV systems was developed and applied successfully, using widely-available or open-source software tools. This enabled highly detailed modelling of the technical and economic performance of small scale isolated residential PV and BIPV systems, overcoming some of the identified limitations in current approaches such as high granularity irradiation data accounting for anisotropy and urban shading, façade implementations, inverter options, operating temperature, detailed PV system components modeling, building characteristics for deployment area, lifetime economic behavior and legal and fiscal frameworks, all the while retaining high customizability from the user´s perspective. This makes it adaptable to any other project, paving the way for its implementation on an accessible platform for wide dissemination

[35] The energy payback time is time it takes for the PV system to produce as much energy as was required to create it (i.e. the embodied energy). It can vary as much as 2 to 6 years in continental Europe for c-Si and 1 to 2 years for TF (see Jelle et. al, 2012, and Heinstein et. al., 2013)

taking full advantage of the 3D environment. To the best of the researchers´ knowledge, no other GIS based user-oriented PV system assessment methodology allows for façade inclusion or is as detailed in its calculations of irradiation and PV performance.

This methodology was applied, with the technical and economic potential of a standard rooftop and façade implementation of a PV and BIPV system assessed, with results in line with current market supporting the notion that both technologies are currently economically viable and a justifiable environmental and economic choice from the project developer´s perspective. The correct design of these systems can provide a large return on investment, support continuous savings throughout the lifetime of the project, guarantee a payback on investment in an acceptable timeframe and compete with retail electricity grid prices, making it an alternative source of energy worth considering. The insights provided into the sensitivity of the systems to several variables should help steer the decision process, complement the understanding of the risk factors in these residential PV deployments, and support the design of more robust and economically viable systems in Portugal and elsewhere. The current methodology implemented on a 3D-GIS urban model can further facilitate the deployment of urban PV projects and opens for consideration the inclusion of façades which complement standard rooftop arrays, reducing production costs per kWh and increasing monthly savings, while taking full advantage of the available solar resource.

Current limitations to full deployment of BIPV were identified, and the modeled results lend support to the notion that technology can be cost competitive both on rooftops and façades, as a standalone or as a complement to standard rooftop installation, a step forward in dissipating the mistaken and widely-held beliefs that their integration is more expensive than conventional roof installations and that their lifetime performance is significantly lacking. It is clearly shown that thin film technology can be cost competitive and present a very low-cost investment with economic upside and should be seriously considered for any building that aims to shift part of its load to green technology. It cannot yet cover the total consumption of a building as other PV technologies do, but it is an economically viable solution for distributed generation. This is step forward in BIPV urban integration and spurs the growth of its currently relatively small market share. To achieve full deployment of BIPV, other limitations need to be overcome, including aesthetic, technical and structural requirements of these cladding systems, as well as the development of the business, legal and fiscal frameworks to spur their development. Innovative business models with PV as a service are already deployed and account for over 50% of the residential PV sector in the U.S.A. and a sizeable portion of the market in Germany, Austria, Sweden and Switzerland (IEA, 2017). As the Portuguese legal framework allows for third parties to install PV on their behalf, this should soon be the case in Portugal as well.

This study focuses on bringing a clearer understanding of the possible benefits stemming from an integration of PV technologies in the urban fabric and is a step in the direction of further dissemination of BIPV to the public. Using a GIS tool, decision makers and urban planners can visualize spatio-temporal parameters of their residential PV investments and perform analyzes under different scenarios, supporting the deployment of the technology and the long-term goal of zero-emission cities.

References

Aliaga, D. G. (2012). 3D design and modeling of smart cities from a computer graphics perspective. *Computer Graphics, 2012*(2012), 19.

Antunes, J. (2017). *Os benefícios fiscais na reabilitação urbana*. Retrieved from Negócios: https://www.jornaldenegocios.pt/opiniao/colunistas/detalhe/os-beneficios-fiscais-na-reabilitacao-urbana

APESF (2015). *Regime Jurídico do Autoconsumo*, Retrieved February 2018, from https://www.apesf.pt/images/apesf/pdf/Regime_Jurdico_Autoconsumo.pdf

Banco de Portugal. (2018). *Projeções para a Economia Portuguesa: 2018-2020.* Retrieved March 2018, from https://www.bportugal.pt/sites/default/files/anexos/pdf-boletim/proj_mar2018_p.pdf

Barbose, G., & Darghouth, N. (2016). *Tracking the Sun IX.* Lawerence Berkeley National LAboratory. Retrieved from https://emp.lbl.gov/sites/default/files/tracking_the_sun_ix_report.pdf

Biljecki, F., Stoter, J., Ledoux, H., Zlatanova, S., & Çöltekin, A. (2015). Applications of 3D City Models: State of the Art Review. *ISPRS International Journal of GEo-information, 4*, 2842-2889.

Biyik, E., Araz, M., Hepbasli, A., Shahrestani, M., Yao, R., Shao, L., Essah, E., Oliveira, A.C., del Caño, T., Rico, L., Lechón, J.L., Andrade, L., Mendes, A., Atli, Y. B. (2017). A key review of building integrated photovoltaic (BIPV) systems. (Elsevier, Ed.) *Engineering Scienceand Technology, an International Journal, 20*, 833-858.

Bizjak, M., Zalik, B., & Lukac, N. (2015). Evolutionary-driven search for solar building models using LiDAR data. *Energy and Buildings, 92*, 195-203.

Blair, N. J., & Dobos, A. P. (2013). Comparison of Photovoltaic Models in the System Advisor Model. *Solar 2013.* Baltimore.

Bortolini, M., Gamberi, M., & Graziani, A. (2014). Technical and economic design of photovoltaic and battery energy storage system. *Energy Conversion and Management, 86*, 81-92.

Breyer, C., & Schmid, J. (2010). Global Distribution of Optimal Tilt Angles for Fixed Tilted PV Systems. *5th World Conference on Photovoltaic Energy Conversion, 6-10 September 2010*, (pp. 4716-4721). Valencia, Spain.

Brown, A., Beiter, P., Heimiller, D., Davidson, C., Denholm, P., Melius, J., Lopez, A., Hettinger, D., Mulcahy, D., Porro, G. (2016). *Estimating Renewable Energy Economic Potential in the United States: Methodology and Initial Results.* NREL.

Carneiro, C., Morello, E., & Desthieux, G. G. (2010). Urban Environment Quality Indicators: Application to Solar Radiation and Morphological Analysis on Built Area. *3rd WSEAS international conference on Visualization, imaging and simulation*, (pp. 141-148). Faro, Portugal.

Carneiro, C., Morello, E., Ratti, C., & Golay, F. (2008). Solar Radiation over the Urban Texture: Lidar Data and Image Processing Techniques for Environmental Analysis at City Scale. *Proceedings of the 3D Geoinfo Conference.* Seoul, 13-14 November 2008.

Catita, C., Redweik, P., Pereira, J., & Brito, M. C. (2014). Extending solar potential analysis in buildings to vertical facades. *Computers & Geosciences, 66*, 1-12.

CEC. (2018, March 15). *List of PV Modules*. Retrieved from Go Solar California: http://www.gosolarcalifornia.ca.gov/equipment/pv_modules.php

Chen, Y., Athienitis, A., & Fazio, P. (2012). Modelling of HIgh-Performance Envelope and Façade Integrated Photovoltaic/Solar Thermal Systems for High-Latitude Applications. *Proceedings of eSim 2012: The Canadian Conference on Building Simulation*, (pp. 108-121). Haifax, Nova Scotia.

Cheng, C., Jimenez, C. S., & Lee, M. (2009). Research of BIPV optimal tilted angle, use of latitude concept for south orientated plans. *Renewable Energy, 34*, 1644-1650.

Chow, A., Fung, A., & Li, S. (2014). GIS modeling of solar neighborhood potential at a fine spatiotemporal resolution. *Buildings, 4*(2), 195–206.

Chow, A., Li, S., & Fung, A. (2016). Modeling Urban Solar Energy with High Spatiotemporal Resolution: A Case Study in Toronto, Canada. *International Journal of Green Energy, 13*(11).

CIMLT. (2016). *Guia de Incentivos à Reabilitação Urbana.* Retrieved from http://www.cimlt.eu/todos-os-documentos/1396-guia-incentivos-reabilitacao-urbana/file

Compagnon, R. (2004). Solar and daylight availability in the urban fabric. *Energy and Buildings, 36*, 321-328.

Comparajá.pt. (2018). *Compare Crédito para Renováveis*. Retrieved from Comparajá.pt: https://www.comparaja.pt/credito-pessoal/energias-renovaveis

COP 21. (2016). COP 21 Conference Proceedings. *Report of the Conference of the Parties on its twenty- first*, (p. 2). Paris. Retrieved January 1, 2017, from http://unfccc.int/meetings/paris_nov_2015/session/9057/php/view/documents.php

Couture, T. D., Jacobs, D., Rickerson, W., & Healey, V. (2015). *The Next Generation of Renewable Electricity Policy: How Rapid Change is Breaking Down Conventional Policy Categories.* NREL.

Culligan, M., & Botkin, J. (2007). *Impact of Tilt Angle on System Economics for Area Constrained Rooftops.* SUNPOWER CORPORATION. Retrieved from Sunpower.

Dean, J., Kandt, A., Burman, L., Lisell, L., & Helm, C. (2009). Analysis of Web-Based Solar Photovoltaic Mapping Tools. In NREL (Ed.), *ASME 3rd International Conference on Energy Sustainability.* California: NREL. Retrieved December 2016

Defaix, P., van Sark, W., Worell, E., & de Visser, E. (2012). Technical Potential for photovoltaics on buildings in the EU-27. *Solar Energy, 86*, 2644-2653.
DeSoto, W., Klein, S., & Beckman, W. (2006). Improvement and Validation of a Model for Photovoltaic Array Performance. *Solar Energy, 80*, 78-88.
Despotovica, M., Nedica, V., Despotovicb, D., & Cvetanovicc, D. (2015). Review and statistical analysis of different global solar radiation sunshine models. *Renewable Sustainable Energy Reviews, 52*, 1869–1880.
Diário de Notícias. (2017, October 22). *Casa deixa de contar para o IRS quando se muda o crédito de banco*. Retrieved from Diário de Notícias: https://www.dn.pt/dinheiro/interior/casa-deixa-de-contar-para-o-irs-quando-se-muda-o-credito-de-banco-8863329.html
Dobos, A. P. (2013). *PVWatts Version 1 Technical Reference.* NREL.
Dobos, A. P. (2014, September). *PVWatts Version 5 Manual.*
Dobos, A., & Gilman, P. (2017, April 4). *SSC Reference Manual SDK 2017.1.17 Revision 2, SSC 172.*
DR. (2012). L 32/2012. In *Diário da República n.º 157/2012, Série I de 2012-08-14.*
DR. (2014). DL 153/2014. In *Diário da República, 1.ª série — N.º 202 — 20 de outubro de 2014.*
DR. (2014b). Lei 82-D/2014. In *Diário da República, 1.ª série — N.º 252 — 31 de dezembro de 2014.*
DR. (2018). Portaria 32/2018. In *Diário da República, 1.ª série — N.º 16 — 23 de janeiro de 2018.*
Economias. (2016, December 14). *IRS: deduções com energias renováveis*. Retrieved from Economias: https://www.economias.pt/irs-2010-deducoes-com-energias-renovaveis/
Economias. (2018). *Escalões de IRS para 2018*. Retrieved from Economias: https://www.economias.pt/escaloes-de-irs-para-2018/
EDP Comercial. (2018). *Tarifários*. Retrieved March 18, 2018, from https://www.edp.pt/particulares/energia/tarifarios/?prod=15421
EDP Comercial. (2018b). *O que é a opção horária e qual a melhor para mim?* Retrieved from EDP: https://www.edp.pt/particulares/apoio-cliente/perguntas-frequentes/tarifarios/o-que-preciso-de-saber-para-contratar/o-que-e-a-opcao-horaria-e-qual-a-melhor-para-mim/faq-4823
Eicker, U., Monien, D., Duminil, E., & Nouvel, R. (2015). Energy Performanceassesment in urban planning competitions. *Applied Energy, 155*, 323-333.
Eiffert, P. (2003). *Guidelines for the Economic Evaluation of Building-Integrated Photovoltaic Power Systems.* NREL.
Eiffert, P., & Kiss, G. J. (2000). *Building Integrated Photovoltaic Designs for Commercial and Institutional Structures - A Sourcebook for Architects.* US DOE.
Eiffert, P., & Thompson, A. (2000). *U.S. Guidelines for the Analysis of Building-Integrated Photovoltaic Power Systems.* NREL.
EnergyPlus. (2018). *EnergyPlus Documentation - Engineering Reference - The Reference to EnergyPlus Calculations.* LBNL. Retrieved from https://energyplus.net/sites/default/files/pdfs_v8.3.0/EngineeringReference.pdf
ENERTECH. (2002). *Demand-side Management: End-use metering campaign in 400 households of the European Community - Assessment of the Potential Electricity Savings.* Comission of European Communities.
EPIA. (2011). *Solar Generation 6 - Solar photovoltaic electricity empowering the world.* European Photovoltaic Industry Association.
Esclapes, J., Ferreiro, I., Piera, J., & Teller, J. (2014). A method to evaluate the adaptability of photovoltaic energy on urban façades. *Solar Energy, 105*, 414–427.
EU. (2010, May 19). Directive 2010/31/EU of the European Parliament and of the Council of 19 May 2010 on the energy performance of buildings (recast). *Of. J. Eur. Union*, pp. 13-35.
European Comission. (2017). *Overview of PVGIS data sources and calculation methods*. Retrieved from Photovoltaic Geographical Information System: http://re.jrc.ec.europa.eu/pvg_static/methods.html#!
Eurostat. (2018, January). *Renewable Energy Statistics*. Retrieved March 9, 2018, from Eurostat Statistics Explained: http://ec.europa.eu/eurostat/statistics-explained/index.php/Renewable_energy_statistics
Faiman, D. (2008). Assessing the outdoor operating temperature of photovoltaic modules. *Progress in Photovoltaics: Research & Application, 16*, 307–315.
Falcão, A., Ildefonso, S., & Rua, H. (2016). Applications of 3D city models in the study of urban evolution, Jornadas de Engenharia Civil no Instituto Politécnico de Leiria
Fath, K., Stengel, J., Sprenger, W., Wilson, H., Schultmann, F., & Kuhn, T. (2015). A method for predicting the economic potential of (building-inteegrated) photovoltaics in urban areas based on Radiance simulations. *Solar Energy, 116*, 357-370.
Fiorelli, J., & Zuercher-Martinson, M. (2013, July). How oversizing your array-to-inverter ratio can improve solar-power system performance. *Solar Power World*, pp. 42-46. Retrieved from https://www.solectria.com/site/assets/files/1472/solectria_oversizing_your_array_july2013.pdf
Fogl, M., & Moudry, V. (2016). Influence of vegetation canopies on solar potential in urban environments. *Applied Geography, 66*, 73-80.
Fraunhofer ISE. (2017). *Photovoltaics Report.* Freiburg: Fraunhofer Institute for Solar Energy.
Free Clean Solar. (2018). *Compare String Inverters vs. Optimizers vs. Micro-Inverters: Which is the Best?* Retrieved from Free Clean Solar: http://www.freecleansolar.com/Solar-String-vs-Micro-Inverters-s/4781.htm

Freeman, J., Whitmore, J., Blair, N., & Dobos, A. P. (2014). *Validation of Multiple Tools for Flat Plate Photovoltaic Modeling Against Measured Data.* NREL. Retrieved March 2017

Freitas, S., Catita, C., Redweik, P., & Brito, M. (2015). Modelling solar potential in the urban environment: State-of-the-art review. *Renewable and Sustainable Energy Reviews, 41*, 915-931.

Fu, R., Feldman, D., Margolis, R., Woodhouse, M., & Ardani, K. (2017). *U.S. Solar Photovoltaic System Cost Benchmark: Q1 2017.* NREL.

Fuentes, M. K. (1987). *A Simplified Thermal Model for Flat-Plate Photovoltaic Arrays.* Albuquerque, NM: Sandia National Laboratories.

Gagnon, P., Margolis, R., Melius, J., Phillips, C., & Elmore, R. (2016). *Rooftop Solar Photovoltaic Technical Potential in the United States: A Detailed Assesment.* NREL.

GCSPS. (2011, August 3). *Solar Power Gross or Net Feed in Tariff?* Retrieved April 2, 2017, from Gold Coast Solar Power Solutions: http://gold-coast-solar-power-solutions.com.au/posts/solar-power-gross-or-net-feed-in-tariff/

Gil, J., Almeida, J., & Duarte, J. (2011). The backbone of a City Information Model (CIM): Implementing a spatial data model for urban design. *29th eCAADe Conference Proceedings*, (pp. 143-151). Ljubljana, Slovenia, 21-24 September 2011.

Gilman, P. (2013, July 24). *Introduction to the SAM Software Development Kit (SDK), July 2013 .* Retrieved February 26, 2017, from NREL SAM: https://sam.nrel.gov/content/introduction-sam-software-development-kit-sdk-july-2013

Gilman, P. (2015). *SAM Photovoltaic Model Technical Reference.* NREL.

Gilman, P. (2018). SAM Electrical Load Profile Estimator (ELPEst, version 1.0). *Document available upon request to sam.support@nrel.gov*.

Grana, P. (2016, July 8). *Solar inverters and clipping: What DC/AC inverter load ratio is ideal?* Retrieved from Solar Power World: https://www.solarpowerworldonline.com/2016/07/solar-inverters-clipping-dcac-inverter-load-ratio-ideal/

Hay, J. (1979). Calculation of monthly mean solar radiation for horizontal and inclined surfaces. *Solar Energy, 23*(4), 301–307.

Heinstein, P., Ballif, C., & Perret-Aebi, L.-E. (2013). *Building Integrated Photovoltaics (BIPV): Review, Potentials, Barriers and Myths .* EPFL.

Hendron, R., & Engenbrecht, C. (2010). *Building America House Simulation Protocols.* NREL. Retrieved from https://www.nrel.gov/docs/fy11osti/49246.pdf

Hofierka, J., & Suri, M. (2002). The solar radiation model for open source GIS: implementation and applications. *Open source GIS-GRASS users conference.*

Hofierka, J., & Zlocha, M. (2012). A new 3-D Solar radiation model for 3-D city models. *Transactions in GIS, 16*(5), 681–680.

Horowitz, K. A., Fu, R., Sun, X., Silverman, T., Woodhouse, M., & A. Alam, M. (2017). *An Analysis of the Cost and Performance of Photovoltaic Systems as a Function of Module Area.* NREL. Retrieved from https://www.nrel.gov/docs/fy17osti/67006.pdf

Horvath, M., Kassai-Szoo, D., & Csoknyai, T. (2016). Solar energy potential of roofs on urban level based on building typology. *Energy and Buildings, 111*, 278-289.

Huld, T., & Amillo, A. M. (2015). Estimating PV Module Performance over Large Geographical Regions: The Role of Irradiance, Air Temperature, Wind Speed and Solar Spectrum. *Energies, 8*, 5159-5181.

Huld, T., Friesen, G., Skoczek, A., Kenny, R., Sample, T., Field, M., & Dunlop, E. (2011). A power-rating model for crystalline silicon PV modules. *Solar Energy Materials & Solar Cells., 95*, 3359-3369.

IDAE. (2011). *Analyses of the energy consumption of the household sector in Spain.* Gobierno de España & Eurostat, Planning and Studies Department. Retrieved from https://ec.europa.eu/eurostat/cros/system/files/SECH_Spain.pdf

IEA. (2015). *2015 Snapshot Of Global Photovoltaic Markets.* IEA - PVPS. Retrieved January 1, 2017

IEA. (2016a). *Energy Policies of IEA countries - Portugal 2016 Review.* IEA.

IEA. (2016b). *IEA PVPS Task 15 - Enabling Framework for BIPV acceleration.*

IEA. (2016c). *Key World Energy Statistics 2016.* International Energy Agency. Retrieved January 15, 2017

IEA. (2017). *Trends in Photovoltaic Applications 2017.* IEA PVPS.

INETI. (2015). Weather Data By Location. Lisbon. Retrieved November 11, 2016, from Energy Plus: https://energyplus.net/weather-location/europe_wmo_region_6/PRT//PRT_Lisboa.085360_INETI

Inforestilo . (2015, May 28). *Minuto Fiscal - Condomínios Imóveis Habitação* . Retrieved from Inforestilo : http://www.inforestilo.pt/informacao-util/minuto-fiscal-condominios-imoveis-habitacao.html

ISSOL. (2016). *ISSOL - Architecture BIPV*. Retrieved January 16, 2017, from http://www.issol.eu/

Jakubiec, J. A., & Reinhart, C. F. (2013). A Method for Predicting City-Wide Electricity Gains from Photovoltaic Panels Based on LiDAR and GIS Data Combined with Hourly Daysim Simulations. *Solar Energy, 93*, 127-143.

James, T., Goodrich, A., Woodhouse, M., Margolis, R., & Ong, S. (2011). *Building-Integrated Photovoltaics (BIPV) in the Residential Sector: An Analysis of Installed Rooftop System Prices.* NREL.

Jelle, B. P., Breivik, C., & Rokenes, H. D. (2012). Building integrated photovoltaic products: A state-of-the-art review and future research opportunities. *Solar Energy Materials & Solar Cells, 100*, 69-96.
Jesus, L., Almeida, M., & Pereira, E. (2005, January). A integração de fotovoltaicos nos edifícios em Portugal - DIficuldades e Oportunidades. *Engenharia e Vida*, pp. 38-45.
Jordan, D. R., & Kurtz, S. (2013). Photovoltaic Degradation Rates—an Analytical Review. *Progress in Photovoltaic Research and Applications, 21*, 12-29.
Koinegg, J., Brudermann, T., Posch, A., & Mrotzek, M. (2013). An Analysis of Prospects and Barriers of Building Integrated Photovoltaics. *GAIA, 22*(1), 39-45.
Kuiper, J., Ames, D., Koehler, D., Lee, R., & Quinby, T. (2013). *Web-based Mapping Applications for Solar Energy Project Planning.* Idaho National Laboratory.
Kumar, L., Skidmore, A., & Knowles, E. (1997). Modelling topographic variation in solar radiation in a GIS environment. *International Journal of Geographical Information Science, 11*(5), 475-497.
Lang, T., Ammann, D., & Girod, B. (2016). Profitability in absence of subsidies: A techno-economic analysis of rooftop photovoltaic self-consumption in residential and comercial buildings. *Renewable Energy, 87*, 77-87.
Lazard. (2017). *Lazard´s Levelized Cost of Energy Analysis - Version 11.0.*
Lee, J. B., Yoon, J. H., Baek, N. C., Kim, D. K., & Shin, U. C. (2014). An empirical study of performance characteristics of BIPV (Building Integrated Photovoltaic) system for the realization of zero energy building. *Energy, 66*, 25-34.
Levinson, R., Akbari, H., Pomerantz, M., & Gupta, S. (2009). Solar access of residential rooftops in four California cities. *Solar Energy, 83*(12), 2120-2135.
Liang, J., Gong, J., Zhou, J., Ibrahim, A., & Li, M. (2015). As open-source 3D solar radiation model integrated with a 3D Geographic Information System. *Environmental Modelling Software, 64*, 94-101.
Liu, B. Y., & Jordan, R. C. (1960). The interrelationship and characteristic distribution of direct, diffuse and total solar radiation. *Solar Energy, 4*(3), 1–19.
Machete, R. F. (2016). *Utilização de Modelos SIG-3D na Determinação da Radiação Solar Incidente nos Edifícios - Influência do Contexto Urbano.* Master´s Thesis Dissertation, Instituto Superior Técnico, Engenharia CIvil, Lisboa. Retrieved March 2017
Machete, R., Falcão, A., & Gomes, M. (2015). The use of 3DGIS to analyse the influence of urban context in building solar exposure. *VIII CNCG. Conferência Nacional de Cartografia e Geodesia, 29 e 30 de Outubro de 2015,* Ordem dos Engenheiros, Lisboa
Maia, C. (2017, May 29). *Energias renováveis: quais as opções de financiamento?* Retrieved from Comparaja: https://www.comparaja.pt/blog/energias-renovaveis-financiamento
Mapdwell. (2013). *Mapdwell Solar System*. Retrieved from https://www.mapdwell.com/en/solar
Marion, W., Adelstein, J., Boyle, K., Hayden, H., Hammond, B., Fletcher, T., Canada, B., Naraang, D., Shugar, D., Wenger, H., KImber, A., Mitchell, L., Rich, G., Townsend, T. (2005). Performance Parameters for Grid-connected PV Systems. *Proceedings of 31st IEEE Photovoltaics Specialists Conference.* Lake Buena Vista, Florida.
Marsh, A. (2004). Non-uniformity in incident solar radiation over the facades of high rise buildings. *PLEA. The 21th Conference on Passive and Low Energy Architecture*, (pp. 19-22). Eindhoven, The Netherlands.
Martin, A., Dominguez, J., & Amador, J. (2015). Applying LIDAR datasets and GIS based model to evaluate solar potential over roofs: a review. *AIMS Press, 3*(3), 326-343.
Martin, N., & Ruiz, J. (2001). Calculation of the PV modules angular losses under field conditions by means of an analytical model. *Solar Energy Materials & Solar Cells, 70*, 25-38.
Martin, N., & Ruiz, J. (2013). Corrigendum to "Calculation of the PV modules angular losses under field conditions by means of an analytical model" [Sol. Energy Mater. Sol. Cells 70 (1) (2001) 25-38]. *Solar Energy Materials & Solar Cells, 110*, 154.
Martins, F. M. (2016, March 31). *Poupar com energia solar: consumir ou vender?* Retrieved from Comparaja: https://www.comparaja.pt/blog/poupar-com-energia-solar-consumir-ou-vender
Meeus, J. (2000). *Astronomical Algorithms.* Willmann-Bell.
Melius, J., Margolis, R., & Ong, S. (2013). *Estimating Rooftop Suitability for PV: A Review of Methods, Patents, and Validation Techniques.* NREL. Retrieved December 2016
Menicucci, D. (1986). Photovoltaic Array Performance Simulation Models. *Solar Cells, 18*(3-4), 383-392.
Menicucci, D., & Fernandez, J. (1988). *User´s Manual for PVFORM: A Photovoltaic System SImulation Program for Stand-Alone and Grid-Interactive Applications.* Albuquerque, NM: Sandia National Laboratories.
Michalsky, J. (1988). The Astronomical Almanac´s Algorithm for Approximate Solar Position (1950-2050). *Solar Energy, 40*(3), 227-235.
Microsoft. (2018). *Compatibility Between the 32-bit and 64-bit Versions of Office 2010*. Retrieved from Office Dev Center: https://msdn.microsoft.com/en-us/library/office/ee691831(v=office.14).aspx
Moura, J. P. (2016, April 22). *Encargos com a Reabilitação de Imóveis no IRS*. Retrieved from Economias: https://www.economias.pt/encargos-com-a-reabilitacao-de-imoveis-no-irs/

NOAA. (2018). *Temperature*. Retrieved from Weather.gov: https://www.weather.gov/source/zhu/ZHU_Training_Page/definitions/dry_wet_bulb_definition/dry_wet_bulb.html
NREL. (2017b). *Disclaimer*. Retrieved from http://www.nrel.gov/disclaimer.html
NREL. (2017c, October 3). *NREL Photovoltaic Research - Best Research Cell Efficiencies.* Retrieved from NREL: https://www.nrel.gov/pv/assets/images/efficiency-chart.png
OMIE. (2011-2014). *OMIE Annual Reports.* Retrieved from OMIE: http://www.omie.es/en/home/publications/annual-report
OMIP. (2018). *Market Data Downloads*. Retrieved from OMIP: https://www.omip.pt/Downloads/SpotPrices/tabid/296/language/en-GB/Default.aspx
Paidipati, J., Frantzis, L., Sawyer, H., & Kurrasch, A. (2008). *Rooftop Photovoltaics Market Penetration Scenarios.* NREL. Retrieved December 2016
Pereira, M. C., Joyce, A., & Reis, P. C. (2016a, January 1). O valor e custo da eletricidade produzida por sistemas solares (fotovoltaicos). *Renováveis Magazine, 7*(25), pp. 46-49.
Pereira, M. C., Joyce, A., & Reis, P. C. (2016b, April 1). O valor e o custo da eletricidade produzida por sistemas solares (fotovoltaicos), 2ª parte. *Renováveis Magazine, 7*(26), pp. 48-54.
Perez, R., Ineichen, P., Seals, R., Michalsky, J., & Stewart, R. (1990). Modeling daylight availability and irradiance components from direct and global irradiance. *Solar Energy, 44*, 271-289.
Perez, R., Seals, 0. R., Ineichen, P., Stewart, R., & Menicucci, D. (1987). A new simplified version of the perez diffuse irradiance model for tilted surfaces. *Solar Energy, 39*(3), 221–231.
Peronato, G., & Rey, E. A. (2016). 3D-modeling of vegetation from Lidar point clouds and assessment of its impact on facade solar irradiation. In 1. 3.-2. 2016 (Ed.), *The International Archives of the Photogrammetry, Remote Sensing and Spatial Information Sciences*, *VOL XLII-2/W2*, pp. 67-70. Athens, Greece.
Pickerel, K. (2011, October 6). *Solar Inverters 101.* Retrieved April 14, 2017, from Solar Builder: http://solarbuildermag.com/featured/solar-inverters-101/
PORDATA. (2011). Average household size, according to the Census. Retrieved from https://www.pordata.pt/en/DB/Portugal/Search+Environment/Table
PORDATA. (2016). Electricity consumption per capita: total and by type of consumption. PORTUGAL. Retrieved from https://www.pordata.pt/en/Portugal/Electricity+consumption+per+capita+total+and+by+type+of+consumption-1230
Psomopoulos, C. S., Ioannidis, G. C., Kaminaris, S. D., Mardikis, K. D., & Katsikas, N. G. (2015). A Comparative Evaluation of Photovoltaic Electricity Production Assessment Software (PVGIS, PVWatts and RETScreen). *Environmental Processes, 2*(1). doi:10.1007/s40710-015-0092-4
PVEducation. (2018). *Nominal Operating Cell Temperature*. Retrieved from PVEducation: http://pveducation.org/pvcdrom/modules/nominal-operating-cell-temperature
PWC. (2015). *O ano das reformas 2015.* Retrieved from https://www.pwc.pt/pt/pwcinforfisco/reforma/fiscalidade-verde/analise-pwc-2.html
Quercus. (2017, September 4). *Crescimento do setor deve apostar mais na produção descentralizada*. Retrieved from Quercus: http://www.quercus.pt/comunicados/2017/setembro/5364-solar-fotovoltaico-ainda-representa-menos-de-4-da-capacidade-instalada-para-producao-de-energia-renovavel-em-portugal
Ratti, C., Bakerb, N., & Steemersb, K. (2005). Energy consumption and urban texture. *Energy and Buildings 37 (7),, 37*(7), 762–776.
Redweik, P., Catita, C., & Brito, M. C. (2013). Solar energy potential on roofs and facades in an urban landscape. *Solar Energy, 97*, 332-341.
Rodrigues, F., Cardeira, C., & Calado, J. (2014). The daily and hourly energy consumption and load forecasting using artificial neural network method: a case study using a set of 93 households in Portugal. *Energy Procedia, 62*, 220 – 229.
Rodrigues, F., Cardeira, C., Calado, J., & Melício, R. (2016). Load Profile Analysis Tool for Electrical Appliances in Households Assisted by CPS. *Energy Procedia*(106), 215 – 224.
Rodriguez, L. R., Duminil, E., Ramos, J. S., & Eicker, U. (2017). Assesment of the photovoltaic potential at urban level based on 3D city models: A case study and new methodological approach. *Solar Energy, 146*, 264-275.
Santos, T., Nuno, G., Brito, M., F. S., Fonseca, A., & Tenedório, A. (2011). Solar potential analysis in Lisbon Using LIDAR data. *Remote Sensing and Geoinformation*, (pp. 13-19).
Sarralde, J. J., Quinn, D. J., Wiesmann, D., & Steemers, K. (2015). Solar energy and urban morphology: Scenarios for increasing the renewable energy potential of neighbourhoods in London. *Renewable Energy, 73*, 10-17.
SDK Forum. (2017, February 5). *Pvwatts with user defined POA Irradiance* . Retrieved from NREL: https://sam.nrel.gov/node/73754
SDK Forum. (2017b, February 2). *PVWatts V1 Input Parameters*. Retrieved from NREL: https://sam.nrel.gov/node/73998
Short, W., Packey, D., & Holt, T. (1995). *A manual for the Economic Evaluation of Energy Efficiency and Renewable Energy Technologies.* NREL.

Shukla, A. K., Sudhakar, K., & Baredar, P. (2017, April 1). Recent advancement in BIPV product technologies: A review. *Energy and Buildings, 140*, 188-195.
Silva, J. (2016). *Characterization, Seismic Assessment and Strengthening of a Mixed Masonry-Reinforced Concrete Building.* Lisboa: IST.
Singh, G. (2013). Solar power generation by PV (photovoltaic) technology: a review. *Energy, 53*, 1-13.
Smalley, J. (2015). *How does solar backtracking make projects more productive?* Retrieved from Solar Power World: https://www.solarpowerworldonline.com/2015/07/how-does-solar-backtracking-make-projects-more-productive/
Solar Reviews. (2018). *Pros and Cons of String Inverters vs. Micro Inverters*. Retrieved from Solar Reviews: https://www.solarreviews.com/solar-inverters/pros-and-cons-of-string-inverter-vs-microinverter/
Solar, F. (2017). *Resumo do processo para unidades de pequena produção*. Retrieved from FF Solar: http://www.ffsolar.com/pdf/Resumo_UPP_pt.pdf
Solar, F. (2017b). *Resumo de processo para unidades de produção para autoconsumo sem venda e com venda*. Retrieved from FF Solar: http://www.ffsolar.com/pdf/Resumo_UPAC_pt.pdf
Teke, A., Yildirim, H., & Çelik, O. (2015). Evaluation and performance comparison of different models for the estimation of solar radiation. *Renewable Sustainable Energy Reviews, 50*, 1097-1107.
Tesla. (2017). *Solar Roof*. Retrieved May 14, 2017, from Tesla: https://www.tesla.com/pt_PT/blog/solar-roof?redirect=no
Tooke, T., Coops, N., Christen, A., Gurtuna, O., & Prevot, A. (2012). Integrated irradiance modeling in the urban environment based on remotely sensed data. *Solar Energy, 86*(10), 2923-2934.
UNDP. (2000). *World Energy Assessment - Energy and the Challenge of Sustainability.* United Nations Development Programme. Retrieved January 15, 2017
Yang, R. J., & Zou, P. (2016). Building integrated photovoltaics (BIPV): costs, benefits, risks, barriers and improvement strategy. *International Journal of Construction Management, 16*(1), 39-53.
Yates, T., & Hibberd, B. (2010, April/May). Production Modeling for Grid-Tied PV Systems. *Solar Pro Magazine*(3.3).

Appendix I
Summary of the UP Regime

In DL 153/2014 (DR, 2014) the concept of production unit (UP, *unidade de produção*) was introduced, as the production of electricity by means of decentralized units with associated supply contract with an electricity retailer, subdivided into small production (UPP, *unidade de pequena produção,* with total grid injection) and self-consumption (UPAC, *unidade de produção de auto-consumo*, with provision for grid injection).

The most relevant details of the UP and UPAC regimes are as follows (DR, 2014): For all UPs, the output capacity (e.g. nominal power rating output of the inverter in the case of PV) to the RESP must be equal or below 100% of the contracted capacity to the retailer; For UPAC, the installed capacity (active and apparent power rating of the electrical generators which in the case of PV is the accumulated nominal capacities of the PV panels) must not exceed 200% of the output capacity. UPAC benefit from a monthly net-billing FiT, in which the share of energy produced that is sold to the grid is done so at a discount to the wholesale market price (disincentivizing the oversizing of installations above the expected local consumption), to the Last Resort Retailer (*Comercializador de Último Recurso*, or CUR). Annual production should remain as close to consumption as possible, non-compliance with this obligation being subject to exclusion from any remuneration for injected energy into the grid. For UPAC with capacity above 1.5kW, they must also make a monthly payment of the CIEG (*Compensação de Interesse Económico Geral*, General economic interest compensation), for the first 10 years after obtaining exploration certificate[1].

All the process to manage the bureaucracies related to UPs is done online, on the SERUP platform (*Sistema Electrónico de Registo de Unidades de Produção*) which is managed by the DGEG. The registration of multiple UPs can be done under the same name, therefore a condominium can register as many UPs as there are consumption points in the building and install a single system (legally made up of multiple UPs).

Until 2010 there were specific tax deductions to the IRS available for the acquisition of renewable energy equipment, but these have since been phased out (Economias, 2016). On the other hand, at the beginning of 2015, the Green tax reform (*Reforma de Fiscalidade Verde*, Lei 82-D/2014 (DR, 2014b)) was implemented, with changes at the level of tax depreciation on PV equipment and municipal real estate tax (IMI) for Renewable Energy Sources (RES) power producing buildings (IEA, 2017). Specifically, the maximum straight line accelerated depreciation for corporate tax purposes (IRC, *Imposto sobre rendimento colectivo*) for solar equipment was reduced from 25% to 8% (increasing the lifetime for tax purposes from

[1] This tax attempts to reflect the potential added costs to grid operation resulting from the injection/extraction to and from the grid, and the reduced revenue from consumption proportional to the installed capacity (not yet in effect as UPAC do not yet account for more than 1% of installed production capacity in the national electric system (Quercus, 2017)).

4 to 12.5 years), and urban buildings exclusively assigned to energy production from RES benefit from a 50% real estate tax break (IMI, *Imposto Municipal sobre Imóveis*) for 5 years (PWC, 2015). Beyond this, under the Lei 32/2012 (DR, 2012), the rehabilitation of urban buildings can be subject to extensive tax benefits (with possible reductions to the IMI, IMT, IVA, and IRS), dependent on, among other things, the location and energy certification improvement (CIMLT, 2016). More details concerning these benefits can be found in Moura, J.P., (2016) and Antunes, J., (2017).

In regard to subsidies, those targetted at investment in renewable energies (not specific for PV) for RD&D (Research Development and Demonstration) include FAI (*Fundo de Apoio à Inovação – Energias Renováveis e Eficiência Energética*), FPC (*Fundo Português de Carbono*), and QREN/COMPETE (*Quadro de Referência Nacional, Programa Operacional de Factores de Competitividade*) (IEA, 2016a).

Under the UP regime, the remuneration tariff cannot be accumulated with other types of production incentives that fall under the special production regime. In Portugal there is no specific legislation for BIPV, being that all that applies to PV is applicable to BIPV technology.

Table 18 – Summary UP regime established by DL 153/2014 & Portaria 32/2018; Sources: DR (2014), DR (2018), EDP (2015), APESF (2015), Futursolutions (2016b), Solar (2017d), Solar (2017e) & SPAES (2018)

	UPAC	UPP
Capacity limit	Output Capacity (i.e. inverter rating) ≤100% contracted capacity with the electricity retailer; Installed Capacity (i.e. PV pannel rating) <200% of Output Capacity	Output capacity ≤100% contracted capacity; Max = 250kW
Production	Must be sized so as to approximate the produced energy to the consumed energy (estimated with Y-1 demand load); Can sell instantaneous excess generation to the CUR	Must be sized so as to produce a maximum of 200% of the consumed energy (estimated with Y-1 demand load); Sells all energy to the CUR
Producer & Installation	The consumer (natural or legal person, or condominium) can install a UPAC for each electrical installation of utilization, consume its electricity and export the excess to the RESP. The UP must be installed on the same site as the utilization instalation. Multiple UP registries can be made under the same name as long as for each UP there is a single associated utilization installation	The consumer (natural or legal person, or condominium) or 3rd party duly authorized by the holder of the electricity supply contract to the utilization installation, can install a UPP for each utiliation installation. The UP must be installed on the same site as the utilization instalation. Multiple UP registries can be made under the same name as long as for each UP there is a single associated utilization installation
Quota	N/A	Annual quota ≤ 20 MW for tenders of UPP
Remuneration	Payment for power supplied to the RESP is done according to: $R_{UPAC,m} = E_{supplied,m} \times OMIE_m \times 0.9$ $R_{UPAC,m}$ Payment for month m in € $E_{supplied,m}$ Energy Supplied in month m in kWh $OMIE_m$ Arithmetic average of the daily setllement price of OMIE for month m in €/kWh Sale contract with the CUR has a maximum duration of 10 years, renewable for 5 year periods; UPAC with installed capacity > 1.5kW and connected to the RESP must pay a monthly tax (CIEG) for the first 10 years after obtaining the exploration license; Installed Capacity ≥ 1MW can sell to other than CUR or in the wholesale market; the payment is done according to a net-billing policy, only the instantaneous excess production above demand load is sold to the grid	FiT attributed by public tender where producers bid for a share of the annual quota with discounts to the reference tariff, published in *portaria* for each category: Category I: Installation of one UPP Category II: Installation of UPP with associated electrical vehicle charging outlet Category III: Installation of UPP with a solar thermal colector with area ≥ 2m^2 The FiT will be the resulting price of the tender, is dependent on the primary energy used on the UPP and is valid for 15 years, counting from the first day of electricity supply
Metering	Mandatory metering of produced and injected electricity in the RESP for UPAC with installed capacity ≥1.5kW	Mandatory metering of the injected electricity into the RESP

		Inst. Cap.≤ 200W	200W ≤ Inst. Cap. ≤ 1.5kW; Connected to RESP	1.5kW ≤ Inst. Cap. ≤ 1MW; Connected to RESP	Inst. Cap. ≤ 1MW; non consumed energy injected into RESP	Inst. Cap. ≥ 1MW	Off-Grid	Any UPP
Licensing Process	Exemption of previous control	X						
	Mere previous communication		X				X	
	Registration on SERUP (mandatory if selling on RESP)			X	X	X		X
	Exploration Certificate (mandatory if selling on RESP)			X	X			X
	Production License					X		
	Exploration License					X		
	Liability Insurance (mandatory if registered on SERUP)			X	X	X		X
	Periodic Inspection (mandatory if connected to grid)			Every 10 years, 20% of registration tax				Only if Inst. Capacity ≥ 1.5kW

		W/o sale to Grid	W/ sale to Grid	
Registration fees (VAT = 23%)	Inst. Cap. ≤ 1.5kW	N/A	30€ + VAT	30€ + VAT
	1.5 kW < Inst. Cap. ≤ 5 kW	70€ + VAT	100€ + VAT	100€ + VAT
	5 kW < Inst. Cap. ≤ 100 kW	175€ + VAT	250€ + VAT	250€ + VAT
	100 kW < Inst. Cap. ≤ 250 kW	300€ + VAT	500€ + VAT	500€ + VAT
	250 kW < Inst. Cap. ≤ 1000 kW	500€ + VAT	750€ + VAT	750€ + VAT

Appendix II

System Specifications – System Advisor Model (NREL)

The System Advisor Model (SAM) is a free software developed by the National Renewable Energy Laboratory (NREL) for predicting the performance of renewable energy systems and analyzing the financial feasibility of residential, commercial, and utility-scale grid-connected projects, offering several options for multiple technologies, including performance of photovoltaic systems, with simulation results widely regarded as representative of real world operation (Freeman et al.,2014). Included are also a suite of analysis tools that include parametric, optimization, sensitivity and statistical tools, providing insight on the relationship of system variables and how changes to these variables impact the output metrics such as production and finance indicators. SAM also provides free technical support through the SDK forum, giving direct access to the developers of the software, with timely and comprehensive responses to queries.

SAM Development Kit

Besides having a user-friendly consumer-oriented version of their renewable energy calculators (SAM Desktop), there is a collection of development tools named SSC SDK (SAM Development Kit), which comprehensively extends the capabilities of the Desktop Software by allowing developer access to the SSC (SAM Simulation Core) and permitting customized uses of the energy system models within the SSC library. The SDK allows access to the SAM application programming interface (API) from 3rd party programs, enabling the developer to run his own simulations, vary inputs and automate repetitive tasks, designing bespoke models by combining the different modules in the SSC library. It does not however allow the developer to alter a simulation module´s source code (no access to the library´s contents), only to change the inputs and get the respective outputs. In this way, the user can model systems (e.g. PV system performance) and projects (e.g. financials of the system) without running the SAM Desktop software.

A module in the SSC (also referred to as simulation module or compute module) is a chunk of compiled code that simulates a system component, project cash flow or performs a modeling function. The programmer can write code to combine multiple modules to build a system or project model.

The SCC SDK, found at https://sam.nrel.gov/sdk, includes the following:

1. The SSC Guide explaining how to use the tools in the SDK
2. The SSC API (Application Programming Interface) in ISO-standard C – the header file in native C language (i.e. the API to relay between the SSC and the computer program)
3. The SDKtool (an index of all the modules, functions and variables being used by SAM), to explore the SSC modules´ different variables, and help build and test models.
4. A set of precompiled binary dynamic libraries (.dll) for the following operating systems and architectures (the actual SSC, precompiled, where the different system component modules are housed and where the calculations take place, driven by the inputs from the API): Windows 8/7/Vista 64-bit; Windows 8/7/Vista 32-bit; OS X 10.8 64-bit; Linux 64-bit
5. A set of wrappers for the following languages (wrapper libraries to allow the code written in these languages to interact with the native C API): C#; Java; MATLAB; Python; PHP
6. Code examples.

Within the desktop version of SAM, which is no more than a user-friendly interface to the SSC dynamic library (*.dll files*), one can find production and economic performance models for a slew of renewable technologies. Simulations run on the desktop version of SAM can be exported as source code in multiple formats (including VBA, Python and Matlab), simplifying the access to the SSC from outside the user interface.

Many companies have used the SSC API for their own applications, including SunRun (PVWatts and flat plate PV models (*pvsamv1*) for pricing and system design), SunEdison (PVWatts for energy estimates), Arizona Public Service (PVWatts for grid-integration analysis), Concept3D (Flat Plate PV Model (*pvsamv1*) and residential/commercial financial model in Simuwatt), and Genability (PVWatts for online siting tool) (Gilman P. , 2013). All the results in this dissertation have been obtained through NREL´s SAM software, and as such, and according to the terms in NREL (2017b), the author credits the U.S. Department of Energy (DOE)/NREL/ALLIANCE for use of their data.

In sections II1.1 and II1.2. an in-depth analysis of which of SAM´s models will be relevant to can be found.

Appendix III

VBA code access and interpretation

Table 19 outlines all the variables that go into the SDK´s compute modules, their description, input origin, default values and ranges. This list does not however cover all other variables within routines that had to be created to achieve the final product, but the code is heavily commented to make it easier to follow. It can be accessed through the developer tab in MS Excel, in the *Simulator.xlsm* workbook, in Module 6, the macro´s name being *Run Case*. To run the model on another PC, keep in mind the directory *C:\TESEMD* is automatically defaulted to within the code, and was used to host the folders named *SDK Lib PVWatts* (containing the SSC´s *.dll* and API), *LOAD* (containing *load.csv* file and *PRT Lisboa (EPW).csv*) and *Rates* (containing *ur_ec_sched_weekday.csv, ur_ec_sched_weekend.csv* and *ur_ec_sell_rate.csv),* holding the required files to properly run the model. Also, all outputs of the *Basetable.xlsm* and *Simulator.xlsm* are defaulted to generated folders and files in this directory. If using a different machine, the code must either be altered to reflect a new directory and/or file structure, or this same file structure should be recreated.

Table 19 – VBA Modules Variable Names and Definitions

Module	Variable Name	Variable Description	Input	Default	Range
pvwattsv1	*solar_resource_file*	Weather Data Resource File	User	Filepath	N/A
	enable_user_poa	Overrides inbuilt POA Calculation	Fixed	1	{0,1}
	user_poa	Array of POA Values	User	*	N/A
	system_size	System Nameplate Capacity	User	*	[0,..+]
	derate	System Derate Factor	User	0.85	[0,1]
	inv_eff	Inverter Efficiency	User	0.96	[0,1]
	track_mode	Axis Tracking Mode	Fixed	0	{0,1,2,3}
	tilt	PV Panel Tilt	User	*	[0,90]
	azimuth	PV Panel Azimuth	User	*	[0,360]
	adjust:constant	Constant Loss Adjustment	Fixed	0	[0,100]
	gamma	Max. Power Temp. Coefficient	User	*	[-..,0]
	ar_glass	Enable Anti-reflective Coating	User	*	{0,1}
	inoct	Installed NOCT	Fixed	49	[0,..+]
	gcr	Ground Coverage Ratio	FIxed	1	[0,1]
belpe	*solar_resource_file*	Weather Data Resource File	Fixed	Filepath	N/A
	en_belpe	Enable Load Calculation	Fixed	1	{0,1}
	load	Initial Hourly Load Array	Fixed	Filepath	N/A
	floor_area	Total Surface Area (m2)	User	928.4	[0,..+]
	Stories	Number of Stories in Building	User	4	[1,..+]
	YrBuilt	Year Built	Fixed	1980	[1900,..+]
	Retrofits	Building Energy Saving Measures	Fixed	1	{0,1}
	Occupants	Total Number of Occupants	User	20.8	[0,..+]
	Occ_Schedule	Hourly Occupant Schedule	Fixed	100% All hours	Fraction/hour
	Theat	Heating Setpoint	Fixed	68ºF	[0,..+]
	Tcool	Cooling Setpoint	Fixed	77ºF	[0,..+]
	THeatSB	Heating Setpoint Setback	Fixed	68ºF	[0,..+]
	TCoolSB	Cooling Setpoint Setback	Fixed	77ºF	[0,..+]
	T_Sched	Temperature Schedule	Fixed	100% All hours	{0,1}/hour
	en_heat	Enable ElectricHeat	Fixed	0	{0,1}
	en_cool	Enable Electric Cooling	Fixed	0	{0,1}
	en_fridge	Enable Electric Fridge	Fixed	0	{0,1}
	en_range	Enable Electric Stove	Fixed	0	{0,1}
	en_dish	Enable Electric Dishwasher	Fixed	0	{0,1}
	en_wash	Enable Electric Washing Machine	Fixed	0	{0,1}
	en_dry	Enable Electric Dryer	Fixed	0	{0,1}
	en_mels	Enable Misc. Electric Loads	Fixed	0	{0,1}
	Monthly_util	Montlhy Consumption from Utility Bill	User	*	N/A
utilityrate5	*analysis_period*	Number of Years in Analysis	Fixed	25	[0,100]
	system_use_lifetime_output	Lifetime Hourly System Outputs	Fixed	0	{0,1}
	gen	System Power Generated	pvwattsv1	*	N/A
	inflation_rate	Inflation Rate	User	1.50%	[0,..+]
	degradation	System Yearly Degradation	Fixed	-0.75%/year	[-..,0]
	load_escalation	Annual Load Escalation	Fixed	0%/year	[0,..+]
	rate_escalation	Annual Rate Escalation	Fixed	0%/year	[0,..+]
	ur_metering_option	Metering Options	Fixed	2	{0,1,2,3,4}
	ur_monthly_fixed_charge	Monthly Fixed Charge	Fixed	0	[0,..+]
	ur_monthly_min_charge	Monthly Minimum Charge	Fixed	0	[0,..+]
	ur_annual_min_charge	Annual Minimum Charge	Fixed	0	[0,..+]
	ur_en_ts_sell_rate	Enable TOU Sell Rates	Fixed	1	{0,1}
	ur_ts_sell_rates	TOU Sell Rates Array	Fixed	OMIE Price	N/A
	ur_ec_sched_weekday	Energy Charge Weekday Schedule	Fixed	Filepath	N/A
	ur_ec_sched_weekends	Energy Charge Weekend Schedule	Fixed	Filepath	N/A
	ur_ec_tou_mat	Energy Rates Table	User	*	N/A
	ur_dc_enable	Enable Demand Charge	Fixed	0	{0,1}

*Dependent on User PV Panel Selection and Simulation Inputs in ArcGIS

Appendix IV

System Comparison Scenarios Input Variable Description

Table 20 – Rooftop Analysis Scenario Description

Input Variations	PV1	PV2	PV3	PV4	PV5	PV6	PV7	PV8	PV9	PV10	PV11	PV12	PV13	PV14	PV15	PV16	PV17	PV18	PV19
Module Type	Standard	Premium	Thinfilm	Standard	Standard	Standard	Standard	Standard	Standard	Standard	Standard	Standard	Standard	Standard	Standard	Standard	Standard	Standard	Standard
System Losses	11.42%	11.42%	11.42%	11.42%	11.42%	11.42%	11.42%	11.42%	11.42%	11.42%	11.42%	11.42%	11.42%	11.42%	11.42%	11.42%	11.42%	11.42%	11.42%
Inverter Efficiency	96%	96%	96%	96%	96%	96%	96%	96%	96%	96%	96%	96%	96%	96%	96%	96%	96%	96%	96%
Inverter	No	No	No	String	Micro	No	No	No	No	No	No	No	No	No	No	No	No	No	No
	Option	Option	Option	Option		Option	Option	Option	Option	Option	Option	Option	Option	Option	Option	Option	Option	Option	Option
Nº Pers/Household	2.6	2.6	2.6	2.6	2.6	1	2.6	2.6	2.6	2.6	2.6	2.6	2.6	2.6	2.6	2.6	2.6	2.6	2.6
Average Surface Area/Household (m2)	116.05	116.05	116.05	116.05	116.05	116.05	116.05	116.05	116.05	116.05	116.05	116.05	116.05	116.05	116.05	116.05	116.05	116.05	116.05
Nº Stories	4	4	4	4	4	4	4	4	4	4	4	4	4	4	4	4	4	4	4
Nº Households	8	8	8	8	8	8	8	8	8	8	8	8	8	8	8	8	8	8	8
Cycle	Bi-hourly	Bi-hourly	Bi-hourly	Bi-hourly	Bi-hourly	Bi-hourly	Simple	Bi-hourly	Bi-hourly	Bi-hourly	Bi-hourly	Bi-hourly	Bi-hourly	Bi-hourly	Bi-hourly	Bi-hourly	Bi-hourly	Bi-hourly	Bi-hourly
Household Contracted Capacity (kVA)	6.9	6.9	6.9	6.9	6.9	6.9	6.9	6.9	6.9	6.9	6.9	6.9	6.9	6.9	6.9	6.9	6.9	6.9	6.9
New Construction	0	0	0	0	0	0	0	1	0	0	0	0	0	0	0	0	0	0	0
VAT (%)	23%	23%	23%	23%	23%	23%	23%	23%	15%	23%	23%	23%	23%	23%	23%	23%	23%	23%	23%
Debt Fraction (%)	50%	50%	50%	50%	50%	50%	50%	50%	50%	100%	0%	50%	50%	50%	50%	50%	50%	50%	50%
Loan Interest (%)	3%	3%	3%	3%	3%	3%	3%	3%	3%	3%	3%	5%	3%	3%	3%	3%	3%	3%	3%
Loan Term (Years)	7	7	7	7	7	7	7	7	7	7	7	7	10	7	7	7	7	7	7
IRS (%)	35%	35%	35%	35%	35%	35%	35%	35%	35%	35%	35%	35%	35%	35%	35%	35%	35%	35%	35%
Inflation (%T)	1.5%	1.5%	1.5%	1.5%	1.5%	1.5%	1.5%	1.5%	1.5%	1.5%	1.5%	1.5%	1.5%	0.5%	2.5%	1.5%	1.5%	1.5%	1.5%
Discount Rate	WACC	WACC	WACC	WACC	WACC	WACC	WACC	WACC	WACC	WACC	WACC	WACC	WACC	WACC	WACC	WACC	WACC	WACC	WACC
Sell Rate	Standard	Standard	Standard	Standard	Standard	Standard	Standard	Standard	Standard	Standard	Standard	Standard	Standard	Standard	Standard	Standard + 25%	Standard - 25%	Energy+ + 25%	Energy+ -25%
Irradiation (W/m2)	Energy+	Energy+	Energy+	Energy+	Energy+	Energy+	Energy+	Energy+	Energy+	Energy+	Energy+	Energy+	Energy+	Energy+	Energy+	Energy+	Energy+		

Table 21 – Façade Analysis Scenario Description

Input Variations	TF1	TF2	TF3	TF4	TF5	TF6	TF7	TF8	TF9	TF10	TF11	TF12	TF13	TF14	TF15	TF16	TF17
Module Type	Thinfilm	Thinfilm	Thinfilm	Thinfilm	Thinfilm	Thinfilm	Thinfilm	Thinfilm	Thinfilm	Thinfilm	Thinfilm	Thinfilm	Thinfilm	Thinfilm	Thinfilm	Thinfilm	Thinfilm
System Losses	11.42%	11.42%	11.42%	11.42%	11.42%	11.42%	11.42%	11.42%	11.42%	11.42%	11.42%	11.42%	11.42%	11.42%	11.42%	11.42%	11.42%
Inverter Efficiency	96%	96%	96%	96%	96%	96%	96%	96%	96%	96%	96%	96%	96%	96%	96%	96%	96%
Inverter	No Option	String	Micro	No Option	No Option	No Option	No Option	No Option	No Option	No Option	No Option	No Option	No Option	No Option	No Option	No Option	No Option
Nº Pers/Household	2.6	2.6	2.6	1	2.6	2.6	2.6	2.6	2.6	2.6	2.6	2.6	2.6	2.6	2.6	2.6	2.6
Average Surface Area/Household (m2)	116.05	116.05	116.05	116.05	116.05	116.05	116.05	116.05	116.05	116.05	116.05	116.05	116.05	116.05	116.05	116.05	116.05
Nº Stories	4	4	4	4	4	4	4	4	4	4	4	4	4	4	4	4	4
Nº Households	8	8	8	8	8	8	8	8	8	8	8	8	8	8	8	8	8
Cycle	Bi-hourly	Bi-hourly	Bi-hourly	Bi-hourly	Simple	Bi-hourly	Bi-hourly	Bi-hourly	Bi-hourly	Bi-hourly	Bi-hourly	Bi-hourly	Bi-hourly	Bi-hourly	Bi-hourly	Bi-hourly	Bi-hourly
Household Contracted Capacity (kVA)	6.9	6.9	6.9	6.9	6.9	6.9	6.9	6.9	6.9	6.9	6.9	6.9	6.9	6.9	6.9	6.9	6.9
New Construction	0	0	0	0	0	1	0	0	0	0	0	0	0	0	0	0	0
VAT (%)	23%	23%	23%	23%	23%	23%	15%	23%	23%	23%	23%	23%	23%	23%	23%	23%	23%
Debt Fraction (%)	50%	50%	50%	50%	50%	50%	50%	100%	0%	50%	50%	50%	50%	50%	50%	50%	50%
Loan Interest (%)	3%	3%	3%	3%	3%	3%	3%	3%	3%	5%	3%	3%	3%	3%	3%	3%	3%
Loan Term (Years)	7	7	7	7	7	7	7	7	7	7	10	7	7	7	7	7	7
IRS (%)	35%	35%	35%	35%	35%	35%	35%	35%	35%	35%	35%	35%	35%	35%	35%	35%	35%
Inflation (%T)	1.5%	1.5%	1.5%	1.5%	1.5%	1.5%	1.5%	1.5%	1.5%	1.5%	1.5%	0.5%	2.5%	1.5%	1.5%	1.5%	1.5%
Discount Rate	WACC	WACC	WACC	WACC	WACC	WACC	WACC	WACC	WACC	WACC	WACC	WACC	WACC	WACC	WACC	WACC	WACC
Sell Rate	Standard	Standard	Standard	Standard	Standard	Standard	Standard	Standard	Standard	Standard	Standard	Standard	Standard	Standard +25%	Standard - 25%	Standard	Standard
Irradiation (W/m2)	Energy+	Energy+	Energy+	Energy+	Energy+	Energy+	Energy+	Energy+	Energy+	Energy+	Energy+	Energy+	Energy+	Energy+	Energy+	Energy+ +25%	Energy+ -25%

Appendix V

System Comparison Scenarios Result Comparison

Table 23 – Rooftop Simulation Scenarios Result Comparison

	Module Type			Inverter Type		↓Occup.	Flat Elec. Rate	New Construction	↓VAT	Debt Fraction		↑Loan Interest	↑Loan Term	Inflation		Sell Rate		Irradiation	
	Standard	Premium	Thin film	String	Micro					100%	0%			Lower	Higher	Higher	Lower	Higher	Lower
Results	PV1	PV2	PV3	PV4	PV5	PV6	PV7	PV8	PV9	PV10	PV11	PV12	PV13	PV14	PV15	PV16	PV17	PV18	PV19
Total Installed Capacity (kW)	4.25	5.01	2.81	4.250	4.250	4.25	4.25	4.25	4.25	4.25	4.25	4.25	4.25	4.25	4.25	4.25	4.25	4.25	4.25
Number Panels	16	16	16	16	16	16	16	16	16	16	16	16	16	16	16	16	16	16	16
Tilt (º)	30	30	30	30	30	30	30	30	30	30	30	30	30	30	30	30	30	30	30
Azimuth (º)	247.9	247.9	247.9	247.9	247.9	247.9	247.9	247.9	247.9	247.9	247.9	247.9	247.9	247.9	247.9	247.9	247.9	247.9	247.9
Local	Rooftop	Rooftop	Rooftop	Rooftop	Rooftop	Rooftop	Rooftop	Rooftop	Rooftop	Rooftop	Rooftop	Rooftop	Rooftop	Rooftop	Rooftop	Rooftop	Rooftop	Rooftop	Rooftop
Total Area (m2)	27.78	27.78	27.78	27.78	27.78	27.78	27.78	27.78	27.78	27.78	27.78	27.78	27.78	27.78	27.78	27.78	27.78	27.78	27.78
Annual Production Y1 (kWh)	5111.15	6141.79	3463.40	5067.73	5112.07	5111.15	5111.15	5111.15	5111.15	5111.15	5111.15	5111.15	5111.15	5111.15	5111.15	5111.15	5111.15	6387.18	3762.36
Annual Consumption (kWh)	28861.3	28861.3	28861.3	28861.3	28861.3	20381.7	28861.3	28861.3	28861.3	28861.3	28861.3	28861.3	28861.3	28861.3	28861.3	28861.3	28861.3	28861.3	28861.34
Electric Bill W/ System Y1 (€)	4519.71	4334.28	4858.02	4528.07	4519.48	2995.45	4690.66	4519.71	4224.92	4519.71	4519.71	4519.71	4519.71	4519.71	4519.71	4516.54	4522.88	4291.36	4791.91
Electric Bill W/o System Y1 (€)	5700.50	5700.50	5700.50	5700.50	5700.50	4042.38	5633.72	5700.50	5329.81	5700.50	5700.50	5700.50	5700.50	5700.50	5700.50	5700.50	5700.50	5700.50	5700.50
Savings in Y1 (€)	1180.80	1366.21	842.52	1172.44	1181.02	1046.94	943.04	1180.80	1104.82	1180.80	1180.80	1180.80	1180.80	1180.80	1180.80	1183.96	1177.63	1409.12	908.62
Total Installed Cost (€)	11624.42	12073.49	4197.20	11049.35	12977.87	11624.42	11624.42	10317.86	10868.36	11624.42	11624.42	11624.42	11624.42	11624.42	11624.42	11624.42	11624.42	11624.42	11624.42
Debt (€)	5812.21	6036.74	2098.60	5524.67	6488.94	5812.21	5812.21	5158.93	5434.18	11624.42	0.00	5812.21	5812.21	5812.21	5812.21	5812.21	5812.21	5812.21	5812.21
NPV (€)	8276.28	10985.87	9933.57	8677.47	8305.77	6013.32	3640.09	9563.97	7749.83	7128.34	9960.29	5939.27	8334.11	9470.44	7190.59	8321.76	8230.79	12850.98	2851.58
Payback Period (Years)	9.87	8.94	5.20	9.49	10.91	11.03	14.40	8.85	9.86	9.87	9.87	9.87	9.87	10.35	9.46	9.85	9.89	8.26	14.99
Project IRR (%)	9.06%	10.37%	19.34%	9.56%	8.50%	7.68%	6.21%	10.50%	9.07%	9.06%	9.06%	9.06%	9.06%	7.98%	10.15%	9.09%	9.03%	11.60%	5.69%
Equity IRR (%)	10.55%	12.30%	25.84%	11.21%	9.78%	8.74%	6.90%	12.48%	10.56%	13.99%	9.06%	10.05%	11.16%	9.20%	11.90%	10.59%	10.51%	13.98%	6.26%
Real LCOE (€c/kWh)	16.40	14.59	10.33	15.90	16.37	16.40	16.40	14.96	15.34	16.90	15.54	18.11	16.34	16.10	16.72	16.40	16.40	13.13	22.28
Nominal LCOE (€c/kWh)	19.35	17.21	12.18	18.76	19.31	19.35	19.35	17.65	18.09	19.82	18.44	21.21	19.27	17.06	21.73	19.35	19.35	15.48	26.28
Higher than PV1	Lower Than PV1																		

Table 22 – Façade Simulation Scenarios Result Comparison

	Inverter Type			↓Occup.	Flat Elec. Rate	New Construction	↓VAT	Debt Fraction		↑Loan Interest	↑Loan Term	Inflation		Sell Rate		Irradiation	
	No Option	String	Micro					100%	0%			Lower	Higher	Higher	Lower	Higher	Lower
Results	TF1	TF2	TF3	TF4	TF5	TF6	TF7	TF8	TF9	TF10	TF11	TF12	TF13	TF14	TF15	TF16	TF17
Total Installed Capacity (kW)	2.66	2.659	2.659	2.66	2.66	2.66	2.66	2.66	2.66	2.66	2.66	2.66	2.66	2.66	2.66	2.66	2.66
Number Panels	56	56	56	56	56	56	56	56	56	56	56	56	56	56	56	56	56
Tilt (º)	90	90	90	90	90	90	90	90	90	90	90	90	90	90	90	90	90
Azimuth (º)	247.86	247.9	247.9	247.9	247.9	247.9	247.9	247.9	247.9	247.9	247.9	247.9	247.9	247.9	247.9	247.9	247.9
Local	Façade	Façade	Façade	Façade	Façade	Façade	Façade	Façade	Façade	Façade	Façade	Façade	Façade	Façade	Façade	Façade	Façade
Total Area (m2)	26.31	26.31	26.31	26.31	26.31	26.31	26.31	26.31	26.31	26.31	26.31	26.31	26.31	26.31	26.31	26.31	26.31
Annual Production Y1 (kWh)	1589.25	1425.59	3361.89	1589.25	1589.25	1589.25	1589.25	1589.25	1589.25	1589.25	1589.25	1589.25	1589.25	1589.25	1589.25	2100.07	1081.96
Annual Consumption (kWh)	28861.34	28861.34	28861.34	20381.66	28861.34	28861.34	28861.34	28861.34	28861.34	28861.34	28861.34	28861.34	28861.34	28861.34	28861.34	28861.34	28861.3
Electric Bill W/ System Y1 (€)	5309.49	5349.54	4922.25	3657.5	5323.52	5309.49	4964.18	5309.49	5309.49	5309.49	5309.49	5309.49	5309.49	5309.49	5309.49	5187.08	5433.72
Electric Bill W/o System Y1 (€)	5700.50	5700.50	5700.50	4042.38	5633.72	5700.50	5329.81	5700.50	5700.50	5700.50	5700.50	5700.50	5700.50	5700.50	5700.50	5700.50	5700.50
Savings in Y1 (€)	391.03	350.99	778.27	384.88	310.21	391.03	365.60	391.03	391.03	391.03	391.03	391.03	391.03	391.04	391.03	513.43	266.78
Total Installed Cost (€)	3981.63	3788.70	4436.95	3981.63	3981.63	3456.86	3722.67	3981.63	3981.63	3981.63	3981.63	3981.63	3981.63	3981.63	3981.63	3981.63	3981.63
Debt (€)	1990.82	1894.35	2218.48	1990.82	1990.82	1728.43	1861.33	3981.63	0.00	1990.82	1990.82	1990.82	1990.82	1990.82	1990.82	1990.82	1990.82
NPV (€)	1553.84	976.92	9586.72	1479.02	5.89	2071.04	1452.78	1272.47	2004.44	899.60	1573.65	1945.53	1198.81	1553.84	1553.84	3914.93	-826.13
Payback Period (Years)	13.5	15.56	5.91	13.83	18.43	10.90	13.50	13.50	13.50	13.50	13.50	14.37	12.50	13.50	13.50	8.26	21.65
Project IRR (%)	6.84%	5.82%	17.59%	6.69%	3.67%	8.39%	6.84%	6.84%	6.84%	6.84%	6.84%	5.67%	8.01%	6.84%	6.84%	11.00%	1.70%
Equity IRR (%)	7.72%	6.43%	22.68%	7.52%	3.80%	9.74%	7.72%	9.41%	6.84%	7.26%	8.09%	6.25%	9.17%	7.72%	7.72%	13.23%	1.47%
Real LCOE (€c/kWh)	21.34	23.03	9.41	21.34	21.34	19.48	19.95	21.86	20.41	23.19	21.27	21.05	21.64	21.34	21.34	16.15	31.35
Nominal LCOE (€c/kWh)	25.17	27.16	11.10	25.17	25.17	22.98	23.54	25.65	24.21	27.16	25.09	22.30	28.12	25.17	25.17	19.05	36.98
Higher than TF1	Lower Than TF1																